Investigating intermolecular interactions motifs in ammonium carboxylate salts

by

James Arthur Odendal

Thesis presented in partial fulfilment of the requirements for the degree of Master of Science

at

Stellenbosch University

Department of Chemistry and Polymer Science

Faculty of Science

Supervisor: Prof. Klaus R. Koch

Co-supervisor: Dr. Delia A. Haynes

Dec 2009

Declaration

By submitting this dissertation electronically, I declare that the entirety of the work contained therein is my own, original work, that I am the owner of the copyright thereof (unless to the extent explicitly otherwise stated) and that I have not previously in its entirety or in part submitted it for obtaining any qualification.

Date: December 2009

Dedicated to my late father ***Arthur Julius Odendal***

(1964/04/17 - 2001/12/22)

"I have this one little saying, when things get too heavy just call me helium, the lightest known gas to man."

by *Jimi Hendrix*

Acknowledgements

- Firstly, I would like to thank my supervisor Prof Klaus Koch for giving me the opportunity to do my M.Sc under his supervision, for his guidance and support throughout this project and for believing in me.

- My co-supervisor Dr. Delia Haynes for her open door policy, patience, enthusiasm, guidance and support throughout this project. I am truly grateful for everything you have done for me ☺

- To Dr. Jocelyn Bruce for her initial input and work done on this project.

- Then to my friends and colleagues in the Platinum Metals Chemistry Research Group old and new, *Sakkie, Terblanchie, Piet-Neet, Liezel, Stjani, Ugo* and *Geswint*. Thank you for making our working environment so pleasurable.

- To Dr. Jan Gertenbach for training me to operate the instrument needed for this study. Special thanks to Leigh Loots for reading through thesis chapters

- To my loving mother and two brothers for their supports and prayers.

- The University of Stellenbosch and NRF for Financial assistance

ABSTRACT

This thesis reports an in-depth investigation of the intermolecular interaction motifs in secondary, primary and ammonium carboxylate salts. The investigation was conducted using the Cambridge Structural Database (CSD), together with a systematic steric-specific experimental study.

The tendency in the literature has been to analyse organic salt crystal structures in terms of hydrogen bonding patterns, almost ignoring cation-anion interactions. This study focuses on the cation-anion interactions in secondary, primary and ammonium carboxylate salts, which have a direct effect on the formation of specific structural motifs. The ideas of ring-stacking and ring-laddering, which arise from the tendency of cations and anions to arrange themselves so as to maximise electrostatic interactions, have been applied to ammonium carboxylate salts.

An extensive survey of organic ammonium carboxylate salt structures in the CSD has been carried out. The structural motifs in ammonium carboxylates were investigated, and a set of predictive rules for the pattern of intermolecular interactions in these salts was developed. Using these results, the formation of ring-stacking or ring-laddering in primary ammonium carboxylate salts can be predicted. The results from the CSD survey are discussed in Chapter 3.

An experimental study has been carried out, which complements the results obtained from the CSD survey. The experimental study formed 19 novel ammonium carboxylate salts, of which 2 formed hydrates and 2 co-crystals of salts. The experimental results confirm what was found in the CSD survey, and this is discussed in Chapter 4.

This study has found that the principle of ring-stacking and ring-laddering can be applied in a general form to the crystal structures of organic ammonium carboxylate salts. The size of the cation and the anion in these salts has a significant effect on the formation of structural motifs in the solid state. Interactions between cation and anion substituents also play an important role in the formation of particular structural motifs in ammonium carboxylate salts.

OPSOMMING

In hierdie tesis word die intermolekulêre interaksie motiewe in die sekondêre, primêre en ammonium karbosilaat soute in-diepte ondersoek. Die studie is gedoen met behulp van die Cambridge Strukturele Databasis (CSD), saam met ’n sistematiese steries-spesifieke eksperimentele studie.

Die neiging in die literatuur is om organiese sout kristal strukture in terme van waterstofbindings patrone te analiseer sonder om katioon-anioon interaksies in ag te neem. Die studie fokus juis op hierdie katioon-anioon interaksies tussen sekondêre, primêre en ammonium karbosilaat soute wat ’n direkte effek het op die vorming van spesifieke strukturele motiewe naamlik ‘ring-stacking’ en ‘ring-laddering’ wat hul oorsprong kry vanaf die neiging van katione en anione om hulself op so ’n wyse te rangskik sodat die elektrostatiese interaksies ’n maksimum kan bereik, op die ammonium karboksilaat soute.

’n Volledige ondersoek van ammonium karboksilaat soute in die CSD is gedoen. Die strukturele motiewe in ammonium karboksilaat is ondersoek, en ’n stel reels wat die patrone van intermolekulêre interaksies in hierdie soute voorspelis ontwikkel. Hierdie resultate kan gebruik word om die vorming van ‘ring-stacking’ en ‘ring-laddering’ in primêre ammonium karbosilaat soute te voorspel. Die resultate van die CSD ondersoek word bespreek in Hoofstuk 3.

’n Eksperimentele studie is uitgevoer en die resultate hiervan komplimenteer die resultate van die CSD ondersoek. In die eksperimentele studie is 19 nuwe ammonium karboksilaat soute gekristaliseer, waarvan 2 hidraat-soute en 2 ko-kristal-van-soute is. Die eksperimentele resultate bevestig die bevindings van die CSD ondersoek, en dit word bespreek in Hoofstuk 4.

Hierdie studie het gevind dat die beginsel van ‘ring-stacking’ en ‘ring-laddering’ kan in ‘n algemene vorm in die kristal strukture van organiese ammonium karboksilaat soute toegepas word. Die grootte van die katioon en anion in hierdie soute het ’n beduidende effek op die vorming van strukturele motiewe in die vaste toestand. Interaksie tussen die katioon en anioon substituente speel ‘n belangrike rol in die vorming van spesifieke motiewe in ammonium karbosilaat soute.

Conferences

1. **SACI 2008 – *39th National Convention of the South African Chemical Institute***

   Stellenbosch, South Africa, 30 November – 5 December 2008

   Poster Presentation – Investigating intermolecular interactions motifs in ammonium carboxylate salts

2. **ISIC-2009 – *12th International Seminar on Inclusion Compounds***

   Stellenbosch, South Africa, 4 – 9 April 2009

   Poster Presentation – Investigating intermolecular interactions motifs in ammonium carboxylate salts

Abbreviations

0-D	Zero Dimensional
1-D	One Dimensional
2-D	Two Dimensional
3-D	Three Dimensional
CSD	Cambridge Structural Database
CE	Crystal Engineering
HB	Hydrogen bonding
LMOG	Low Mass Organic Gelation
MeOH	Methanol
SCD	Single-Crystal X-ray Diffraction
TGA	Thermogravimetric Analysis
XRPD	X-ray Powder Diffraction

Atomic Colour Key

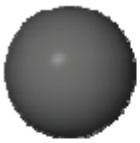

Carbon

Oxygen

Nitrogen

Hydrogen

Table of Contents

CHAPTER 4

CRYSTAL STRUCTURES OF NOVEL AMMONIUM CARBOXYLATE SALTS

LIST OF FIGURES

LIST OF TABLES

LIST OF SCHEMES

Chapter 1

Introduction

Crystal engineering is "… *the understanding of intermolecular interactions in the context of crystal packing and in the utilization of such understanding in the design of new solids with desired physical and chemical properties.*"[1] by G. R. Desiraju

1.1 CRYSTAL ENGINEERING IN SUPRAMOLECULAR CHEMISTRY

Desiraju's definition has stood the test of time as it covers the basic fundamentals of crystal engineering. Crystal engineering (CE) is a subdiscipline of supramolecular chemistry; it looks at crystal design and is based on understanding intermolecular interactions in the solid-state.[2] The concepts of CE were introduced by Pepinsky[3] in the 50s and later implemented by Schmidt[4] when he looked at the design of molecular crystals for use in photodimerization in the solid-state. The field of CE has not just been of interest to chemists; but also has potential application in molecular biology,[5] material sciences,[6] physical sciences[7], and pharmaceutical sciences.[8] This field has brought together an interesting combination of interdisciplinary scientists to advance the science of CE.

CE seeks a way of understanding intermolecular interactions and molecular recognition phenomena between molecules in the solid-state. Molecular recognition between molecules in the solid-state refers to specific interactions between two or more molecules through noncovalent interactions i.e. hydrogen bonds, van der Waals forces, π···π interactions and electrostatic effects.[9] The behaviour of a functional group in CE is dependent on the position and location of these functionalities on the molecule.[10] In organic chemistry the long-chain aliphatic groups have no molecular recognition functionality, but in CE the entire molecule has molecular functionality: alkyl-alkyl interactions are well documented in the literature.[2,42] This shows the importance of steric effects in CE - the size and the functionalities of the molecules play an important role and these are a key factor in the design strategy of crystals.

If molecules are built by connecting atoms with covalent bonds, solid-state supermolecules (crystals) are built by connecting molecules with intermolecular interactions. The supermolecule consists of smaller structural units called supramolecular synthons, these supramolecular

synthons assemble by means of molecular recognition functionality in a way which is reproducible from structure-to-structure.[10,11] In Scheme 1 some examples of supramolecular synthons are shown, displaying both homo and heterosynthons.

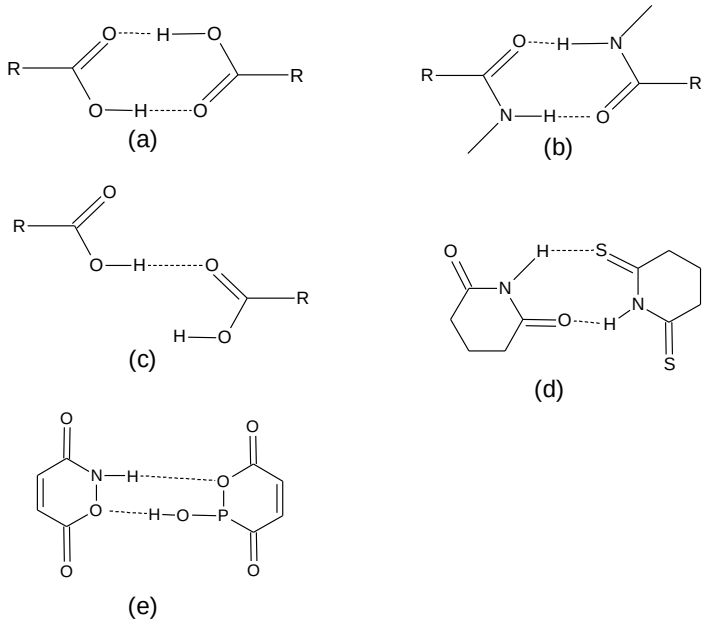

Scheme 1 Representative supramolecular synthons: homosynthons (a, b and c) and heterosynthons (d, e) – Dotted lines represent non-covalent interactions.

The investigation of intermolecular interactions has been made easier with the advances in technology, with crystallographic software and crystallographic databases containing vast amounts of structural information. The Cambridge Structural Database (CSD)[12] is, to date, one of the most powerful sources of crystallographic data on small organic/inorganic crystal structures obtained from X-ray and neutron diffraction. This database provides the researcher with vital information on published crystal structures such as the nature of certain bond types and other intermolecular interactions. It has been used extensively by various supramolecular research groups to study intermolecular interactions and crystal packing, giving fundamental knowledge for CE and crystal design.[13]

There are various intermolecular interactions which play an important role in CE. These intermolecular interactions in the solid-state are well documented in the literature. The hydrogen bonding interaction[14] is the strongest and most important interaction in CE because it is direction-specific, which makes it advantageous in crystal design.[1] The increasing interest in different types of stable aromatic type interactions,[15] charge-assisted hydrogen bonding[16] and alkyl-alkyl interactions[2,17] is also well documented in the literature. These interactions play a fundamental role in designing crystals with desired physical and chemical properties. The attempts made by various research groups to understand the different effects of intermolecular interactions in CE gives the modern-day crystallographer great insight into the design strategy of new solids.

1.2 INTERMOLECULAR INTERACTIONS

In recent years there has been considerable interest in the relative importance of various intermolecular interactions as they play an important role in CE,[18,24] molecular recognition,[19] supermolecular assemblies[20,21] and ultimately crystal structure prediction and determination.[22]

1.2.1 HYDROGEN BONDING IN THE SOLID-STATE

What is a hydrogen bond? With the advances made in understanding intermolecular interactions to the present day one might think that it is a rhetorical question to ask. If we look at the progress in developing an understanding of the hydrogen bond this question might not sound so rhetorical after all. I would like to bring your attention to a quote directly out of a paper by Cotton and Luck.[23]

"There is a kind of conventional wisdom that neutron diffraction finds hydrogen atoms better than X-ray diffraction does. But is this even a meaningful statement, let alone a true one? It can be argued that it is not meaningful and thus incapable of being true. The simple facts are that neutrons and X-rays see two different parts of the hydrogen atom and that these parts do not coincide. It is then a Solomonic question whether either technique is justifiably considered to 'see' the hydrogen atom. The neutron experiment sees, with considerable accuracy (ca. f 0.001Å), the location of the hydrogen atom's nucleus, the proton. In a very favourable case, the

X-ray experiment sees, with less accuracy, the hydrogen atom's electron cloud. Which of these is 'the hydrogen atom'? Both the nucleus and the electron density of an atom are essential parts, and it is therefore impossible to assert rationally that the position of either the one or the other is 'the' position of the atom."

This statement is important to understand if you are a scientist and the main focus of your research is hydrogen bonding and what effects it has in the solid-state.[24] Scientists have been looking at hydrogen bonding interactions dating back to the 1920s when Latimer and Rodebush[25] investigated and postulated the hydrogen bonding phenomenon in water using varying temperatures. Pauling[26] in the 1940s then postulated that hydrogen bonding is fairly ionic in nature and forms between only the most electronegative atoms. He then mentioned that the hydrogen bond is of great significance in determining the properties of substances and today we can bear witness to the truth of that statement. Pimentel and McClellan[27] during the 1960s defined a hydrogen bond between a functional group A-H and an atom, or a group, B in the same or different molecule when

a) *there is evidence of bond formation be it association or chelation*

b) *there is evidence that this new bond linking A-H and B specifically involves the hydrogen atom already bonded to A.*

This definition does not take into account the chemical nature of the participants, including the polarities, and net charges are widely unspecified. The definition has no restrictions on interaction geometry; it only makes the assumption that a hydrogen atom must be involved.[14] It took about 40 years for the advancement of this statement thus showing the controversy around the hydrogen bond. Steiner[14] gave a definition of hydrogen bonding which states the following:

An A-H···B interaction is called a "hydrogen bond", if 1. it constitutes a local bond, and 2. A-H acts as a proton donor to B.

This definition has widely been accepted as the general chemical definition for hydrogen bonding as it addresses the acid/base properties of ***A-H*** **(donor)** and ***B*** **(acceptor)**, which in principle can be understood by the incipient proton-transfer reaction from ***A-H*** to ***B***. There are

many specialized definitions of hydrogen bonding which are based on certain properties that are studied using particular techniques.[14]

The terminology on hydrogen bonding is not uniformly used within the literature; therefore some of the terms used here will be explained. In a particular hydrogen bond ***A-H···B***, the group ***A-H*** is called the proton donor and ***B*** is called the proton acceptor. Some authors refer to it as electron-acceptors and electron-donors. Due to the hydrogen bond having such a long range a single donor can interact with up to three acceptors simultaneously (Figure 1.1).

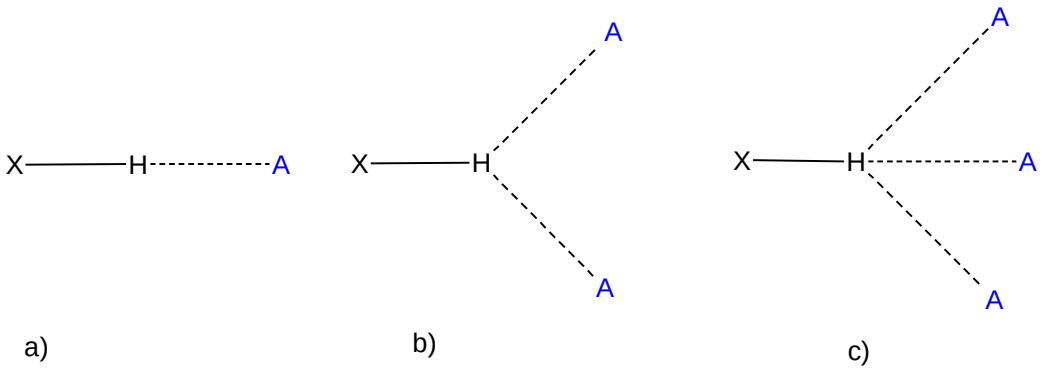

Figure 1.1 The different types of hydrogen bonding a) a single hydrogen bond, b) bifurcated hydrogen bond c) trifurcated hydrogen bond.

The energy of hydrogen bonds in the solid-state cannot be measured with any standard crystallographic technique, but it can be explained by its geometry, which makes it possible to be calculate energies computationally. The typical hydrogen bond geometry between a donor (X-H) and acceptor (A), is related by an angle θ (Figure 1.2) which ranges between 160 - 180°.[14] Since hydrogen bonds have such a long range it raises a question: Can hydrogen bonding be characterized into "strong", "moderate" and "weak" hydrogen bonds? According to Jeffery[28] this is possible (see Table 1.1).

Figure 1.2 Schematic of a typical hydrogen bonding geometry between donor and acceptor.

	Strong	Moderate	Weak
interaction type	strongly covalent	mostly electrostatic	electrostatic
Examples	[F – H – F] $^-$	O – H ⋯ H – O	O – H ⋯ π
	P – OH ⋯ O = P	N-H ⋯ O = C	C – H ⋯ O
Bond lengths in Å			
H⋯A	1.2 – 1.5	1.5 – 2.2	> 2.2
X⋯A	2.2 – 2.5	2.5 – 3.2	> 3.2
Directionality	strong	moderate	weak
Bond angles in °	170 – 180	> 130	> 90
Bond energies in kcal/mol	15 – 40	4 – 15	< 4

Table 1.1 Hydrogen bonds categorized into strong, moderate and weak hydrogen bonds as classified by Jeffrey.[28]

1.2.1.1 GRAPH-SET NOTATION

Many research groups, dating back to the 1920s,[25] have attempted to categorize hydrogen bonding systems based on the topology of the atoms involved in hydrogen bonding. Etter[29,30] was one of the pioneers to explain the topology of hydrogen atoms involved in the different kinds of hydrogen bonding. Etter used graph theory for categorizing hydrogen bonding motifs in the organic solid-state using graph set notation. Graph set notation describes the topology of the

atoms involved in hydrogen bonding with great detail. This graph set notation categorizes hydrogen bonds into four different types. The modes of hydrogen bonding are classified into four designators (G): self bonding (S) (intermolecular interaction within the same molecule), chain (C), discrete (D) and ring (R) and they are depicted as follows:

$$G_d^a(r)$$

where

G = pattern designator

r = the degree (total number of atoms involved in the hydrogen bonding)

a = number of hydrogen bond acceptors

d = number of hydrogen bond donors

Using this nomenclature various hydrogen bonding motifs can be classified into the above pattern designators. Figure 1.3 shows the graph set notation for different hydrogen bonds.

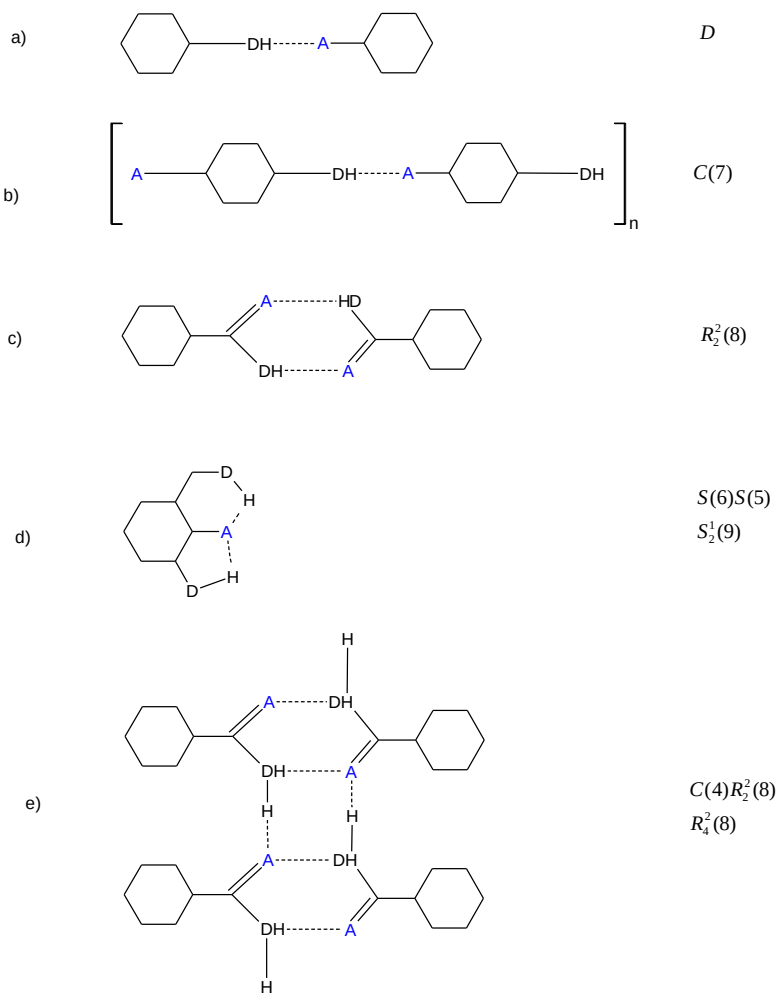

Figure 1.3 Examples of hydrogen bonding motifs assigned with their respective graph-set notations.[30]

1.2.2 WEAK HYDROGEN BONDING AND THE van der WAALS INTERACTION

It has been well documented that the C-H group acts as a weak hydrogen bond donor.[31,32] All atoms and molecules attract one another as a result of transient dipole-dipole interactions. Molecules need not have a net charge to participate in a dipole interaction. This transient dipole-dipole interaction is known as a van der Waals interaction. This is a weak interaction and its effects are based on the distance between the atoms/molecules involved.[33]

What is the difference between a hydrogen bond and a van der Waals interaction? This is a fundamental question when dealing with intermolecular interaction classifications. A paper published by Cotton[34] states that a typical C-H···O/N hydrogen bond represents nothing more

than a classical van der Waals interaction, but this statement was later challenged by Steiner and Desiraju.[35] Steiner and Desiraju did a complete CSD survey and their results show that the fundamental difference between the hydrogen bond and van der Waals interactions lies in the difference in directionality of these interactions. The hydrogen bond is directional and very close to linear geometry; the van der Waals contacts are fairly isotropic, thus the bond is independent of the angle θ. This difference allows us to distinguish between the two contacts.

1.2.3 C-H···π and π···π INTERACTIONS

C-H···π interactions between a hydrogen atom and the π-system of an aromatic ring only recently gained interest in the literature[37] but the geometry of this interaction is poorly understood. The C-H···π interaction is considered to be a weak hydrogen bonding interaction where the π-system acts as a hydrogen bond acceptor. Hanton[36] observed that structures containing no hydrogen bonding acceptors will make use of π-systems of aromatic ring as acceptors. It is therefore important for us to understand how this intermolecular interaction influences the mode of packing in the crystal. The aromatic type interaction has two basic orientations: the face-to-face (stacked) or edge-to-face[37] shown in Figure 1.4. The face-to-face stacking appears to be more favourable if the molecules are different and share similar isoelectronic systems. The edge-to-face is normally found in structures of small aromatic molecules.[38] The distance between the parallel and off-set packed aromatics rings (Figure 1.4) is approximately 3.3 – 3.8 Å.[39]

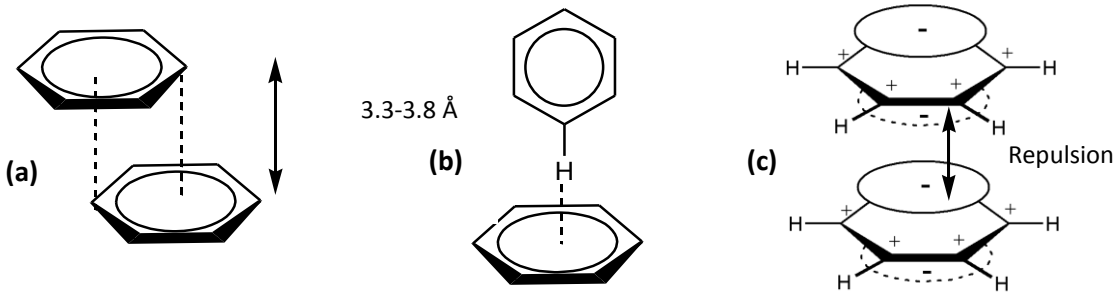

Figure 1.4: The types of aromatic π-π interactions: (a) face-to-face (interplanar distance about 3.3-3.8 Å) and (b) edge-to-face orientations. (c) The repulsion between negatively charged π-electron clouds of facially oriented aromatic rings.[38,40]

1.2.4 ALKYL-ALKYL INTERACTIONS

The alkyl-alkyl interaction is known for being non-covalent in nature. This interaction has recently been investigated[2] for its effects on the packing of molecules in the crystal. These interactions play an important role in the gelation of low mass organic salts[41] (LMOG). Research in LMOG has potential application in photography, cosmetics, food and the petroleum industry which plays an important role in our modern society. A systematic study was conducted by Dastidar and Trivedi[2] to look at the effects these interactions had on gelation of LMOG in ammonium carboxylate salts. This systematic study confirmed the importance of alkyl-alkyl interaction in CE. These long alkyl chains stack on top of one another in a parallel fashion (Figure 1.5) displaying a high degree of interdigitation of long alkyl chains, to maximize the alkyl-alkyl interactions in the crystal lattice.[42] The alkyl-alkyl interactions in the solid-state display a unique characteristic unlike other intermolecular interactions that need very specific molecular recognition to control the mode of packing. In alkyl-alkyl interactions the interdigitation between the of the alkyl groups is so overwhelming that it has an enormous effect on the packing in the solid-state, which makes this an ideal interaction to use in crystal engineering.

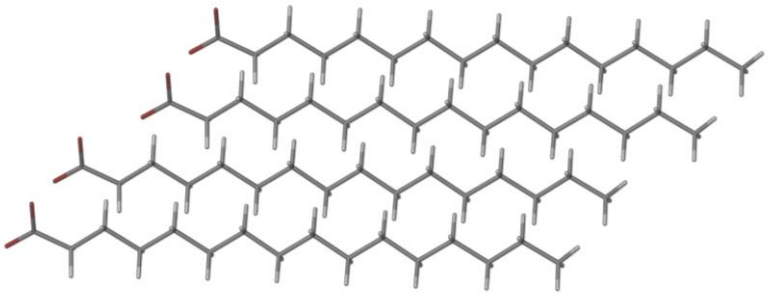

Figure 1.5 Alkyl-alkyl interactions in *ammonium palmitate* (GUKZOB).

1.3 CRYSTAL EXPLORER

Crystal Explorer[43] has become an essential tool in CE. It explores the packing modes and intermolecular interactions in molecular crystals using Hirshfeld surfaces,[44] from which information about all the intermolecular interactions can be encoded.[45] The Hirshfeld surface reflects the position of atoms and molecules in the crystal structure thus giving vital information on intermolecular interactions between the molecules.[46] The Hirshfeld surface uses sophisticated interactive graphics (SIG) to encode information about all the intermolecular interactions and it is quite time consuming to compute these surfaces. The 2-D fingerprint plot has been developed to include all intermolecular interactions without using SIG software.[45] The 2-D fingerprint plot gives an elaborate visual account of the type of intermolecular interactions experienced in the crystal structure i.e. hydrogen bonding, close and distant van der Waals contacts, C-H$\cdots\pi$ interactions and $\pi\cdots\pi$ interactions on 2-D axes. The 2-D fingerprint plot is extensively used in Chapter 4 of this thesis and a more detailed account on recognising specific intermolecular interaction will be given at this point.

1.4 RING-STACKING AND RING-LADDERING

The concept of ring-stacking and ring-laddering was introduced by Snaith and co-workers [47] from their study of alkali metal complexes in structural inorganic chemistry. They looked at the association of discrete cation and anion pairs which formed polymeric ladders (ring-laddering) and extended stacks (ring-stacking). Bond[48] has extended this concept to organic ammonium halide analogues using the CSD[12]. This association of the cation-anion pairs to form ring-stacking and ring-laddering is mainly driven by electrostatic forces to maximize the Coulombic energy within the crystal lattice. This study focused on the dimeric ring of association cation-anion pairs forming 3-D ring-stacks and 2-D ring-ladders in organic ammonium carboxylate salts (Figure 1.6). Using the CSD, together with a systematic experimental study, the ring-stacking and laddering concept has been extended to the organic ammonium carboxylate salts. Ring-stacking and laddering is discussed in greater detail in Chapter 3 of this thesis.

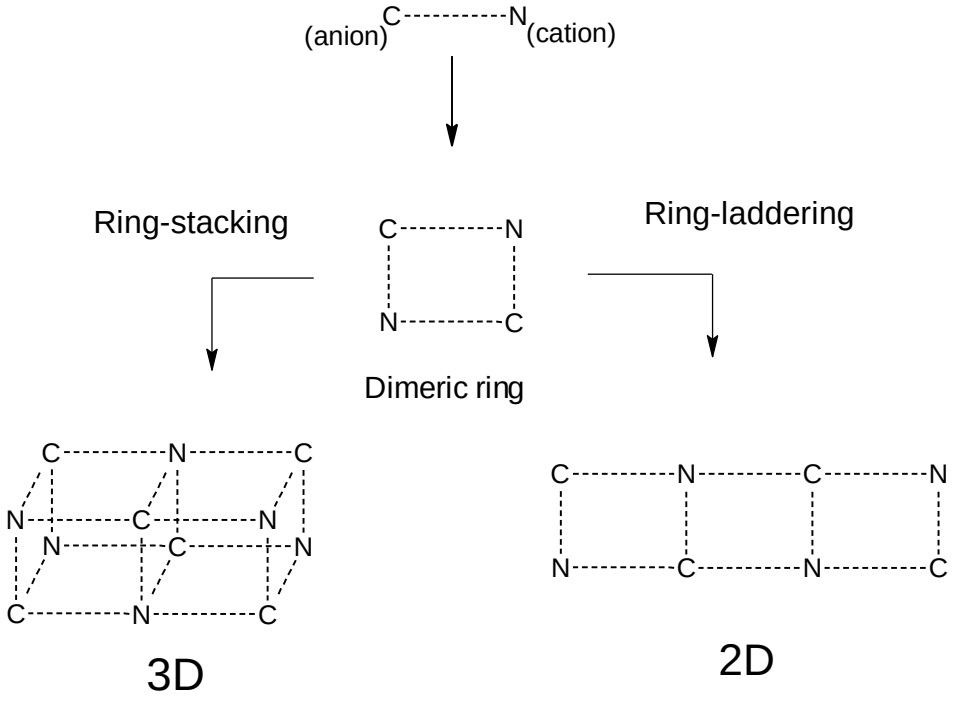

Figure 1.6 Schematic of ring-stacking and ring-laddering in ammonium carboxylate salts.

1.5 OBJECTIVES OF THIS STUDY

Salts are used in the pharmaceutical industry to modify properties of compounds such as the solubility, toxicity, and reducing the hydroscopicity of products.[49,50] The secondary, primary and ammonium carboxylate salts have been studied separately and extensively by various research groups[2,51], with their main focus on the hydrogen bonding patterns. Hydrogen bonding in ammonium carboxylate salts might be the main "recognition synthon" due to its bonding directionality, but the subtleties of various other intermolecular interactions play as important a role in the mode of packing in the crystal structure.

A Cambridge Structural Database (CSD) survey was conducted to look for the specific intermolecular interaction motifs formed in ammonium, primary and secondary carboxylate salts. The occurrence of ring-stacking and ring-laddering in ammonium carboxylate salts was investigated with the results obtained from the survey. The statistics of this study are discussed in detail in Chapter 3, where trends in the formation of stacks and ladders and other structural motifs in these salts are described.

The results from a series of steric-specific experiments on secondary, primary and ammonium carboxylate salts are discussed in Chapter 4. The single crystal structures obtained from these experiments are compared with the CSD data to confirm the stacking and laddering phenomena and structural motifs founds in ammonium carboxylate salts. Crystal Explorer is used to generate 2-D fingerprint plots which help to identify the intermolecular interactions present in secondary, primary and ammonium carboxylate salts, and assisted in investigating the role these interactions play in the mode of packing.

An initial hypothesis is made that the size of the molecule and conformation of the cation and anion play an important role in the formation of stacks, ladders and specific intermolecular interaction motifs. Thus studying the intermolecular interactions between the non-ionic functional groups of the ions can give great insight as to why these structures form stacks and ladders. The results from the study will firstly confirm if the concept of ring-stacking and ring-laddering is applicable to ammonium carboxylate salts. They will also help formulate rules as to

why these systems form nets, stacks, ladders and other structural motifs. This will ultimately help in the design of crystals.

REFERENCES:

1. G. R. Desiraju, *Angew. Chem., Int. Ed.*, 2007, **46**.

2. R. T. Darshak, P. Dastidar, *Cryst.Growth & Des.*, 2006, **6**, 1022.

3. P. Pepinsky, *Phys. Rev.* 1955, **100**, 971.

4. G. M. J. Schmidt, *Pure Appl. Chem*., 1971, **27**, 647.

5. L. Addadi and M. Geva, *CrystEngComm.,* 2003, **5**, 410.

6. A. Nangia, *Curr. Opin. Solid State Mater*. Sci. 2001, **5**, 115.

7. P. Rabl, A. J. Daley and P. O. Fredicher, *Phys. Rev. Lett*., 1998, **81**, 110403- 1 .

8. O. Almarsson and M. J. Zaworotko, *Chem. Commun*., 2004, **17**, 1889.

9. I. Cosic, *IEEE transactions on bio-medical engineering*, 1994, **41**, 1101.

10. V. R. Vangala, B. R. Bhogala, A. Dey, G. R. Desiraju, C. K. Broder, P. S. Smith, R. Mondal, J. A. K. Howard and C. C. Wilson, *J. Am. Chem. Soc.,* 2003, **125**, 14495.

11. G. R. Desiraju, *Angew. Chem., Int. Ed., Eng*, 1995, **34**, 2311.

12. F. Allen, *Acta Crystallogr. Sect. B.,* 2002, **58**, 380.

13. J. Chisholm, E. Pidcock, J. van de Streek, L. Infantes, S. Motherwell and F.H. Allen, *CrystEngComm*, 2006, **8**, 11.

14. T. Steiner, *Angew. Chem., Int. Ed.*, 2002, **41**, 48.

15. S.V. Lindeman, D. Kosynkin, and J.K. Kochi, *J. Am. Chem. Soc*., 1998, **120**, 13268.

16. S. Nagahama, K. Inoue, K. Sada, M. Miyata and A. Matsumoto, *Cryst. Growth & Des.*, 2003, **2**, 247.

17. A. Ballabh, T. K. Adalder and P. Dastidar, *Cryst.Growth Des*, 2008, **8**, 4144.

18. G. R. Desiraju, *The Crystal as a Superamolecular Entity Vol. 2*, Wiley, New York, 1996.

19. A. D. Hamilton, *Angew. Chem. Int. Ed. Engl.*, 1993, **115,** 5314.

20. G. M. Whitesides, *Chem. Soc. Rev.*, 1994. **94**, 2388.

21. J. M. Lehn, *Angew. Chem., Int. Ed. Engl.*, 1990, **29,** 1304

22. A. Gavezzoti, *Acc. Chem. Res.*, 1994, **27**, 309.

23. F.A. Cotton and R. L. Luck, *Inorg. Chem.*,1989, **28**, 3210.

24. C. B. Aakeröy and K. R. Seddon, *Chem. Soc. Rev.*, 1993, **22**, 397.

25. W. M. Latimer and W. H. Rodebush, *J.Am.Chem.Soc.*, 1920, **42**, 1419.

26. L. Pauling, '*The Nature of the Chemical Bond and the Structure of Molecules and Crystals - An Introduction to Modern Structural Chemistry'*, 2nd Edn, Oxford University Press, London, 1940.

27. G. C. Pimentel and A. L. McClellan, *'The Hydrogen Bond'*, Freeman, San Francisco, 1960.

28. G. A. Jeffrey, *An Introduction to Hydrogen Bonding*, Oxford University Press, Oxford, 1997.

29. M. C. Etter, *Acc. Chem. Res.*, 1990, **23**, 120.

30. M. C. Etter, J. C. Macdonald and J. Bernstein, *Acta Crystallogr., Sect. B*, 1990, **46**, 256.

31. G. R. Desiraju, *Acc. Chem. Res*., 1991, **24**, 290; 1996, **29**, 441.

32. T. Steiner, *Chem. Commun*., 1997, 727.

33. P. W. Kuchel and G. B. Racston, *Biochemistry Second Edition*, 1998, 85

34. F. A. Cotton, L. M. Daniels, G. T. Jordan IV and C. A. Murillo, *Chem. Commun.*, 1997, 1673.

35. T. Steiner and G. R. Desiraju, *Chem. Commun.*, 1998, 891.

36. L. R. Hanton, C. A. Hunter and D. H. Purvis, *J. Chem. Soc., Chem. Commun*., 1992, 1134.

37. J. F. Malone, C. M. Murray, M. H. Charlton, R. Dochetry and A. J. Lavery, *J. Chem. Soc., Faraday Trans*., 1997, **93,** 3429.

38. J. W. Steed and J. L. Atwood, *Supramolecular Chemistry*, John Wiley & Sons Ltd, 2000.

39. B. Sarma, L. S. Reddy and A. Nangia, *Cryst.Growth Des.*, 2008, **8**, 4546.

40. S. Kiviniemi, PhD Thesis, *University of Oulu*, 2001.

41. P. Terech and R. G. Weiss, *Chem. Re*v.1997, **97**, 3133; L. A. Estroff and A. D. Hamilton, *Chem. Re*v. 2004, **104**, 1201; O. Grownwald and S. Shinkai, *Curr. Opin. Colloid Interface Sci.*, 2002, **7**, 148; J. H. van Esch and B. L. Ferringa, *Angew. Chem., Int. Ed.* 2000, **39**, 2263; N. M. Sangeetha and U. Maitra, *Chem. Soc. Rev*., 2005, **34**, 821.

42. A. Ballabh, D. R. Trivedi and P. Distidar, *Org. Lett.*, 2006, **8**, 1271.

43. S. K. Wolff, D. J. Grimwood, J. J. McKinnon, D. Jayatilaka and M. A. Spackman, *Crystal Explorer 2.1 (381)*, University of Western Australia, Perth, 2007.

44. F. L. Hirshfeld, *Theor. Chim. Acta*, 1977, **44**, 129.

45. M. A. Spackman and J. J. McKinnon, *CrystEngComm*, 2002, 378.

46. J. J. McKinnon, A. S. Mitchell and M. A. Spackman, *Chem. Eur. J.*, 1998, **4**, 2136.

47. D. Barr, W. Clegg, R. E. Mulvey, R. Snaith and K. Wade, *J. Chem. Soc. Chem. Commun.*, 1986, 295-297; D. R. Armstrong, D. Barr, W. Clegg, R.E. Mulvey, D. Reed, R. Snaith and K. Wade, *J. Chem. Soc. Chem. Commun*., 1986, 869; D. Barr, W. Clegg, R. E. Mulvey, R. Snaith, and K. Wade, *Chem. Commun.*, 1986, 295; K. Gregory, P. von R. Schleyer and R. Snaith, *Adv. Inorg. Chem*., 1991, 47.

48. A. D. Bond, *Chem. Eur. J.*, 2004, **10**, 1885 - 1898; A. D. Bond, *Cryst. Growth Des*., 2005, **5**, 755.

49. Handbook of *Pharmaceutical Salts: Properties, Selection and Use, ed*. P. H. Stahl and C. G. Wermuth, Wiley-VCH/VHCA Weinheim/Zürich, 2002.

50. P. J. Gould. *Int. J. Pharm*., 1986, **33**, 201.

51. A. Lemmerer, S. A. Bourne and M. A. Fernandes, *CrystEngComm*, 2008, **10**, 1750; A. Lemmerer, S. A. Bourne and M. A. Fernandes, *CrystEngComm*, 2008, **10**, 1605.

Chapter 2

Experimental and Analytical Techniques

This study involved an extensive analysis of the Cambridge Structural Database[1], as well as an experimental study of ammonium carboxylate salts. A number of analytical techniques were used, as well as several different software and graphics packages. This chapter gives details of the techniques used in this study.

2.1 ANALYTICAL TECHNIQUES

Single-Crystal Diffraction Analysis (SCD)

SCD is undoubtedly one of the most powerful analytical techniques used to characterise structures at a molecular level. It makes use of X-ray radiation to map electron densities to determine the atomic topology of the molecules in the solid-state. This technique yields information on the structure of the molecule in 3-D, from which crucial information on chemical formula, bond lengths, bond angles, molecular motifs, intramolecular and intermolecular interactions can be elucidated.

Before the crystals in this study were analysed they had to be carefully selected while suspended in paratone oil. The selection was primarily based on the crystal morphology, and the crystals were selected based upon observations of the crystal under polarised light. The crystal selected for analysis was mounted on a MiTeGen mount (under some circumstances glass-fibres were used). This was then placed onto the goniometer head of the single-crystal diffractometer on which the data collection was done. X-ray intensity data were collected on a Bruker-Nonius SMART Apex diffractometer equipped with a fine-focus sealed tube and a 0.5 mm Monocap collimator (monochromated Mo-Kα radiation, λ = 0.71073 Å). Data were captured with a CCD (Charge-Coupled Device) area-detector with the generator powered at 40 kV and 30 mA. The diffractometer came equipped with a 700 Series Cryostream Plus produced by Oxford Cryogenic Cryostat. This produced a constant stream nitrogen for low temperature data collection at 100K.
Data reduction, absorption corrections and unit cell determination were carried out using the diffractometer software (APEXII, Bruker). Structure solution and refinement were carried out using the X-Seed software (section 2.2). All hydrogen atoms involved in proton transfer reactions were located on the difference map. Details of structure sdolution and refinement can be found on the Appendix CD.

X-ray Powder Diffraction (XPRD)

Powder diffraction is common practice for supramolecular chemists and various other disciplines to characterise solid materials. It is used to monitor the phase and structural changes of materials, it also verifies the composition of the bulk material from which a suitable crystal was selected for single-crystal diffraction.

The powder diffractometer used for the purpose of this study was a Bruker D8 ADVANCE model with Bragg-Brentano geometry using Cu Kα radiation (λ = 1.5406Å) and fitted with a Dynamic scintillation (point type) detector. Data were collected with the instrument set at 40 kV and 30 mA, and samples were spun at 15 rotations per minute to reduce preferred orientation. Simulated powder patterns were also generated from crystal structures obtained via single crystal diffraction using Mercury[2] and X-seed[3,4]. These could then be compared to measured powder patterns. All powder patterns are included in the CD Appendix.

Thermal Gravimetric Analysis (TGA)

TGA is an analytical technique often used in supramolecular chemistry. It measures the weight loss or gain of materials as a function of temperature. This loss or gain of weight can be in the form of drying, structural water release, structural decomposition, gas evolution and re-hydration.

TGA was carried out using a TA Instrument Q500 analyser under N_2 with a flow rate of 50ml/min which was used to purge the furnace. The resulting thermogram was analysed using the TA instrument Universal analysis program.

2.2 SOFTWARE INTERFACES

Cambridge Structure Database (CSD)

The CSD is currently the world repository of small molecule crystal structures; it records the bibliographic, chemical and crystallographic information for organic molecules and metal-organic compounds. Only the 3-dimensional atomic coordinates from structures that have been determined with analytical techniques such as X-ray Diffraction and Neutron Diffraction are used in the database. This is a very important database for crystallographers.

The database also provides the following software interfaces to make the navigation of the database easier:

- Search and information with ConQuest[5]
- Structural visualisation with Mercury
- Numerical analysis with Vista[6]
- Database creation with PreQuest[7]

A more elaborate explanation of the function of the CSD during my study is given in Chapter 3 of this thesis.

Crystal Explorer

Crystal Explorer is a software interface that uses calculations made from Hirshfeld surfaces.[8] These surfaces are used to encode all the intermolecular interactions in molecular crystals.[9] This is a novel tool to explore packing modes in various molecular crystals.[3] These Hirshfeld surfaces use sophisticated interactive graphics (SIG) in order to extract the information efficiently.[9] To overcome the slowness of this SIG a two-dimensional (2-D) mapping has been devised that quantitatively summarises the nature and type of intermolecular interactions within the molecular crystal[4]. These 2-D mapping (fingerprint plots) will be demonstrated and discussed in Chapter 4.

X-seed

X-Seed is a software interface used to analyse data obtained from SCD experiments, to solve and refine the single-crystal data. This software is an interface for the Shel-X[10] suite of programs, which use the .ins and .hkl files generated by X-prep in the APEX II software to elucidate the crystal structure obtained from the experiment. X-seed also contains some other software that plays an important role in the final structure presented including ,

POV-RAY[11] was used to generate figures

LAZY-PULVERIX[12] is used to generate powder diffraction patterns form the single crystal data

The following programs are integrated into the X-seed software package to simplify and modify the structural refinement process.

SADABS[13] (Siemens Area Detector Absorption Correction) used .raw files generated by the APEX II

XPREP[14] is used to look at possible space groups that was incorrectly assigned by the APEX II software

2.3 EXPERIMENTAL METHODOLOGY

2.3.1 STARTING MATERIALS USED

All the compounds and solvents used in the experiments were supplied by Sigma-Aldrich. These were used without any future purification with the exception of aniline; it had to be distilled before use. A summary of physical properties of all compounds used is listed in Table 2.1

Table 2.1 Physical properties of starting materials used in formation of ammonium carboxylate salts.

Compounds	Molecular Formula	Molecular mass (M_r) /g mol^{-1}	Physical Appearance	Densities /g cm^{-3}
Diethyl amine	$C_4H_{11}N$	73.17	Colourless liquid	0.707
Dibutyl amine	$C_8H_{19}N$	129.24	Colourless liquid	0.767
Dihexyl amine	$C_{12}H_{27}N$	185.35	Colourless liquid	0.795
Dioctyl amine	$C_{16}H_{35}N$	241.35	Colourless liquid	0.799
Diphenyl amine	$C_{12}H_{11}N$	169.22		
Dicylohexyl amine	$C_{12}H_{23}N$	181.32	Colourless liquid	0.91
Propyl amine	C_3H_9N	59.11	Colourless liquid	0.72
Butyl amine	$C_4H_{11}N$	74.11	Colourless liquid	0.74
Cyclohexyl amine	$C_6H_{13}N$	99.17	Colourless liquid	0.86
Aniline	C_6H_7N	93.12	Orange liquid	1.02
1-phenylmethanamine	C_7H_9N	107.15	Colourless liquid	0.98
2-phenylethanamine	$C_8H_{11}N$	121.18	Colourless liquid	0.96
Formic acid	CH_2O_2	46.03	Colourless liquid	1.22
Acetic acid	$C_2H_4O_2$	60.05	Colourless liquid	1.05
Propionic acid	$C_3H_6O_2$	74.08	Colourless liquid	0.99
Benzoic acid	$C_7H_6O_2$	122.12	White powder	
Cyclohexane carboxylic acid	$C_8H_{12}O_2$	128.17	Colourless solid/liquid	1.03
Phenylacetic acid	$C_8H_8O_2$	136.15	White powder	
Diphenylacetic acid	$C_{14}H_{12}O_2$	228.37	White powder	

Densities were obtained from Sigma-Aldrich catalogue 2008-2009

2.3.2 EXPERIMENTAL TECHNIQUES

Crystal Growth

Various crystal growing methods were employed to obtain crystal suitable for single-crystal analysis. The standard slow solvent evaporation method, liquid and vapour diffusion and seeding were used to grow crystals.

The crystal growth times ranged from two minutes to three weeks. Crystals were grown at various different temperatures; ambient room temperature at 25°C, in the fridge at roughly at 0-4°C and in the deep freezer at -8°C. Some of the solvents were heated to dissolve the solid starting materials.

Solvent-free grinding experiments

The conventional way of growing crystals suitable for single crystal analysis is by slow evaporation of solvent and vapour diffusion[15] just to name a few of the methods. These methods still use solvents which have harmful effects on the environment.[16] With the advancements made in green chemistry[16] solvent free solid-state grinding plays an important role in crystal engineering. Grinding experiments are a very quick and effective way of checking for the formation of new solid materials and have the potential of being used to grow suitable crystals for X-ray diffraction studies. Since our study focused on the formation of ammonium carboxylate salts, grinding offered an easy method to look for potential formation of solids for X-ray diffraction studies. It is not always possible to obtain single crystals suitable for SCD analysis, but the powder can be used in PXRD analysis and from the resulting in a powder pattern a Rietveld refinement[17] can be performed to obtain possible 3-D structures.

2.3.3 SALT FORMATION EXPERIMENTS

The grids in Table 2.3 and Table 2.4 were used to set up acid:base reactions in various ratios to study the formation of ammonium carboxylate salts. The tables display all the ratios used in experiments to obtain single-crystals for SCD analysis and other standard crystallographic solid-state analysis. An experiment for each ratio was repeated for each solvent listed in Table 2.2.

The ratios from the experimental tables are all highlighted in two different colours: red ratios formed a solid (not all the solid were suitable for single crystal analysis), ratios in blue gave oils which were not suitable for any solid state characterisation techniques.

Table 2.2 Solvents used in experiments

Solvent	Symbols
Acetone	a
Acetonitrile	b
Dichloromethane	c
Diethyl ether	d
Ethanol	e
Ethyl acetate	f
Methanol	g
Water	h

AMMONIUM CARBOXYLATE SALTS (Table 2.3)

The series of experiments with ammonium hydroxide series in combination with the acids gave only four crystalline powders, whilst the other three solutions in the vials completely evaporated. These four solids, *ammonium benzoate*, *ammonium cyclohexanecarboxylate*, *ammonium phenylacetate* and *ammonium diphenylacetate* were analysed with PXRD. None of the four solids formed suitable crystals for single-crystal diffraction (SCD) analysis, even after recrystallisation. The vapour diffusion crystallisation method was then used to obtain crystals. The four solids were dissolved in methanol (MeOH) and dichloromethane was diffused into the solutions. Only the ammonium benzoate formed crystals that were suitable for single crystal analysis. Experimental details are given in Section 2.3.

Table 2.3 Summary of acid:base ratios used in experiments involving primary amines

RED = SOLID BLUE = OIL	Formic 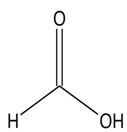	Acetic 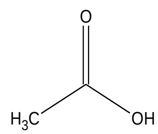	Propionic 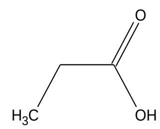	Benzoic 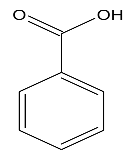	CyclohexaneC 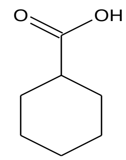	Phenylacetic 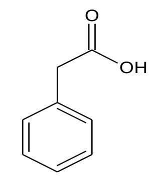	Diphenylacetic 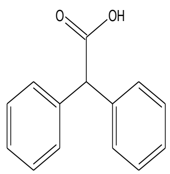
Ammonium Hydroxide H_4N^+—OH	1:1 1:2 1:3	1:1 1:2 1:3	1:1 1:2 1:3	1:1 1:2 1:3	1:1 1:2 1:3	1:1 1:2 1:3	1:1 1:2 1:3
Propyl 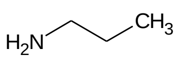	1:1 1:2 1:3 1:4 1:5 2:1 2:3 2:4 2:5 3:1 3:2 3:4 3:5 4:1 4:3 4:5 5:1 5:2 5:3 5:4	1:1 1:2 1:3 1:4 1:5 2:1 2:3 2:4 2:5 3:1 3:2 3:4 3:5 4:1 4:3 4:5 5:1 5:2 5:3 5:4	1:1 1:2 1:3 1:4 1:5 2:1 2:3 2:4 2:5 3:1 3:2 3:4 3:5 4:1 4:3 4:5 5:1 5:2 5:3 5:4	1:1 1:2 1:3 1:4 1:5 2:1 2:3 2:4 2:5 3:1 3:2 3:4 3:5 4:1 4:3 4:5 5:1 5:2 5:3 5:4	1:1 1:2 1:3 1:4 1:5 2:1 2:3 2:4 2:5 3:1 3:2 3:4 3:5 4:1 4:3 4:5 5:1 5:2 5:3 5:4	1:1 1:2 1:3 1:4 1:5 2:1 2:3 2:4 2:5 3:1 3:2 3:4 3:5 4:1 4:3 4:5 5:1 5:2 5:3 5:4	1:1
Butyl 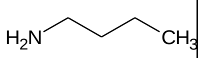	1:1 1:2 1:3 1:4 1:5 2:1 2:3 2:4 2:5 3:1 3:2 3:4 3:5 4:1 4:3 4:5 5:1 5:2 5:3 5:4	1:1 1:2 1:3 1:4 1:5 2:1 2:3 2:4 2:5 3:1 3:2 3:4 3:5 4:1 4:3 4:5 5:1 5:2 5:3 5:4	1:1 1:2 1:3 1:4 1:5 2:1 2:3 2:4 2:5 3:1 3:2 3:4 3:5 4:1 4:3 4:5 5:1 5:2 5:3 5:4	1:1 1:2 1:3 1:4 1:5 2:1 2:3 2:4 2:5 3:1 3:2 3:4 3:5 4:1 4:3 4:5 5:1 5:2 5:3 5:4	1:1 1:2 1:3 1:4 1:5 2:1 2:3 2:4 2:5 3:1 3:2 3:4 3:5 4:1 4:3 4:5 5:1 5:2 5:3 5:4	1:1 1:2 1:3 1:4 1:5 2:1 2:3 2:4 2:5 3:1 3:2 3:4 3:5 4:1 4:3 4:5 5:1 5:2 5:3 5:4	1:1 1:2 1:3 1:4 1:5 2:1 2:3 2:4 2:5 3:1 3:2 3:4 3:5 4:1 4:3 4:5 5:1 5:2 5:3 5:4
Cyclohexyl 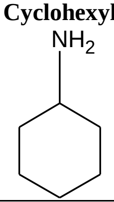	1:1 1:2 1:3 1:4 1:5 2:1 2:3 2:4 2:5 3:1 3:2 3:4 3:5 4:1 4:3 4:5 5:1 5:2 5:3 5:4	1:1 1:2 1:3 1:4 1:5 2:1 2:3 2:4 2:5 3:1 3:2 3:4 3:5 4:1 4:3 4:5 5:1 5:2 5:3 5:4	1:1 1:2 1:3 1:4 1:5 2:1 2:3 2:4 2:5 3:1 3:2 3:4 3:5 4:1 4:3 4:5 5:1 5:2 5:3 5:4	1:1	1:1 1:2	1:1 1:2 1:3	1:1 1:2 1:3 1:4

Aniline 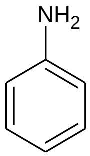	1:1 1:2 1:3 1:4 1:5 2:1 2:3 2:4 2:5 3:1 3:2 3:4 3:5 4:1 4:3 4:5 5:1 5:2 5:3 5:4	1:1 1:2 1:3 1:4 1:5 2:1 2:3 2:4 2:5 3:1 3:2 3:4 3:5 4:1 4:3 4:5 5:1 5:2 5:3 5:4	1:1 1:2 1:3 1:4 1:5 2:1 2:3 2:4 2:5 3:1 3:2 3:4 3:5 4:1 4:3 4:5 5:1 5:2 5:3 5:4	1:1 1:2 1:3 1:4 1:5 2:1 2:3 2:4 2:5 3:1 3:2 3:4 3:5 4:1 4:3 4:5 5:1 5:2 5:3 5:4	1:1 1:2 1:3 1:4 1:5 2:1 2:3 2:4 2:5 3:1 3:2 3:4 3:5 4:1 4:3 4:5 5:1 5:2 5:3 5:4	1:1 1:2 1:3 1:4 1:5 2:1 2:3 2:4 2:5 3:1 3:2 3:4 3:5 4:1 4:3 4:5 5:1 5:2 5:3 5:4	1:1 1:2 1:3 1:4 1:5 2:1 2:3 2:4 2:5 3:1 3:2 3:4 3:5 4:1 4:3 4:5 5:1 5:2 5:3 5:4
Benzyl 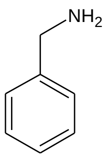	1:1 1:2 1:3 1:4 1:5 2:1 2:3 2:4 2:5 3:1 3:2 3:4 3:5 4:1 4:3 4:5 5:1 5:2 5:3 5:4	1:1 1:2 1:3 1:4 1:5 2:1 2:3 2:4 2:5 3:1 3:2 3:4 3:5 4:1 4:3 4:5 5:1 5:2 5:3 5:4	1:1 1:2 1:3 1:4 1:5 2:1 2:3 2:4 2:5 3:1 3:2 3:4 3:5 4:1 4:3 4:5 5:1 5:2 5:3 5:4	1:1 1:2 1:3 1:4 1:5 2:1 2:3 2:4 2:5 3:1 3:2 3:4 3:5 4:1 4:3 4:5 5:1 5:2 5:3 5:4	1:1 1:2 1:3 1:4 1:5 2:1 2:3 2:4 2:5 3:1 3:2 3:4 3:5 4:1 4:3 4:5 5:1 5:2 5:3 5:4	1:1 1:2 1:3 1:4 1:5 2:1 2:3 2:4 2:5 3:1 3:2 3:4 3:5 4:1 4:3 4:5 5:1 5:2 5:3 5:4	1:1 1:2 1:3 1:4 1:5 2:1 2:3 2:4 2:5 3:1 3:2 3:4 3:5 4:1 4:3 4:5 5:1 5:2 5:3 5:4
1-phenylethyl 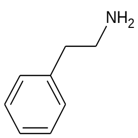	1:1 1:2 1:3 1:4 1:5 2:1 2:3 2:4 2:5 3:1 3:2 3:4 3:5 4:1 4:3 4:5 5:1 5:2 5:3 5:4	1:1 1:2 1:3 1:4 1:5 2:1 2:3 2:4 2:5 3:1 3:2 3:4 3:5 4:1 4:3 4:5 5:1 5:2 5:3 5:4	1:1 1:2 1:3 1:4 1:5 2:1 2:3 2:4 2:5 3:1 3:2 3:4 3:5 4:1 4:3 4:5 5:1 5:2 5:3 5:4	1:1 1:2 1:3 1:4 1:5 2:1 2:3 2:4 2:5 3:1 3:2 3:4 3:5 4:1 4:3 4:5 5:1 5:2 5:3 5:4	1:1 1:2 1:3 1:4 1:5 2:1 2:3 2:4 2:5 3:1 3:2 3:4 3:5 4:1 4:3 4:5 5:1 5:2 5:3 5:4	1:1 1:2 1:3 1:4 1:5 2:1 2:3 2:4 2:5 3:1 3:2 3:4 3:5 4:1 4:3 4:5 5:1 5:2 5:3 5:4	1:1 1:2 1:3 1:4 1:5 2:1 2:3 2:4 2:5 3:1 3:2 3:4 3:5 4:1 4:3 4:5 5:1 5:2 5:3 5:4

Table 2.4 Summary of acid:base ratios used in experiments involving secondary amines

RED = **SOLID** **BLUE** = **OIL**	**Formic** 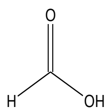	**Acetic** 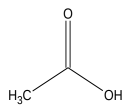	**Propionic** 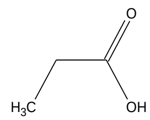	**Benzoic** 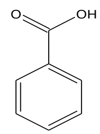	**CyclohexaneC** 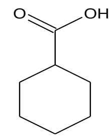	**Phenylacetic** 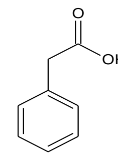	**Diphenylacetic** 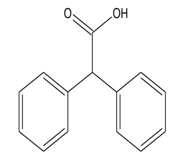
Diethyl 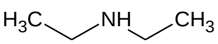	1:1 1:2 1:3 1:4 1:5 2:1 2:3 2:4 2:5 3:1 3:2 3:4 3:5 4:1 4:3 4:5 5:1 5:2 5:3 5:4	1:1 1:2 1:3 1:4 1:5 2:1 2:3 2:4 2:5 3:1 3:2 3:4 3:5 4:1 4:3 4:5 5:1 5:2 5:3 5:4	1:1 1:2 1:3 1:4 1:5 2:1 2:3 2:4 2:5 3:1 3:2 3:4 3:5 4:1 4:3 4:5 5:1 5:2 5:3 5:4	1:1 1:2 1:3 1:4 1:5 2:1 2:3 2:4 2:5 3:1 3:2 3:4 3:5 4:1 4:3 4:5 5:1 5:2 5:3 5:4	1:1 1:2 1:3 1:4 1:5 2:1 2:3 2:4 2:5 3:1 3:2 3:4 3:5 4:1 4:3 4:5 5:1 5:2 5:3 5:4	1:1 1:2 1:3 1:4 1:5 2:1 2:3 2:4 2:5 3:1 3:2 3:4 3:5 4:1 4:3 4:5 5:1 5:2 5:3 5:4	1:1 1:2 1:3 1:4 1:5 2:1
Dibutyl 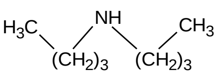	1:1 1:2 1:3 1:4 1:5 2:1 2:3 2:4 2:5 3:1 3:2 3:4 3:5 4:1 4:3 4:5 5:1 5:2 5:3 5:4	1:1 1:2 1:3 1:4 1:5 2:1 2:3 2:4 2:5 3:1 3:2 3:4 3:5 4:1 4:3 4:5 5:1 5:2 5:3 5:4	1:1 1:2 1:3 1:4 1:5 2:1 2:3 2:4 2:5 3:1 3:2 3:4 3:5 4:1 4:3 4:5 5:1 5:2 5:3 5:4	1:1 1:2 1:3 1:4 1:5 2:1 2:3 2:4 2:5 3:1 3:2 3:4 3:5 4:1 4:3 4:5 5:1 5:2 5:3 5:4	1:1 1:2 1:3 1:4 1:5 2:1 2:3 2:4 2:5 3:1 3:2 3:4 3:5 4:1 4:3 4:5 5:1 5:2 5:3 5:4	1:1 1:2 1:3 1:4 1:5 2:1 2:3 2:4 2:5 3:1 3:2 3:4 3:5 4:1 4:3 4:5 5:1 5:2 5:3 5:4	1:1 1:2 1:3 1:4 1:5 2:1
Dihexyl 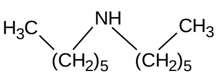	1:1 1:2 1:3 1:4 1:5 2:1 2:3 2:4 2:5 3:1 3:2 3:4 3:5 4:1 4:3 4:5 5:1 5:2 5:3 5:4	1:1 1:2 1:3 1:4 1:5 2:1 2:3 2:4 2:5 3:1 3:2 3:4 3:5 4:1 4:3 4:5 5:1 5:2 5:3 5:4	1:1 1:2 1:3 1:4 1:5 2:1 2:3 2:4 2:5 3:1 3:2 3:4 3:5 4:1 4:3 4:5 5:1 5:2 5:3 5:4	1:1 1:2 1:3 1:4 1:5 2:1 2:3 2:4 2:5 3:1 3:2 3:4 3:5 4:1 4:3 4:5 5:1 5:2 5:3 5:4	1:1 1:2 1:3 1:4 1:5 2:1 2:3 2:4 2:5 3:1 3:2 3:4 3:5 4:1 4:3 4:5 5:1 5:2 5:3 5:4	1:1 1:2 1:3 1:4 1:5 2:1	1:1 1:2 1:3 1:4 1:5 2:1 2:3 2:4 2:5 3:1 3:2 3:4 3:5 4:1 4:3 4:5 5:1 5:2 5:3 5:4
Dioctyl 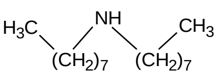	1:1 1:2 1:3 1:4 1:5 2:1 2:3 2:4 2:5 3:1 3:2 3:4 3:5 4:1 4:3 4:5 5:1 5:2 5:3 5:4	1:1 1:2 1:3 1:4 1:5 2:1 2:3 2:4 2:5 3:1 3:2 3:4 3:5 4:1 4:3 4:5 5:1 5:2 5:3 5:4	1:1 1:2 1:3 1:4 1:5 2:1 2:3 2:4 2:5 3:1 3:2 3:4 3:5 4:1 4:3 4:5 5:1 5:2 5:3 5:4	1:1 1:2 1:3 1:4 1:5 2:1 2:3 2:4 2:5 3:1 3:2 3:4 3:5 4:1 4:3 4:5 5:1 5:2 5:3 5:4	1:1 1:2 1:3 1:4 1:5 2:1 2:3 2:4 2:5 3:1 3:2 3:4 3:5 4:1 4:3 4:5 5:1 5:2 5:3 5:4	1:1 1:2 1:3 1:4 1:5 2:1 2:3 2:4 2:5 3:1 3:2 3:4 3:5 4:1 4:3 4:5 5:1 5:2 5:3 5:4	1:1 1:2 1:3 1:4 1:5 2:1 2:3 2:4 2:5 3:1 3:2 3:4 3:5 4:1 4:3 4:5 5:1 5:2 5:3 5:4
Dicyclohexyl 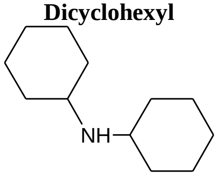	1:1 1:2 1:3 1:4 1:5 2:1	1:1 1:2 1:3 1:4 1:5 2:1 2:3 2:4 2:5 3:1 3:2 3:4 3:5 4:1 4:3 4:5 5:1 5:2 5:3 5:4	1:1	1:1	1:1 1:2 1:3 1:4 1:5 2:1 2:3	1:1 1:2 1:3 1:4 1:5 2:1	1:1 1:2 1:3 1:4 1:5 2:1

PRIMARY AMMONIUM CARBOXYLATE SALTS (Table 2.3)

The grid (Table 2.3) was used to set up acid:base reactions in various ratios in order to study the formation of primary ammonium carboxylate salts. The table displays all the ratios used in the experimental attempts to obtain single crystals for SCD analysis. Experiments for each ratio in Table 2.2 were repeated with each of the solvents in Table 2.2.

Propylamine in combination with the acids always formed yellow oils, except for the *propylammonium diphenylacetate* which formed orange single crystals from the 1:1 ratio of acid:base using diffusion crystallisation methods (MeOH:dichloromethane). The oils were all put in the fridge at 4 °C and in the deep freezer at -8 °C but none of the solutions yielded any crystals.

Butylamine in combination with the acids formed yellow oils; none of the experimental ratios yielded a solid. These oils were then put in the fridge at 4°C and in the deep freezer at -8°C to check for any crystal growth, no crystals were obtained over three weeks. Crystals from other primary ammonium carboxylate salts were used to seed the solutions, but after several weeks no solids were obtained. An attempt was also made to grow crystals from vapour diffusion crytstallisation techniques, but these experiments gave oils at the bottoms of the vials. Solvent-free grinding in various acid:base ratios also did not yield any solids.

Cyclohexylamine in combination with the acids formed seven viscous colourless oils. Crystals of *cyclohexylammonium benzoate* suitable for SCD analysis were obtained from a 1:1 acid:base reaction. The *cyclohexylammonium cylohexanecarboxylate*, *phenylacetate* and *diphenylacetate* crystals were not suitable for SCD even after several attempts AT at recrystallisation. These reactions were then done using solvent-free grinding experiments. Increasing amounts of cyclohexylamine was added to an approximately determined amount of each acid, with grinding (see Section 2.4 for details). Surprisingly, all seven of these reactions yielded white crystalline powders. These powders (1g) were then dissolved in 2 ml of MeOH and the solutions put in the fridge. After one day three of the

vials contained crystals. The *cyclohexylammonium formate* and *cyclohexylammonium propionate* crystals redissolved immediately on removal from the fridge. The *cyclohexylammonium acetate* formed colourless hexagonal single crystals that were used for SCD analysis.

Aniline in combination with all the acids formed viscous orange oils. The six oils were put in the fridge at 4 °C and remained oils, in the freezer at -8 °C all the solutions froze but melted after standing at room temperature. Solvent free grinding experiments (as described above) yielded some solids. Aniline in combination with *benzoic, cyclohexanecarboxylic, and phenylacetic acid* formed yellow solids on solvent free grinding. These solids were then recrystallised from MeOH and yielded crystals. Only the *anilinium phenylacetate* crystals were suitable for SCD analysis.

Benzylamine in combination with all the acids formed oils and no solid with any of the acid:base ratios shown Table 2.3. These reactions were then done using solvent-free grinding experiments (see above), and all seven combinations yielded a white crystalline powder. These powders (1g) were then dissolved in 2 ml of MeOH and put in the fridge at 4 °C. After one day three of the vials contained crystals that were suitable for SCD analysis. The three solids *benzylammonium formate*, *benzylammonium acetate* and *benzylammonium propionate* were stable when removed from the fridge, unlike any of the cyclohexylamine series. The remaining four vials did not yield any crystals. These were then put in the deep freezer at -8 °C, but the solutions froze and melted back into oil when left at room temperature for some time.

Combination of 1-phenylethylamine with all the acids formed oils in all the different acid:base ratios in the above table. These reactions were then done using solvent free grinding experiments, and four of these reactions yielded yellow crystalline powders: *1-phenylethylammonium benzoate*, *1-phenylethylammonium cylohexanecarboxylate*, *1-phenylethylammonium phenylacetate* and *1-phenylethylammonium diphenylacetate*. These powders were then recrystallised using 2 ml of MeOH in the fridge. After a week

one of the vials contained crystals suitable for SCD analysis (*1-phenylethylammonium diphenylacetate)*.

SECONDARY AMMONIUM CARBOXYLATE SALTS (Table 2.4)

Diethylamine in combination with the acids formed viscous yellow oils in all cases except for the *diethylammonium diphenylacetate,* which formed single crystals with all the solvents listed in Table 2.2 in ratios 1:1, 1:2 and 1:3. All the *diethylammonium diphenylacetate* crystals obtained from the different solvents and different acid:base ratios were checked using SCD analysis for similarities in the unit cells, and a powder pattern was collected for all of them. The results from the PXRD and SCD analysis were the same, indicating that the structures obtained were representative of the bulk material.

Dibutylamine in combination with all the acids formed colourless oils, except for the *dibutylammonium diphenylacetate* which gave single crystals with all solvents used. This salt exhibits polymorphism: one structure was determined from data collected at room temperature (299 K), the other from data collected at 100 K.

Dihexylamine in combination with all the acids formed viscous yellow oils with all solvents except acetonitrile. In acetonitrile the reactions formed thin needle-like crystals that were not suitable for SCD analysis, except in the case of *dihexylammonium phenylacetate*. This formed one suitable crystal within the viscous oil after a week, which appeared to have nucleated on foreign matter in the vial.

The dioctylamine had to be dissolved in the solvents as it solidified if kept in ambient conditions for too long. Dioctylamine in combination with the acids formed a fine white powdered precipitate with all the solvents used. The PXRD analysis done with all the dioctylamine series confirmed that the product was not any of the starting materials used, and the solids were recrystallised from MeOH. *Dioctylammonium formate* and *dioctylammonium benzoate* gave promising crystals, but none of the datasets collected from SCD analysis could be solved.

Diphenylamine was soluble in all of the solvents except water; upon dissolving the amine in water it formed an insoluble oil droplet. Diphenylamine in combination with all the acids formed very fine coloured powders which were not suitable for SCD analysis. A powder pattern was collected for all of the products formed. Upon recrystallising these powders from MeOH, *diphenylammonium benzoate*, *diphenylammonium phenylacetate* and the *diphenylammonium diphenylacetate* looked promising for SCD analysis. However the crystals were not single, they were very intergrown.

Dicyclohexylamine formed single crystals that were suitable for SCD analysis in four cases. The *dicyclohexylammonium formate*, *dicyclohexylammonium phenylacetate* and *dicyclohexylammonium diphenylacetate* were all crystallised out of methanol. The *dicylohexylammonium formate* was crystallised out of a MeOH and water mixture in a 1:1 ratio (v/v). Powder patterns were collected for all the solids obtained for this series.

2.4 EXPERIMENTAL DETAILS

The powder patterns obtained from the acid:base experiments can be found in the CD Appendix.

Ammonium carboxylate salts

Ammonium benzoate

Ammonium hydroxide (0.1007 g, 2.86 mmol) and benzoic acid (0.1197 g, 0.98 mmol) were separately dissolved in 1 ml of MeOH then added together. Dichloromethane was then allowed to diffuse into the solution containing the acid and the base. Immediately after the dichloromethane started to diffuse into the MeOH solution colourless crystals formed.

Primary ammonium carboxylate salts

Propylammonium diphenylacetate

Propylamine (0.0324 g, 0.54 mmol) and diphenylacetic acid (0.1026 g, 0.48mmol) were separately dissolved in hot MeOH, dichloromethane was then allowed to diffuse into the MeOH solution resulting in the formation of orange plate-like crystals.

Benzylammonium propionate hydrate

Benzylamine (2.012 g 18.7 mmol) were added to a motar and propionic acid (5.245 g, 70.8 mmol) were added and ground, resulting in white powder. About 0.750 g of the powder was dissolved in 2 ml of MeOH and the solution was then put in the fridge at 0°C resulting in colourless crystals.

Benzylammonium acetate

Benzyl amine (2.023 g, 18.8 mmol) were added to a motar and acetic acid (4.210 g, 70.10 mmol) was added and ground; this resulted in white powder. Thereafter about 1.000g of the powder was dissolved in 2 ml of warm MeOH. This was slowly evaporated in the fridge at 4°C and resulted in colourless crystals.

Anilinium phenylacetate

Aniline (2.021g, 21.70 mmol) were added to a motar and phenylacetetic acid (4.032 g, 33.01 mmol) were added and ground resulting in an orange powder. Thereafter about 5.123 g of the powder was dissolved in 6 ml of warm MeOH. This was slowly evaporated at room temperature and resulted in colourless crystals.

Cyclohexylammonium acetate

Cyclohexylamine (2.054 g, 16.02 mmol) were added to a motar and acetic acid (5.101 g, 84.94 mmol) were added and ground; this resulted in white powder. Thereafter about 0.750 g of the powder was dissolved in 2 ml of warm MeOH. This was slowly evaporated in the fridge at 4°C and resulted in a colourless hexagonal crystal.

Cyclohexylammonium benzoate

Cyclohexylamine (0.1003 g, 0.782 mmol) and benzoic acid (0.170 g, 1.39 mmol) were added to a mortar and ground, resulting in white powder. Thereafter about 0.750g of the powder was dissolved in 2 ml of warm MeOH. This was slowly evaporated at room temperature, and resulted in a colourless crystal.

Secondary ammonium carboxylate salts

Diethylammonium diphenylacetate

Diethylamine (0.0172 g, 0.23 mmol) and diphenylacetic acid (0.0512 g, 0.24 mmol) were separately dissolved in 2 ml of methanol (MeOH) and then added together. This was slowly evaporated for one week at room temperature and resulted in cube-shaped colourless crystals.

Dibutylammonium diphenylacetate

Dibutylamine (0.0175 g, 0.13 mmol) and diphenylacetic acid (0.0501 g, 0.23 mmol) were separately dissolved in dissolved in 2 ml of MeOH and then added together. This was slowly evaporated for one week at room temperature and resulted in plate-like colourless crystals. The single crystal data was collected at 100K.

Dihexylammonium phenylacetate

Dihexylamine (0.0068 g, 0.36 mmol) and phenylacetic acid (0.051 g, 0.374 mmol) were separately dissolved in 2 ml of acetonitrile (CH_3CN) then added together. This was slowly evaporated for one week at room temperature and resulted in colourless crystals.

Dicyclohexylammonium formate

Dicyclohexylamine (0.201 g, 1.10 mmol) and formic acid (0.0601 g, 1.31 mmol) were separately dissolved in 2 ml of (MeOH) added together. This was then slowly evaporated for one week at room temperature and resulted in needle-like colourless crystals.

Dicyclohexylammonium formate hydrate

Dicyclohexylamine (0.2097g, 1.15 mmol) and formic acid (0.058g, 1.26 mmol) were separately dissolved in 2 ml of a 1:1 ratio MeOH:H_2O then added together. This was then slowly evaporated for one week at room temperature and resulted in needle-like colourless crystals.

Dicyclohexylammonium cyclohexancarboxylate

Dicyclohexylamine (0.2883 g, 1.59 mmol) and cyclohexanecarboxylic acid (0.2097 g, 1.63 mmol) were separately dissolved in 2 ml of MeOH then added together. This was then slowly evaporated for three days at room temperature and resulted in colourless cubic crystals.

Dicyclohexylammonium phenylacetate

Dicyclohexylamine (0.0784 g, 0.43 mmol) and phenylacetic acid (0.0800 g, 0.58 mmol) were separately dissolved in 2 ml of MeOH then added together. This was slowly evaporated for three days at room temperature and resulted in plate-like colourless crystals.

Dicyclohexylammonium diphenylacetate

Dicyclohexylamine (0.179 g, 0.98 mmol) and diphenylacetic acid (0.213 g, 1.00 mmol) were separately dissolved in (MeOH) then added together. This was then slowly evaporated for three days at room temperature and resulted in colourless crystals.

REFERENCES

1. F. Allen, *Acta Crystallogr. Sect. B*, 2002, **58**, 380.
2. C. F. Macrae, P. R. Edgington, P. McCabe, E. Pidcock, G. P. Shields, R. Taylor, M. Towler and J. van de Streek, *J. Appl. Cryst.*, 2006, **39**, 453.
3. L. J. Barbour, *J. Supramol. Chem.*, 2001, **1**, 189.
4. J. L. Atwood and L. J. Barbour, *Cryst. Growth Des.*, 2003, **3**, 3.
5. I. J. Bruno, J. C. Cole, P. R. Edgington, M. Kessler, C. F. Macrae, P. McCabe, J.Pearson and R. Taylor, *Acta Cryst.*, 2002, B **58**, 389.
6. J. Bruno, J. C. Cole, J. P. M. Lommerse, R. S. Rowland, R. Taylor and M. L. Verdonk, *J. Comput.-Aided Mol. Des.*, 1997, **11**, 525.
7. PreQuest - A program for the validation of crystal structure and chemical information for entry to the CSD Cambridge Crystallographic Data Centre, 12 Union Road, Cambridge, England
8. F. L. Hirshfeld, *Theor. Chim. Acta*, 1977, **44,** 129.
9. M. A. Spackman and J. J. McKinnon, *CrystEngComm*, 2002, 378.
10 G. M. Sheldrick, *Acta Crystallogr., Sect. A*, 2008, **64**, 112.
11. *POV-Ray for Windows, Version 3.6.1a.icl8.win32*, Persistence of Vision Team, Persistence of Vision Pty. Ltd., 2003-2004.
12. Y. von, W. Jeitshko and E. Parthe, *J. Appl. Crystallogr.*, 1997, 10, 73.
13. R. Blessing, *Acta Crystallogr., Sect. A*, 1995, 51, 33.
14. *XPREP - Reciprocal space exploration, Version 6.14 - w95/98/NT/2000/ME*, Bruker Nonius, 2003.
15. W. Clegg, A. J. Blake, R. O. Gould and P. Main, *Crystal Structure Analysis Principles and Practice*, International Union of Crystallography, Oxford University Press, 2001.
16. P. T. Anastas and J. C. Warner, *Green Chemistry: Theory and Practice*,Oxford Science Publications, New York, 1998; P. Anastas and T.Williamson, *Green Chemistry, Frontiers in Benign Chemical Synthesis and Processes*, Oxford Science Publications, New York, 1998; *Green Chemistry: Challenges and Opportunities*, J.

H. Clark, *GreenChem.*, 1999, **1**, 1; J. H. Clark, *The Greening of Chemistry*, *Chem. Brit.*,1998, October, 43.

17. H. M. Rietveld, *J. Appl. Crystal*. 1969, **2**, 65.

Chapter 3

Survey of Crystal Structures of Ammonium Carboxylates in the Cambridge Structural Database

3.1 RING-STACKING AND RING-LADDERING

The concept of ring-stacking and ring-laddering in the solid-state has been developed and well documented by Snaith and co-workers.[1] This came from the initial study of alkali metal complexes from structural inorganic chemistry. They looked at the association of discrete cation and anion pairs which formed polymeric ladders (ring-laddering)[2] and extended stacks (ring-stacking).[3] This association of the cation-anion pairs to form ring-stacking and ring-laddering is mainly driven by electrostatic forces to maximize the Coulombic energy within the crystal lattice. Bond[4] extended this ring-stacking and ring-laddering concept to structural chemistry of organic ammonium halides. He investigated the crystal structures of organic ammonium halides using the Cambridge Structural Database (CSD)[5]. The study confirmed the existence of ring-stacking and ring-laddering in organic ammonium halides, expanding the concept to the organic solid-state.[6] This work described in this thesis has extended this concept to organic primary, secondary and ammonium carboxylate salts (Figure 3.1) using the crystal structures in the CSD.

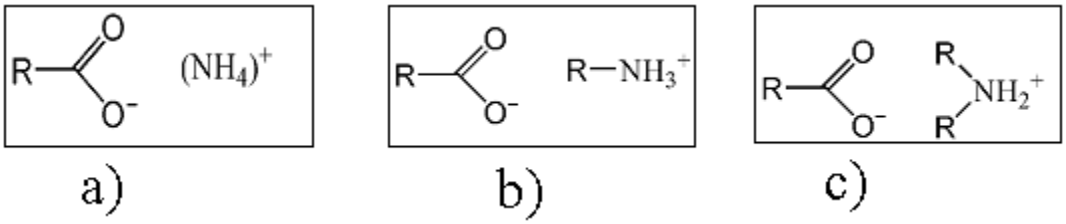

Figure 3.1 a) Ammonium carboxylate salts, b) primary ammonium carboxylate salts and c) secondary ammonium carboxylate salts.

The CSD is a database of all published organic small molecule crystal structures. The crystal structures of the ammonium carboxylate salts obtained from the CSD survey were viewed with emphasis on applying the concept of ring-stacking and ring-laddering to these salts. The tendency in the literature has been to analyse crystal structures of secondary, primary and ammonium carboxylate salts based on hydrogen bonding patterns, due to the strength and directionality of this interaction. This study will look at the influence that both the size and functionality (i.e. C-H···π, π···π and alkyl-alkyl interactions) of the cation and anion have on the formation of ring-stacking and ring-laddering in the organic solid-state.

The association of ammonium carboxylate salts is strongly driven by electrostatic forces between cations and anions, thereby maximising Coulombic energy. The

association of the cation and anion forms a cation-anion pair which can associate with each other to form a dimeric ring. The dimeric rings then associate with one another to form 2-D ring-laddering or 3-D ring-stacking (Figure 3.2). The formation of either ring-stacking or ring-laddering is controlled by steric constraints imposed by both the anion and cation; therefore our study looked at what effects the steric constraints have on the formation of stacks and ladders.

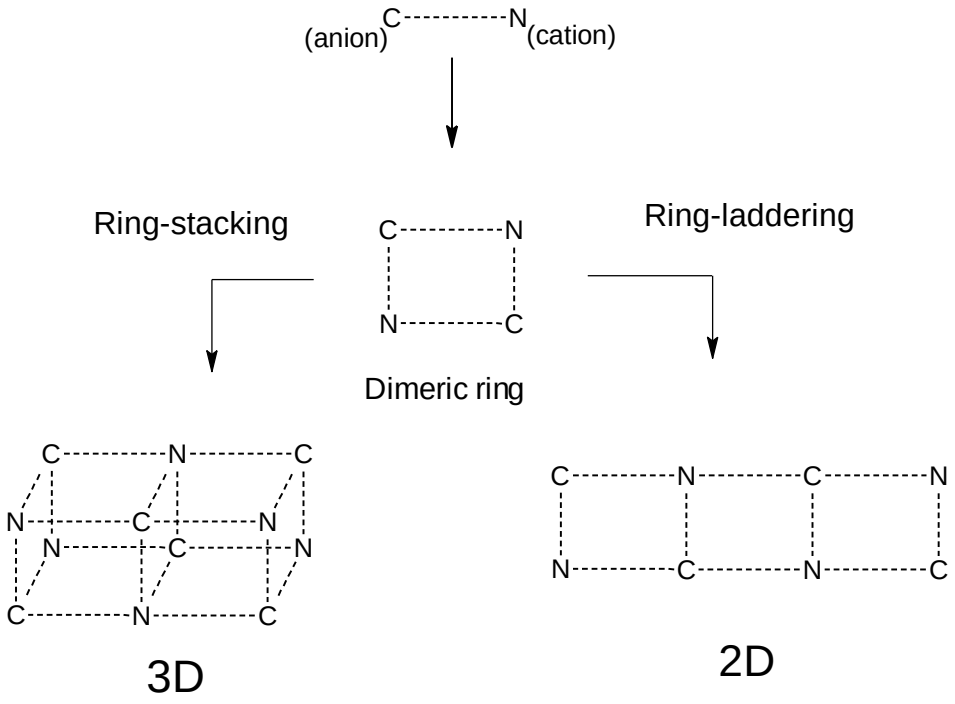

Figure 3.2 Schematic representation of the ring-stacking and ring-laddering concept in ammonium carboxylate salts.

The results obtained from this CSD survey will firstly give us an idea if the concept of ring-stacking and ring-laddering can be applied to ammonium carboxylate salts. It will also give us an idea how intermolecular interactions lead to the formation of stacking and laddering and why some of the salts do not form these stacks and ladders. The hypothesis is that cation-anion interactions are strongly structure directing in ammonium carboxylate salts, i.e. the cation-anion interactions will be maximized in these structures. The most effective arrangement of cations and anions is in an extended grid, as in NaCl. However, the existence of organic substituents of the cations and anions interferes with this arrangement and the dimensionality on the motif is reduced, resulting in nets, ladders and stacks. In this study a hypothesis is

made that ammonium carboxylate will form nets unless prevented by steric constraints. Ultimately this study would like to predict the formation of stacks and ladders in ammonium carboxylate salts based on the functionality and size of the cation and anion.

3.2 EXPERIMENTAL AND RESULTS

The CSD searches were done using ConQuest 1.11[7] (software supplied by the CSD to perform searches) and restricted to organic structures with known 3D coordinates. Searches were done on the best representative polymorph list 530[8] (best R-factor) in order to exclude repeat determinations of the same structure. The cation-anion contacts were defined as contacts between the nitrogen (N) atom of the cation and the carboxylate carbon (C) atom of the anion. The C atom was chosen as being the 'centre' of the negative charge on the anion with an intermolecular contact distance to N of 4.3 Å, (the sum of the default van der Waals radii + 1.1 Å). In order to determine a reasonable value for this distance cut-off, a search for $N^+H\cdots\ ^-OOC$ contacts of less than the default van der Waals radii was carried out and the distance between the cationic N and C of the carboxylate measured for each hit. The maximum value of these distances was used as the cut-off distance for N···C contacts (i.e. van der Waals + 1.1 Å).

Most searches were done on subsets of ammonium carboxylate salts obtained by removing zwitterions (through a combination of searches for intermolecular contacts between the cationic and anionic groups and manual removal of remaining zwitterions), solvates and co-crystals (number of residues <3), and structures containing other hydrogen bonding functionality. Lists of CSD refcodes are given in the CD Appendix.

3.2.1 Ammonium carboxylate salts

A CSD search for ammonium $(NH_4)^+$ and carboxylate (COO^-) gives 101 hits. After removing all the zwitterions, solvates and co-crystals, 65 structures remained. The manual removal of all the structures containing competing hydrogen bonding functionality (COOH, OH, =O, NH, N^+H_2, N^+H_3) left a subset of 23 ammonium carboxylate salts. The 23 salts can be further subdivided into structures containing dicarboxylates and those only containing monocarboxylates. In total there are 9

monoammonium monocarboxylate salts and these structures were inspected for stacking and laddering.

3.2.2 Primary ammonium carboxylate salts

A CSD search for primary ammonium (C-N^+H_3) and carboxylate (COO^-) gave 1484 hits. After the removal of all the zwitterions, solvates and co-crystals, 531 structures remain. The manual removal of all the structures containing competing hydrogen bonding functionality (COOH, OH, =O, NH, N^+H_2) left a subset of 193 primary ammonium carboxylate salts. The 193 salts can be further subdivided into structures containing dicarboxylates or diammonium, and those only containing monoanions and monocations. In total 147 monoammonium monocarboxylic salts were found, and inspected for the formation of stacking and laddering.

3.2.3 Secondary ammonium carboxylate salts

A search for secondary ammonium (C-N^+H_2-C) and carboxylate (COO^-) gave 566 hits with intermolecular interactions between C and N. After manual removal of all the zwitterions only 413 crystal structures remained. The remaining 413 crystal structure were manually inspected to remove all solvates, residues >3 and co-crystals, thus reducing the subset to 260 structures. The manual removal of all the structures containing competing hydrogen bonding functionalities (COOH, OH, =O, NH, N^+H_3) left a subset of 95 salts. The 95 salts can be further subdivided into structures containing dicarboxylates or diammonium, and those containing only monoanions and monocations. The 52 structures containing only monoanions and monocations were inspected for the formation of stacking, laddering and hydrogen bonding networks.

3.3 DISCUSSION

Hydrogen bonding is a dominant interaction in ammonium carboxylate salts due its strength and directionality, and good donor (ammonium) and acceptor (carboxylate) capabilities of the ions.[9] This interaction plays an important role as it is an important molecular recognition synthon in ammonium carboxylate salts. The effects of other competing hydrogen bonding donors and acceptors complicated this study. These competing donors and acceptors can also be involved in stacking and laddering motifs, thus making analysis of the formation of these motifs complex. For this reason they were excluded from this study.

3.3.1 Ammonium carboxylate salts

The 65 crystal structures were inspected for a hydrogen bonding contact between $(NH_4)^+$ and the COO^-, and all 65 structures contain a contact between N and O at less than the sum of the van der Waals radii. Manually removing all the structures containing competing hydrogen bonding functionality (COOH, OH, =O) a subset of 23 salts remained. Of the 23 structures all the dianions were removed. The remaining 9 structures were then investigated for the formation of nets, stacks and ladders.

In 4 of the 9 structures the motifs formed were extended nets (Figure 3.3); the formation of nets is mainly due to the maximization of Coulombic energy in the crystal lattice. The remaining 5 structures formed ladders (Figure 3.4). The ladders stack on top of one another forming stacks due to the additional C-H···π and π ···π interactions between the R-groups (Figure 3.5). These 5 crystal structures all have additional intermolecular interactions that stabilise the formation of ladders and stacks.

The size of the anion plays an important role in the formation of nets, stacks and ladders in ammonium carboxylate salts as the cation size stays the same. Due to the multiple donor capabilities of the ammonium, multiple hydrogen bonding interactions are possible thus forming extensive nets (Figure 3.2). Upon inspecting 4 of the 9 structures all of them have a small anion resulting in the formation of nets. The small anions in the 4 structures have no additional functionality meaning no additional intermolecular interactions could aid in the formation of stacks or ladders. This shows that not just cation-anion interactions are necessary for the formation of stacks and laddering in ammonium carboxylate salts; subtle intermolecular interactions such as C-H···π and π ···π interactions to name a few play a crucial role in the formation of stacks and ladders.

The remaining 5 structures all form ladders which stack on top of one another to form stacks of ladders. This is due to the size and the additional functional groups (phenyl and long aliphatic chain alkyl groups) on the anion. These form π ···π and alkyl-alkyl interactions, which play a crucial role in the formation of stacks of ladders. The structure *ammonium 4-methoxycinnamate* (EVOQAH) has a C-H···π interaction between the C-H of the phenyl group of the anion and of the π-face of the anion

stabilising the formation of stacking and laddering. The structures *ammonium palmitate* (GUKZOB) and *ammonium myristate* (GUKZUH) have very long alkyl chains on the anion resulting in alkyl-alkyl interactions which stabilise the formation of stacking and laddering. The structures *ammonium 3-bromocinnamate* (ICUJIA) and *ammonium 3-chlorocinnamate* (ICUJUM) have multiple π ···π interactions which again reinforce the formation of stacking and laddering. This shows that the size of the anion and its functionality can be used in the design of stacks, ladders and nets. Large anions with substituents able to form π···π or alkyl-alkyl interactions will result in stacked ladders.

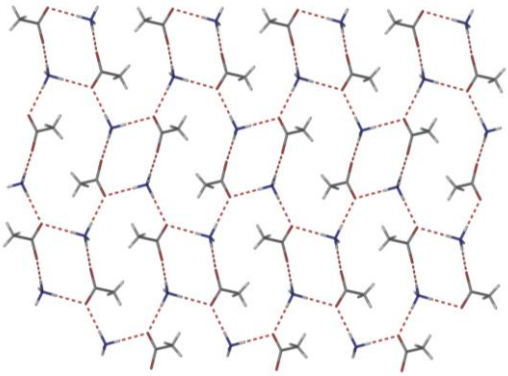

Figure 3.3 Hydrogen bonding nets in *ammonium acetate* (AMACET).

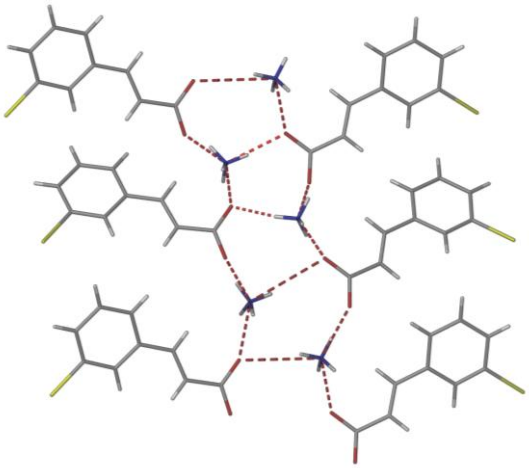

Figure 3.4 Ring-laddering in *ammonium 3-bromocinnamate* (ICUJIA).

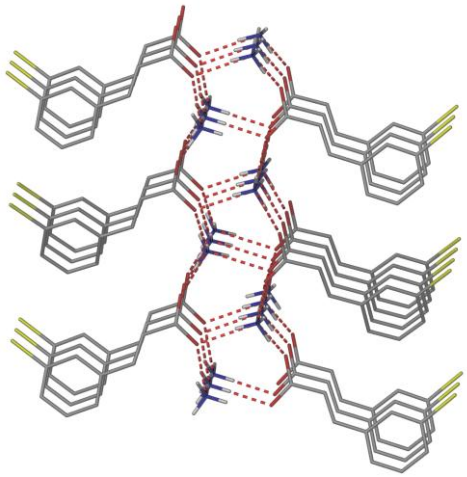

Figure 3.5 Ring-stacking in *ammonium 3-bromocinnamate* (ICUJIA) (hydrogens from the anion have been removed for clarity.

3.3.2 Primary ammonium carboxylate salts

The first observation made regarding the crystal structures of the primary ammonium carboxylate salts retrieved from the CSD was that 528 of the structures have a hydrogen bond between the $(NH_3)^+$ and the COO^-. This means that out of the 531 primary ammonium carboxylate salts only three, *2-ammonio-5-benzamido-3-cyano-11H-pyrido(2,3-b)(1,5)benzodiazepine benzoate* (ZATYEY), *isopropylammonium N-(phosphonomethyl)glycine* (SAVSOX) and *cyclohexylammonium phosphonomethylglycinate* (SOXWUX), do not contain a hydrogen bond between the N^+H_3 and the COO^-. Inspecting the 3 crystal structures reveals that one of them (SAVSOX) has a stronger hydrogen bond acceptor (a phosphate), and the stronger acceptor competes for the donor. One structure (ZATYEY) is not a carboxylate but a carboxylic acid.

After manual removal of all the structures containing competing hydrogen bonding functionality (COOH, OH, =O, NH, NH_2) a subset of 193 primary ammonium carboxylate salts remained. Of these 193 structures all dicarboxylates and diammoniums were removed. The 147 structures that were left all contain monoanions and monocations, and this subset was used to investigate the formation of nets, stacks and ladders.

This subset showed that 112 of the structures contain extended ladders (Figure 3.6). In 28 of the structures the motifs formed extended nets (Figure 3.7), and the remaining 7

structures formed cubes/stacks (Figure 3.8).The formation of stacks occur due to the size of both the cation and anion, if both are large it will form the cube/stack.

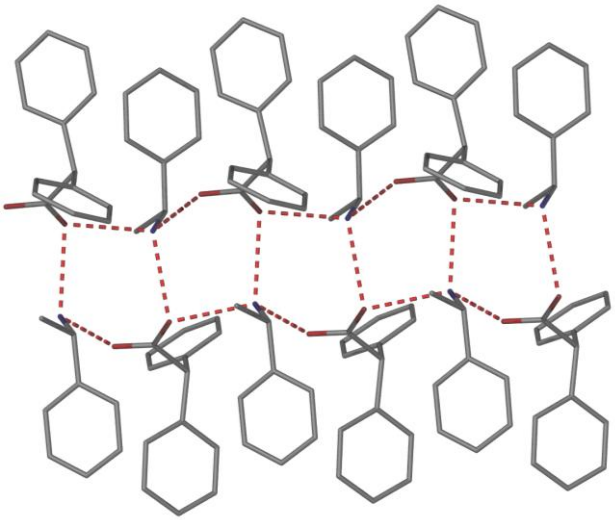

Figure 3.6 Ring-laddering in *1-phenylethylammonium 1,1-diphenylacetate* (ZUSNIK).

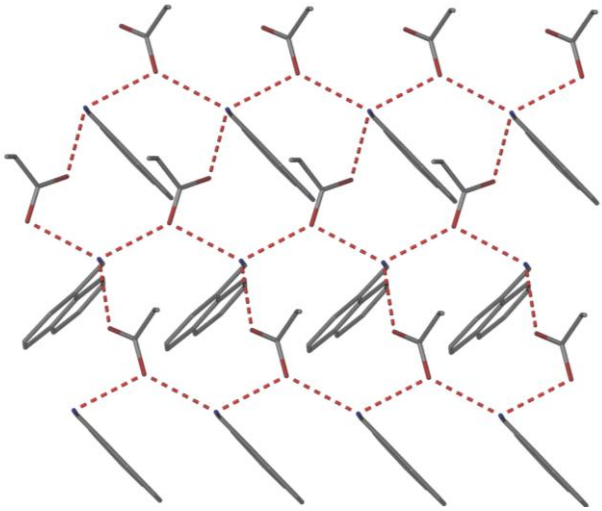

Figure 3.7 Nets in *1-naphthylmethylammonium propanoate* (ISERUT).

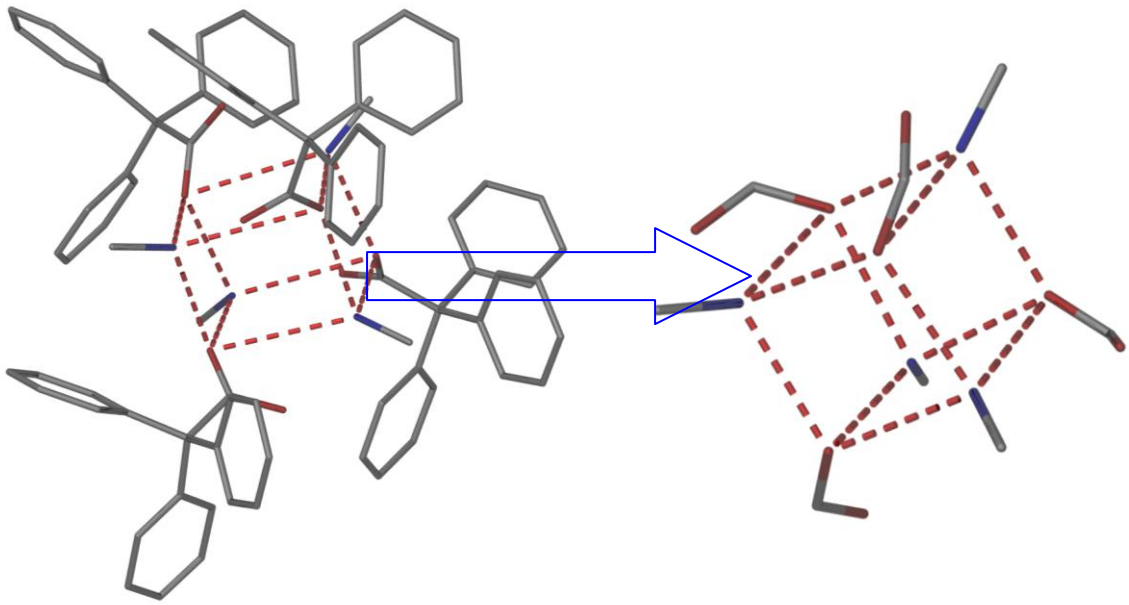

Figure 3.8 Cubes in *n-butylammonium triphenylacetate* (MIBTOH).

Upon investigating the primary ammonium carboxylate salt structures, the size and orientation of the cation are shown to play an important role in the formation of nets and laddering. If the cation is viewed down the N-C bond vector, and a plane is drawn between the two C and N atoms, the remainder of the substituent ions adopt two possible conformations, either perpendicular to the plane (Figure 3.9 (a)) or parallel to the plane (Figure 3.9b(b)). In all the structures showing the perpendicular confirmation the primary ammonium carboxylate salts form ladders (Figure 3.10). In all the structures containing the parallel conformation the primary ammonium carboxylate salts form nets (Figure 3.11). In the parallel conformation the cations stack in such a manner as maximise the electrostatic factors in the crystal lattice which favours the formation of nets.

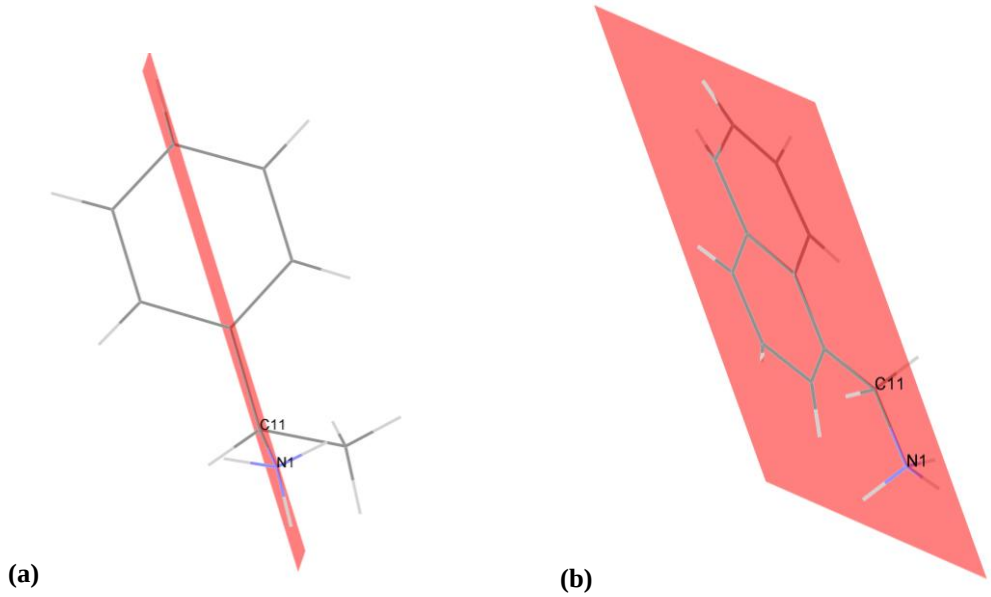

Figure 3.9 (a) Cation substituent perpendicular to the plane in *(R)-1-phenylethylammonium (S)-2-phenylpropanoate* (AFINEJ) and (b) cation parallel within the plane in *1-naphthylmethylammonium octa-2,4-diynoate* (ATEQUL).

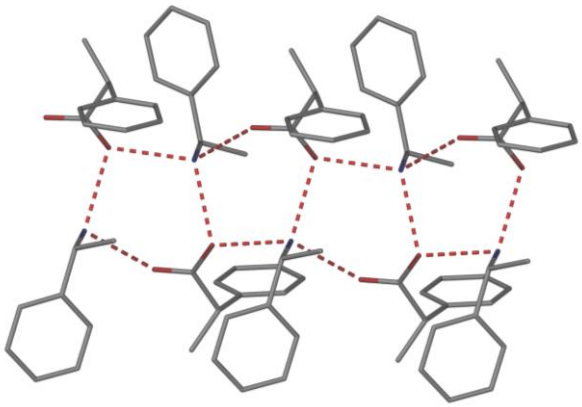

Figure 3.10 Ring-laddering in *(R)-1-phenylethylammonium (S)-2-phenylpropanoate* (AFINEJ).

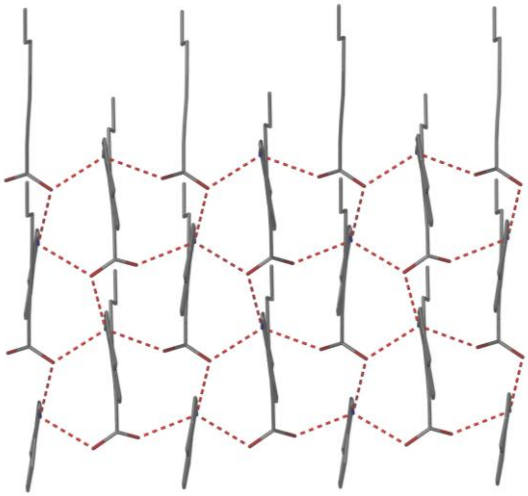

Figure 3.11 Nets in *1-naphthylmethylammonium octa-2,4-diynoate* (ATEQUL).

3.3.3 Secondary ammonium carboxylate salts

The 566 secondary ammonium carboxylate salts were inspected and all zwitterions removed, leaving a subset of 413 structures. The 413 structures still contain numerous diammonium and multiple carboxylate functionalities. These structures were removed leaving a subset of 217 structures. After manual removal of all competing hydrogen bonding functionality a subset of 52 structures remained. The 52 structures were then investigated for the formation of stacking, laddering and nets. In 21 of the structures discrete rings formed (see e.g. Figure 3.12). In the remaining 31 structures, 12 form chains (Figure 3.13) and 19 structures form ladders (Figure 3.14).

The formation of ring-stacking in secondary ammonium carboxylate salts is expected to be very low due to the steric hindrance from both the cation and the anion. This is confirmed by the CSD results (as well as our experimental investigation, see Chapter 4). The secondary ammonium carboxylate salts have a tendency to form 0-D discrete rings, 1-D chains[10] and ladders. Thus depending on the size and the functionality of both the anion and cation the formation of 0-D and 1-D structures can be controlled. If both the cation and anion are large the formation of 1-D chains will be favoured over that of 0-D motifs.

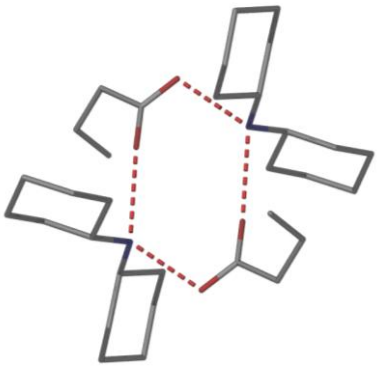

Figure 3.12 Discrete rings in *dicyclohexylammonium butanoate* (JEFYAV) (hydrogen atoms have been removed for clarity).

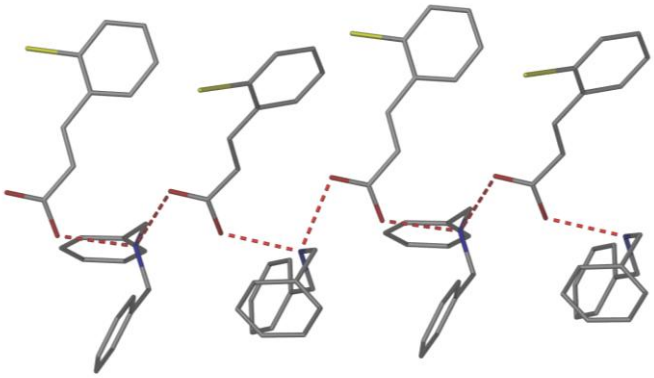

Figure 3.13 The cation-anion chains in *dibenzylammonium 2-bromocinnamate* (PEQGEY) (hydrogen atoms have been removed for clarity).

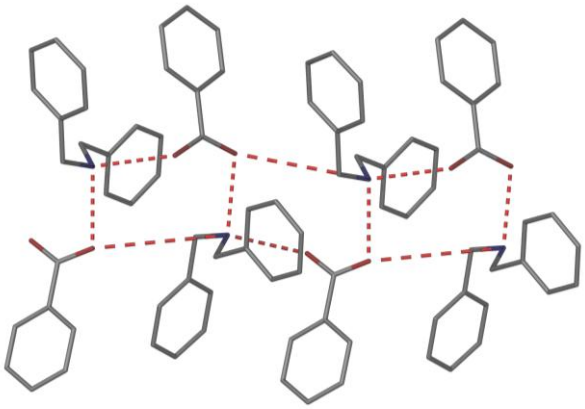

Figure 3.14 Ring-laddering in *dibenzylammonium benzoate* (PEQKIG) (hydrogen atoms have been removed for clarity).

3.4 CONCLUSIONS

The results from the CSD survey of ammonium carboxylate salts show that these salts do form stacks, ladders and nets, thus confirming our hypothesis that cation-anion interactions are structure-directing in these salts. It can also be observed that a hydrogen bond will always form between the ammonium cation and the carboxylate anion in these salts, unless a very strong competitor is present.

Ammonium carboxylate salts $(NH_4)^+$ form nets, ladders and stacks. Primary ammonium carboxylate salts form stacks, ladders, nets or cubes. The survey shows that the formation of ladders dominates over that of nets and stacks in primary ammonium carboxylates. The secondary ammonium carboxylate salts do not form nets or stacks. These salts form discrete 0-D rings, 1-D chains and ladders. The size of the organic substituents influences which motif is formed – smaller substituents are more likely to form nets whilst very large substituents lead to cubes or discrete rings.

In Table 3.1 a summary of the formation of ring-stacking and ring-laddering in the whole series of ammonium carboxylate salts is given. This clearly shows that the formation of stacks and laddering in ammonium carboxylate salts is dependent on the steric effects.

The results from this survey have been compared with the results obtained from the experimental study to look for consistencies in the formation of these motifs found in ammonium carboxylates salts. In the next chapter an in-depth investigation of the intermolecular interactions of new ammonium, primary and secondary carboxylate salts will be discussed.

Table 3.1 Motifs formed in organic ammonium carboxylate salts in the CSD

Type of motifs formed	Ammonium carboxylate salts (9 structures)	Primary ammonium carboxylate salts (147 structures)	Secondary ammonium carboxylate salts (52 structures)
Nets	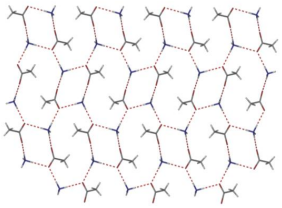 44% of structures	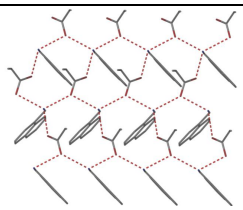 19% of structures	NONE
Stacks	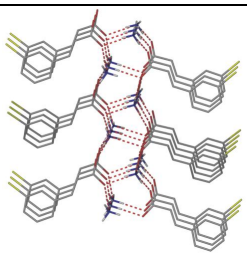 56% of structures	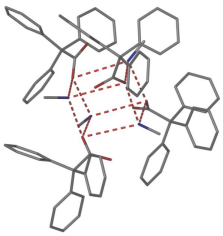 6% of structures	NONE
Ladders	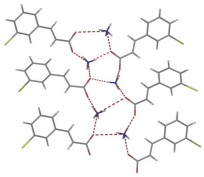 56% of structures	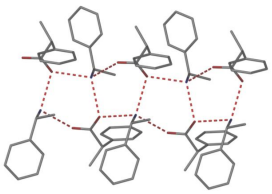 76% of structures	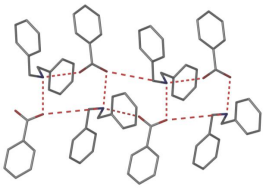 36% of structures
0-D	NONE	NONE	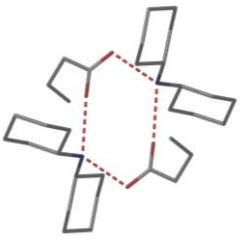 40% of structures
1-D	NONE	NONE	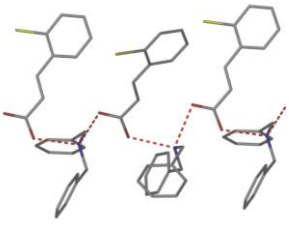 24% of structures

REFERENCES:

1. D. Barr, W. Clegg, R. E. Mulvey, R. Snaith and K. Wade, *J. Chem. Soc. Chem. Commun.*, 1986, 295; D. R. Armstrong, D. Barr, W. Clegg, R.E. Mulvey, D. Reed, R. Snaith and K. Wade, *J. Chem. Soc. Chem. Commun*., 1986, 869; D. Barr, W. Clegg, R. E. Mulvey, R. Snaith, and K. Wade. *J. Chem. Soc. Chem. Commun.*, 1986, 295; K. Gregory, P. von, R. Schleyer and R. Snaith, *Adv. Inorg. Chem*. 1991, 47.
2. D. R. Armstrong, D. Barr, W.Clegg, S. M. Hodgson, R. E Mulvey, D. Reed, R. Snaith and D. S, Wright. *J. Am. Chem. Soc*., 1989, 4719.
3. J. Knizek, I. Krossing, H. Noth, H. Schwenk, T. Seifert. *Chem. Ber*. 1997, 1053.
4. A. D. Bond, *Chem. Eur. J*., 2004, 1885.
5. F. Allen. *Acta, Crystallogr. Sect. B.* 2002, **58**, 380.
6. A. D. Bond, *Cryst. Growth Des.*, 2005, 755.
7. I. J. Bruno, J. C. Cole, P. R. Edgington, M. Kessler, C. F. Macrae, P. McCabe, J. Pearson and R. Taylor, *Acta Cryst., Section B*, 2002, **58**, 389.
8. J. van de Streek, *Acta Cryst*., *Section B,* 2006, **62**, 567.
9. M. C. Etter, *Acc. Chem. Res.* 1990, 120 .
10. T. Darshak and P. Dastidar, *Cryst Growth & Des.*, 2006, **6**, 1022.

Chapter 4

Crystal Structures of Novel Ammonium Carboxylate Salts

This study aims to investigate the occurrence of ring-stacking and laddering in organic ammonium carboxylate salts. To this end, an extensive CSD survey has been done to review the intermolecular interaction motifs in these salts (Chapter 3), and a systematic experimental study were carried out. The results of the experimental study are described in this chapter.

A series of carboxylic acids and amines were allowed to react under various conditions, and the products crystallised (see Chapter 2 for experimental details). A total of 19 new crystal structures were obtained. It was not possible to refine 2 of these structures satisfactorily (*dioctylammonium formate*, *dioctylammonium benzoate* and a polymorph of *dibutylammonium diphenylacetate*), and these 3 structures will not be discussed further.

The crystal structure refinements were done using X-seed[1], some of the hydrogen atoms were placed manually. The hydrogen atoms which were involved in the proton transfer reaction from the acid to the base were found in the difference map and were modelled using the X-seed software. The crystallographic data of all the structures obtained from Single crystal X-ray Diffraction can be found on the Appendix CD.

All the images in this chapter were generated with Pov-Ray[2] using the software interface X-Seed.[1] Ellipsoids are generated at 50% probability.

The 2-D fingerprint plots generated with Crystal Explorer[3] are used extensively in this chapter to look at the intermolecular interactions in the sixteen novel ammonium carboxylate salts. The intermolecular interactions are easily identifiable from the plot which makes this a novel way of viewing intermolecular interaction in the solid-state. The 2-D fingerprint plot[4] makes use of three different colours that represent the distances of the contacts; red (close contacts), blue (most distant contacts) and green (neither close nor distant contacts).

The Hirshfeld surfaces are defined by a simple equation $w = 0.5$, where the weight function $w(r)$ is given by

$$w(r) = \sum_{i \in molecule} \rho_i(r) / \sum_{i \in crystal} \rho_i(r)$$

where $\rho_i(r)$ is the spherical atomic electron distribution located at the *i*-th nucleus. The weight function represents the ratio between the sum of the spherical atom electron density for a molecule (the promolecule) and the same sum for the entire crystal (the procrystal). The Hirshfeld surface covers the entire space surrounding a particular molecule in a crystal where the electron distribution of the promolecule exceeds that due to other molecules.[5]

The 2-D fingerprint plot consists of two axes d_i and d_e in Å (Figure 4.1) and it contains thousands of spots which are positions on the Hirshfeld surface. The fingerprint plot and Hirshfeld surface for the formamide molecule, generated by Crystal Explorer, are shown in Figure 4.1, where

d_i = distance from the surface to the nearest atom interior to the surface

d_e = distance from the surface the nearest atom exterior to the surface.

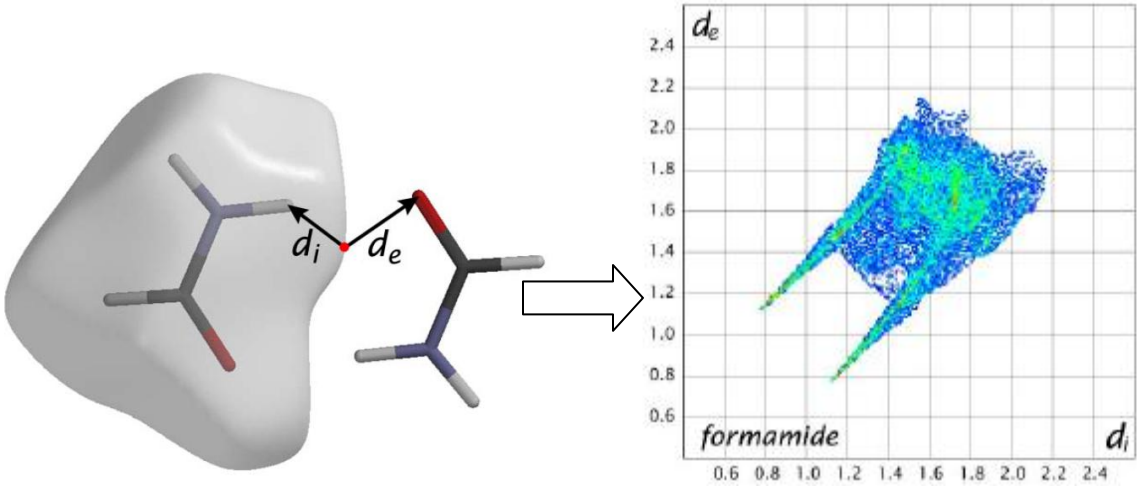

Figure 4.1 2-D fingerprint plot of the dimer formamide.

If the points from the Hirshfeld surface are plotted on axes it produces a 2-D fingerprint plot. The plot can show many different types of intermolecular interaction but examples of hydrogen

bonding, H···H interactions, C-H···π interactions and π···π stacking will be demonstrated as these interactions are the main intermolecular interaction discussed in this work.

With careful inspection of the 2-D fingerprint plot generated with Crystal Explorer all close contacts can be identified. The two sharp peaks at the bottom left of the plot in Figure 4.1 are an indication of a hydrogen bonding donor and acceptor, and arise due to hydrogen bonding between molecules in the formamide dimer.

The H···H interactions are due to intermolecular interactions between the hydrogen (H) atoms interacting with each other and can also arise due to close packing of H atoms, this is visible from the 2-D plot for nonane in Figure 4.2(a) where $d_i = d_e \approx$ 1.2 -1.8 Å.

The small "wings" at the upper left and lower right (marked with stars) of the plot for benzene are characteristic of C-H···π interactions (Figure 4.2 (b)).

The π···π interaction can be found in the $d_i = d_e \approx$ 1.8 region on the plot as seen in the plot for hexabenzocoronene in Figure 4.2 (c).

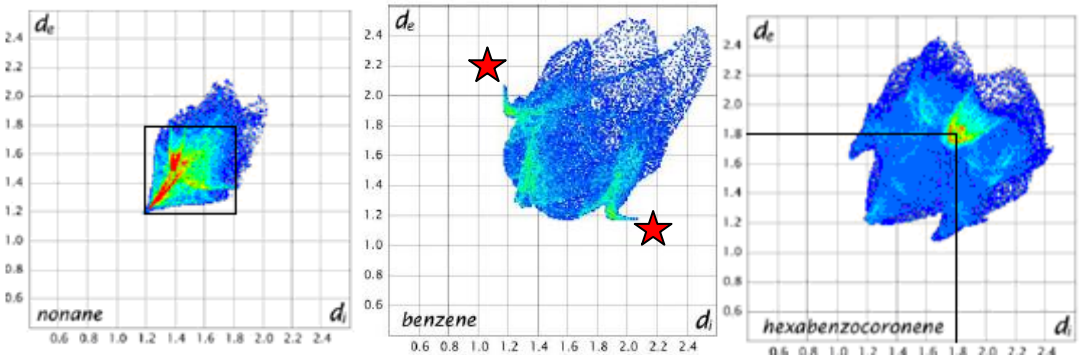

Figure 4.2 (a) H···H interactions, (b) C-H···π interactions and (c) π···π stacking.

4.1 Crystal structure analysis of secondary ammonium carboxylate salts

4.1.1 Diethylammonium diphenylacetate (1)

This salt crystallised in the monoclinic space group $P2_1/c$. There are hydrogen bonds between the diethylammonium and the diphenylacetate (Figure 4.3) [$N_{(4)}^{+}$-$H_{H(1)}$ $\cdots^{-}O_{(1)}OC$ (1.787Å) and $N_{(4)}^{+}$-$H\cdots^{-}O_{(2)}OC$ (1.775 Å)], forming a 1-D hydrogen bonded chain along the ***c***-axis with the graph set notation[6] $C_2^2(7)$. The hydrogen bond donor (N^{+}-H) and acceptor ($^{-}$OOC) can be identified by the two sharp peaks in the 2-D fingerprint plot shown in Figure 4.4. Hydrogen bonding is a common characteristic in ammonium carboxylate salts, due to its donor (ammonium) and acceptor (carboxylate) capabilities[7]. The C-H···π interaction between the C-H of the methylene group and the π–face of the phenyl group shown in Figure 4.5 is evident on the 2-D fingerprint plot, and is identified by the small wings on the sides of the plot. Evidence from the 2-D plot indicates that π···π interactions are present (Figure 4.4) and looking at the molecular packing diagram the phenyl groups stack on top of each other due to this π···π interaction (Figure 4.6). The hydrogen bonded chains pack together in sheets. The sheets stack on top of each other, with C-H···π interactions between sheets, to form the 3-D structure (Figure 4.7).

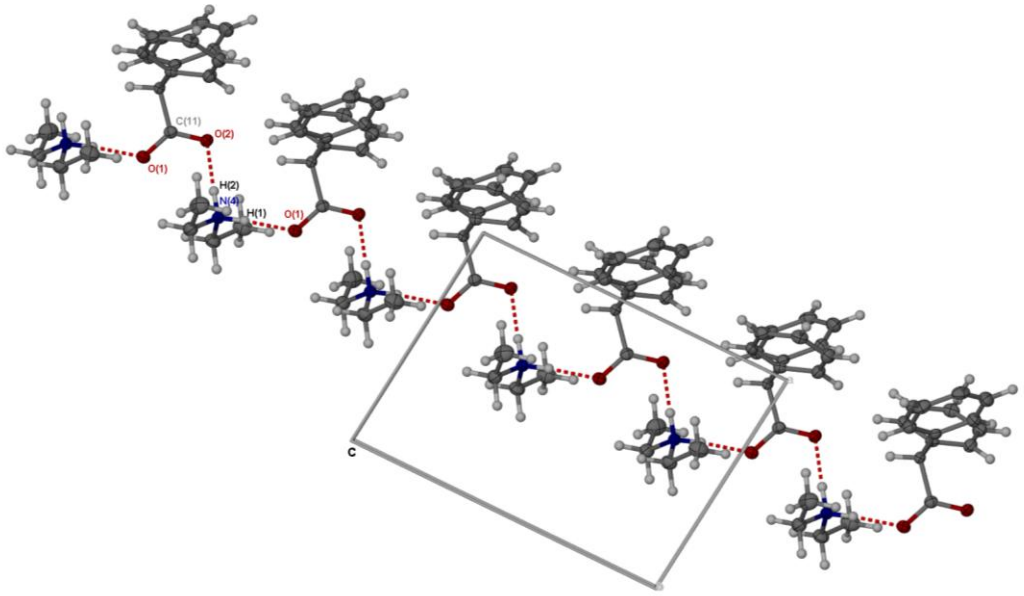

Figure 4.3 1-D hydrogen bonding along *c* in *diethylammonium diphenylacetate*.

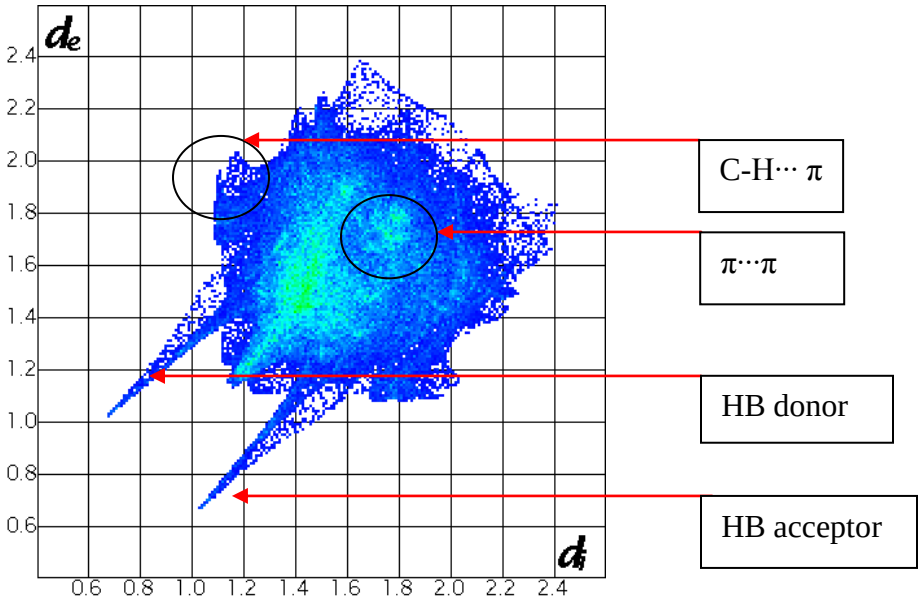

Figure 4.4 The 2-D fingerprint plot of *diethylammonium diphenylacetate* indicating the various interactions.

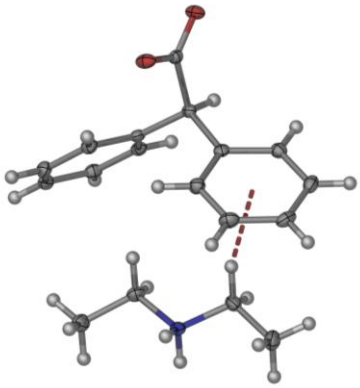

Figure 4.5 C-H···π between anion and cation in *diethylammonium diphenylacetate*.

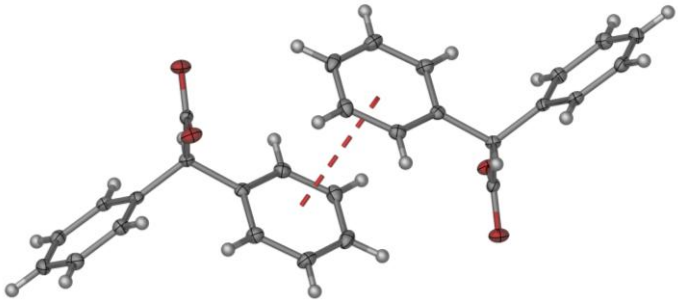

Figure 4.6 π···π stacking between diphenylacetate ions.

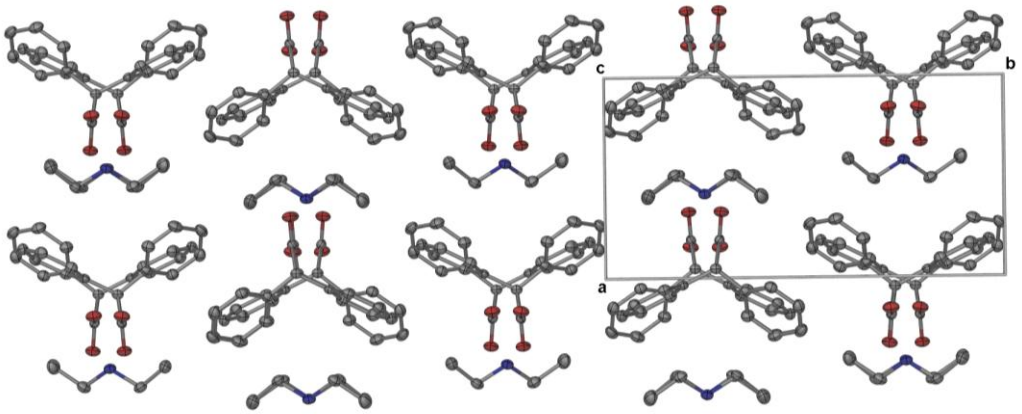

Figure 4.7 The molecular packing diagram of *diethylammonium diphenylacetate* (hydrogen atoms have been removed for clarity).

4.1.2 Dihexylammonium phenylacetate (2)

This salt crystallised in the triclinic space group *P-Ī*. There are hydrogen bonds between the dihexylammonium and phenylacetate ions [$N_{(1)}^{+}$-$H_{(1A)}$···$^{-}O_{(2)}OC$ (1.896 Å) and $N_{(1)}^{+}$-$H_{(1B)}$···$^{-}O_{(2)}OC$ (1.762 Å)], forming a 0-D hydrogen bonding ring with graph set notation $R_4^2(8)$ (Figure 4.8). The two sharp peaks at the bottom left of the 2-D fingerprint plot (Figure 4.9) arise due to hydrogen bonding between the cation and the anion. Evidence of C-H···π interactions is also visible from the fingerprint plot, this is due to the interaction between the C-H group of the methylene and the π-face of the phenylacetate (Figure 4.10). Evidence of multiple H···H interactions is also apparent from the intensity of the spots in the H···H region of the plot (Figure 4.9). These H···H interactions occur between the dihexylammonium ions (Figure 4.11), and this is a good example of the well documented alkyl-alkyl interactions.[8] The 0-D hydrogen bonded motifs results in discrete units strengthened by C-H···π interactions. These units are form sheets with alkyl-alkyl interactions between the sheets (Figure 4.12).

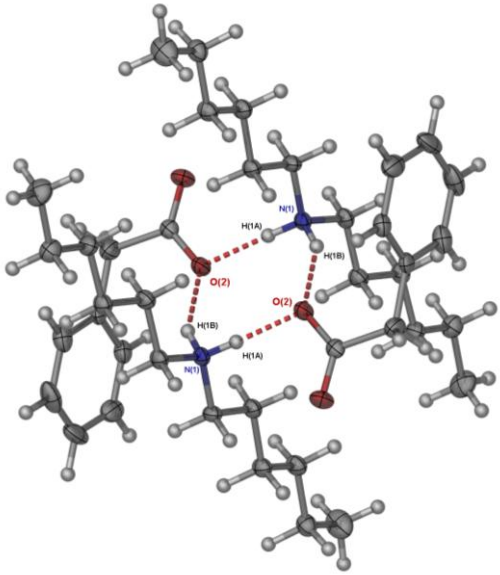

Figure 4.8 0-D hydrogen bonding motif in *dihexylammonium phenylacetate*.

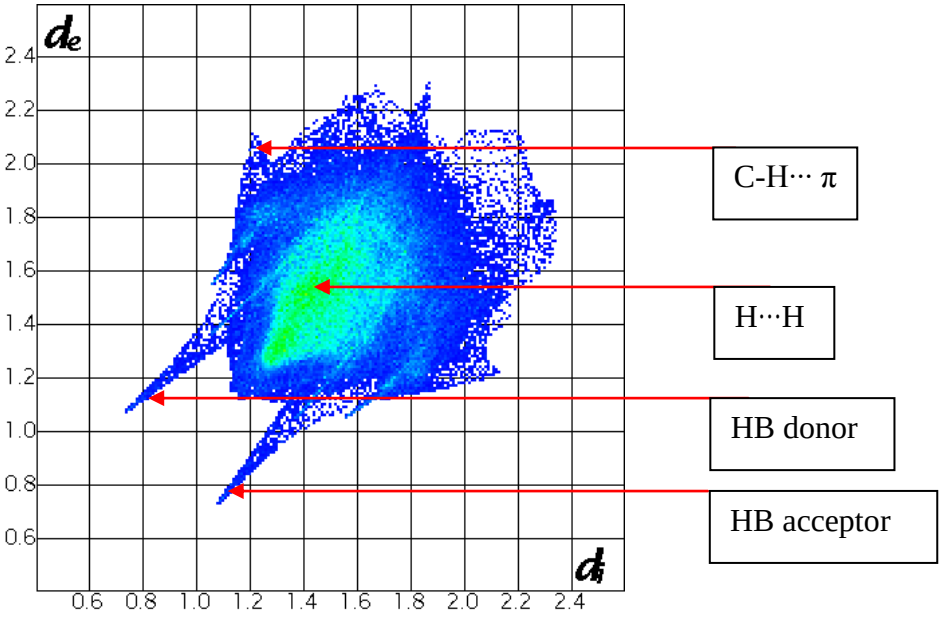

Figure 4.9 The 2-D fingerprint plot of *dihexylammonium phenylacetate* indicating the various interactions.

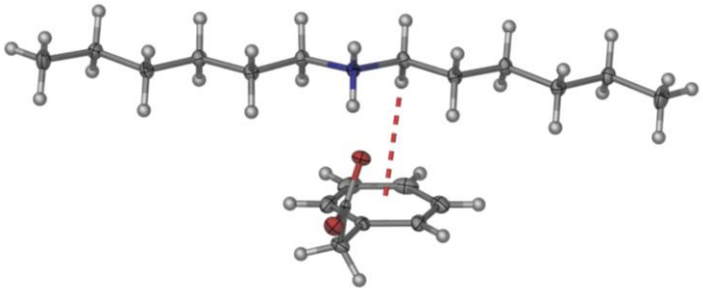

Figure 4.10 C-H···π interaction between methylene group and phenyl group in *dihexylammonium phenylacetate.*

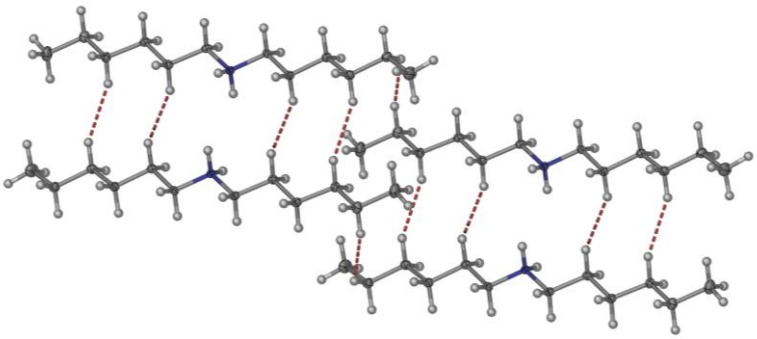

Figure 4.11 Alkyl-alkyl interactions between dihexylammonium ions.

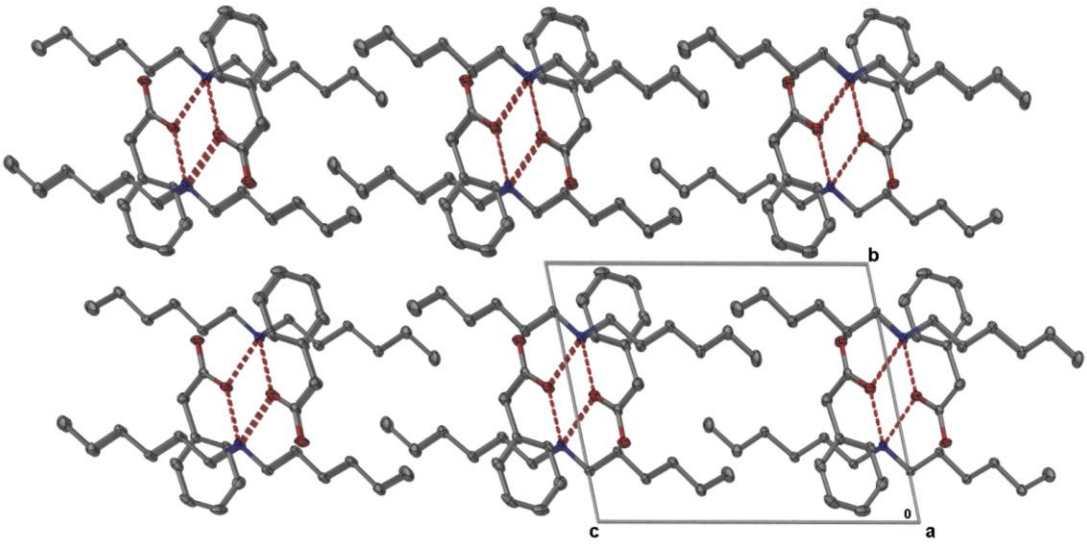

Figure 4.12 Molecular packing diagram of *dihexylammonium phenylacetate* (hydrogen atoms have been removed for clarity).

4.1.3 Dicyclohexylammonium formate (3)

This salt crystallised in the monoclinic space group *C2/c*. There are hydrogen bonds between the dicyclohexylammonium and the formate [$N_{(1)}^{+}$-$H_{(1)}\cdots^{-}O_{(2)}OC$ (1.809 Å) and $N_{(1)}^{+}$-$H_{(2)}\cdots^{-}O_{(4)}OC$ (1.792 Å)], forming a 0-D hydrogen bonding ring with the graph set notation $R_4^4(12)$ (Figure 4.13). The two sharp peaks at the bottom left of the 2-D fingerprint plot (Figure 4.14) arise due to hydrogen bonding between the donor cation (N^{+}-H) and acceptor anion ($^{-}$OOC). The plot also shows evidence for multiple H···H interactions. This arises due to the C-H groups from the cyclohexylammonium interacting with another cyclohexylammonium C-H group (Figure 4.15). The 0-D hydrogen bonding forms a discrete unit which is strengthened by the H···H interactions. The discrete hydrogen bonded units close pack to form sheets that stack on top of and next to each other forming the 3-D structure (Figure 4.16).

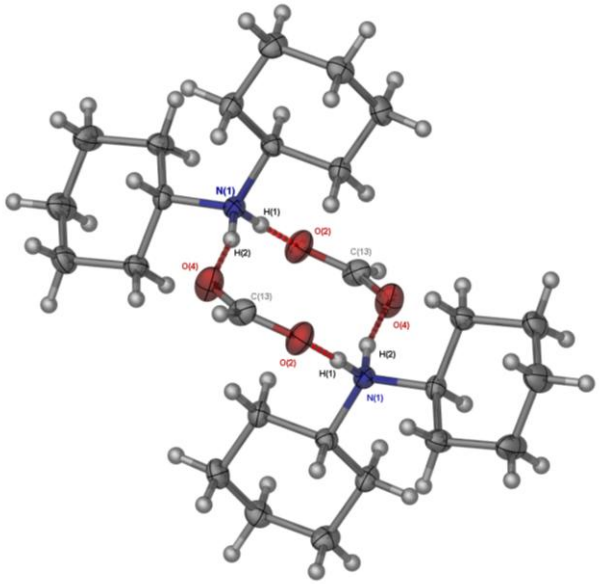

Figure 4.13 0-D hydrogen bonding in *dicyclohexylammonium formate*.

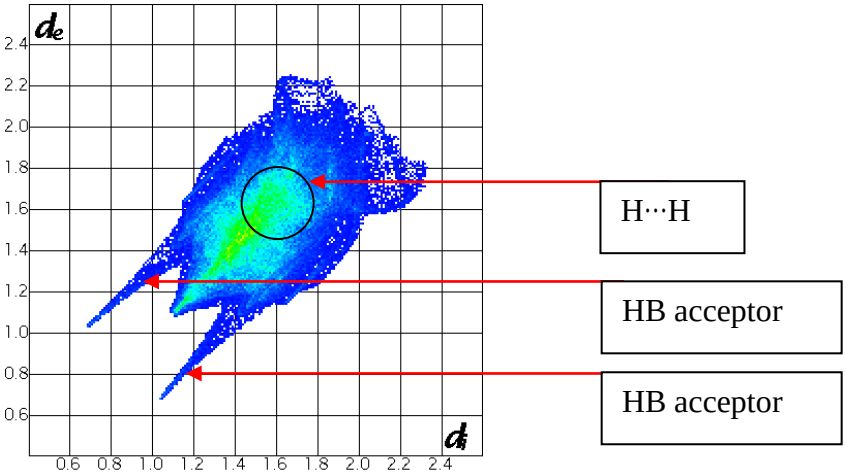

Figure 4.14 The 2-D fingerprint plot of *dicyclohexylammonium formate* indicating the various interactions.

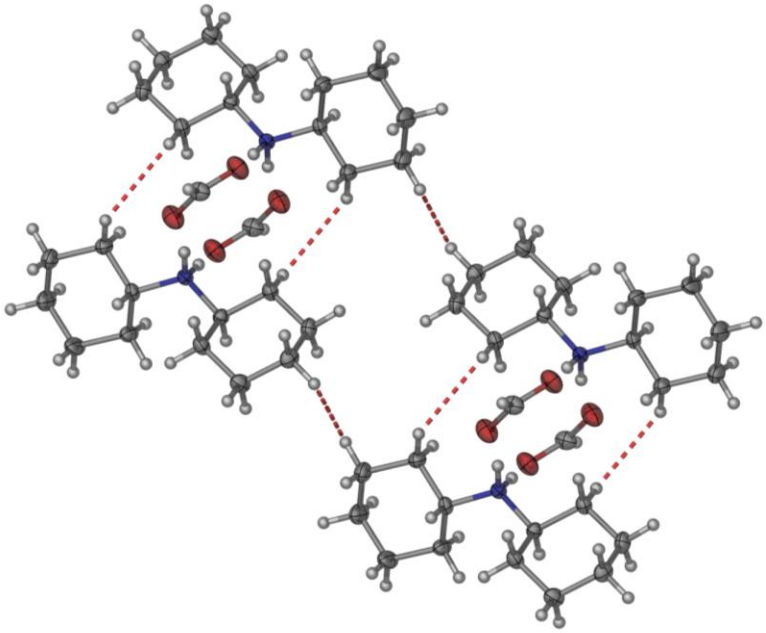

Figure 4.15 H···H interactions between cyclohexylammonium cations.

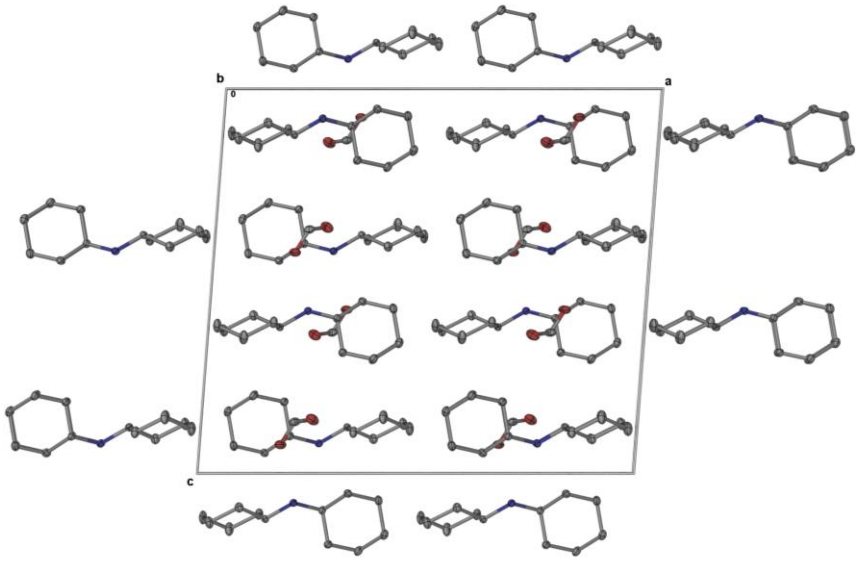

Figure 4.16 Molecular packing diagram of *dicyclohexylammonium formate*.

4.1.4 Dicyclohexylammonium formate hydrate (4)

This salt crystallised in the monoclinic space group $P2_1/n$. There are hydrogen bonds between the dicyclohexylammonium and the formate [$N_{(2)}^{+}$-$H_{(H2A)}\cdots^{-}O_{(1)}OC$ (1.833 Å), $N_{(2)}^{+}$-$H_{(H2B)}\cdots^{-}O_{(3)}OC$ (2.193 Å) and N_2^{+}-$H_{(H2B)}\cdots^{-}O_{(1)}OC$ (2.109 Å)], forming a hydrogen bonding chain along the *a*-axis (Figure 4.17). The two water molecules also form a hydrogen bond (1.552 Å). The two sharp peaks on the 2-D fingerprint plot (Figure 4.18). are due to hydrogen bonding between donor cation (N^{+}-H) and acceptor anion ($^{-}$OOC). The plot indicates that multiple H···H interactions are present in the structure. This is due to the C-H of the cyclohexylammonium interacting with an adjacent C-H of another cyclohexylammonium (Figure 4.19). The intensities of the spots on the donor and acceptor peaks indicate that additional hydrogen bonding interactions are present in **4**. These interactions are due to hydrogen bonding between the water molecules, and the interaction of the OH group of the water molecule with the formate ion. The water molecules act as a bridge between hydrogen bonded chains (Figure 4.20). Two cation-anion chains are held together by a ribbon/tape of hydrogen-bonded water molecules (Figure 4.20).

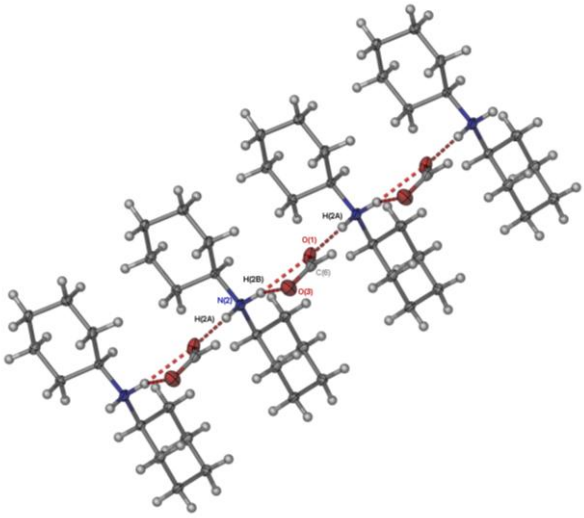

Figure 4.17 1-D hydrogen bonding chain in *dicyclohexylammonium formate hydrate* (hydrogen atoms have been removed for clarity).

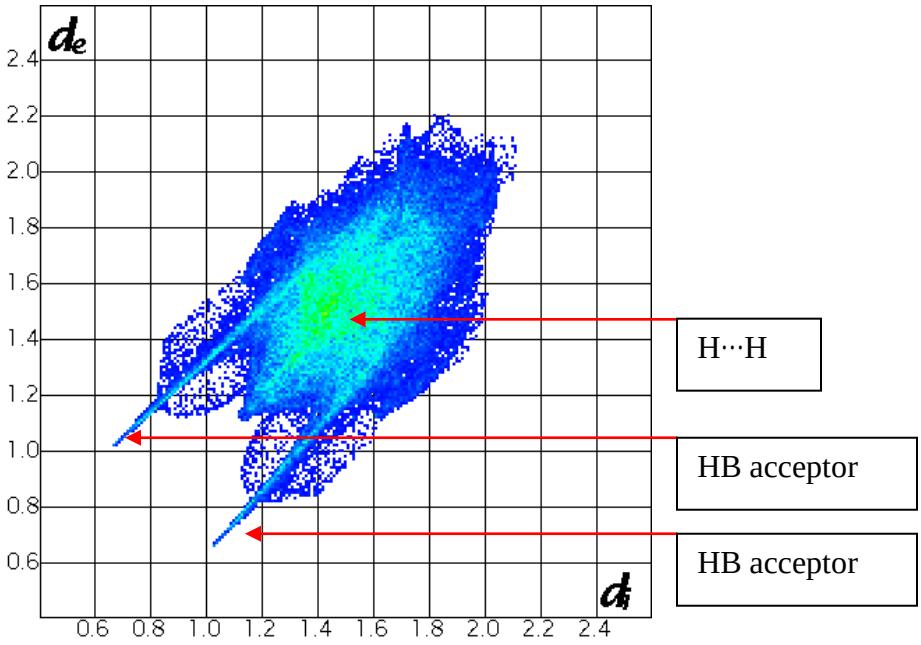

Figure 4.18 The 2-D fingerprint plot of *dicyclohexylammonium formate* hydrate indicating the various intermolecular interactions.

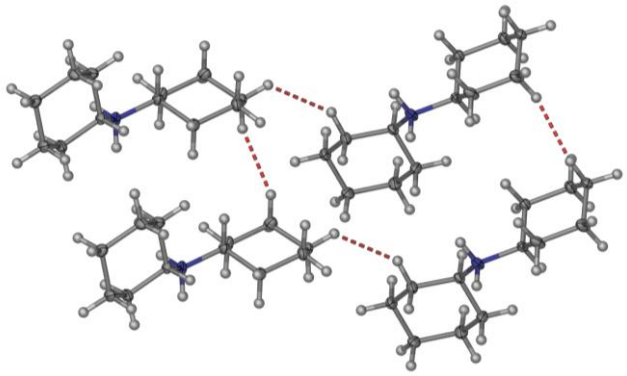

Figure 4.19 H···H interactions in *dicyclohexylammonium formate hydrate*.

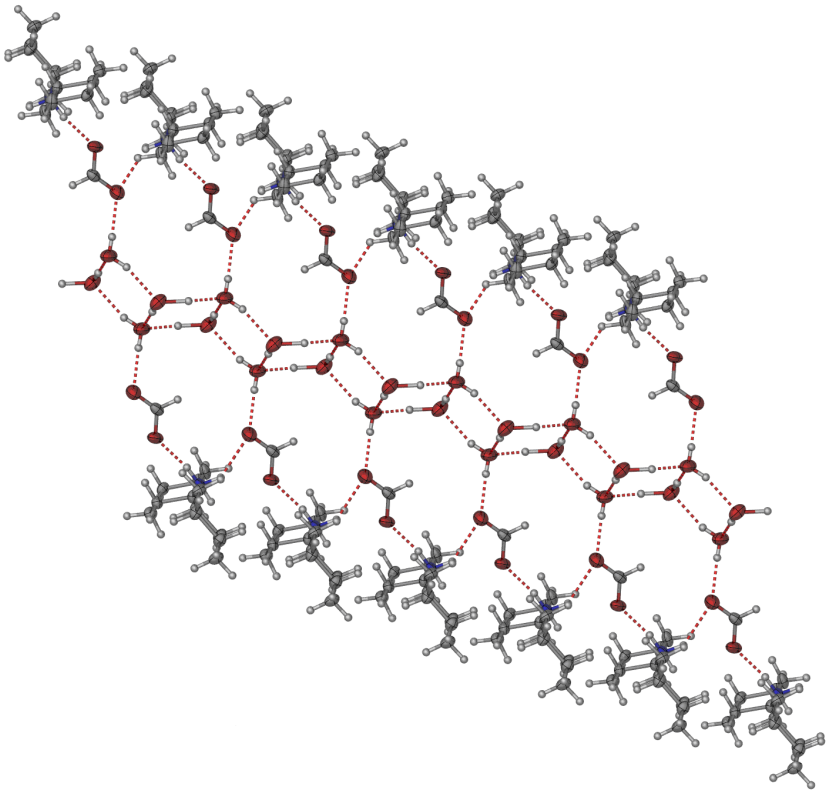

Figure 4.20 Water bridge between anion and cation in *dicyclohexylammonium formate hydrate*.

TGA analysis of **4** (Figure 4.21) shows an initial loss of surface water from the crystal structure followed by the loss of two waters, corresponding to the loss of water molecules between the H-bonded chains. The water loss between the hydrogen bonding chains results in the crystal structure breaking apart. Thus after the loss of the water molecules the complete decomposition of the crystal structure is seen on the thermogram.

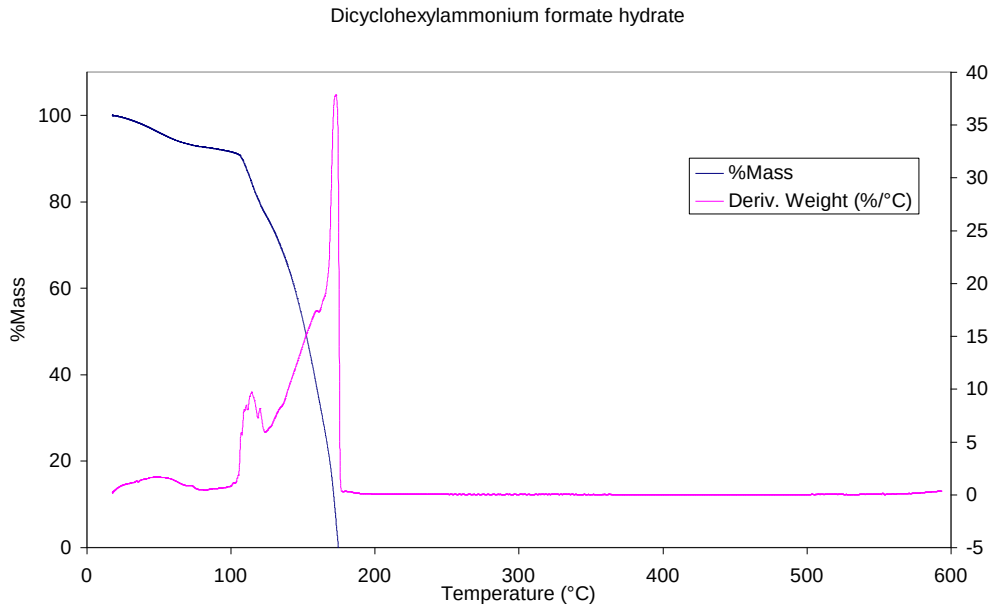

Figure 4.21 TGA of *dicyclohexylammonium formate hydrate*.

4.1.5 Dicyclohexylammonium phenylacetate (5)

This salt crystallised in the triclinic space group *P*-$\bar{I}$. There are hydrogen bonds between the dicyclohexylammonium and the phenylacetate [$N_{(3)}^{+}$-$H_{(H3A)}\cdots^{-}O_2OC$ (1.771 Å) and $N_{(3)}^{+}$-$H_{(H3B)}\cdots^{-}O_{(1)}OC$ (1.799 Å)], forming a 1-D hydrogen bonding chain along the *a*-axis, with the graph set notation $C_4^4(7)$ (Figure 4.22). The 2-D fingerprint plot generated by Crystal Explorer (Figure 4.23) shows all the intermolecular molecular interactions in **5**. The two sharp peaks from the plot are due to the interaction between donor cation (N^{+}-H) and acceptor anion ($^{-}$OOC). The intensity of the spots in the H···H interaction region of the plot indicates the presence of multiple H···H interactions in **5**. This arises due to close packing between the C-H groups of two cyclohexylammonium ions (Figure 4.24). The plot also shows evidence of C-H···π interactions, this is due to the C-H of the cyclohexylammonium interacting with the π-face of the

phenylacetate as shown in Figure 4.24. The hydrogen bonding chains are held together by C-H···π interactions to form sheets. These sheets stack on top of each other resulting in the 3-D structure (Figure 4.25).

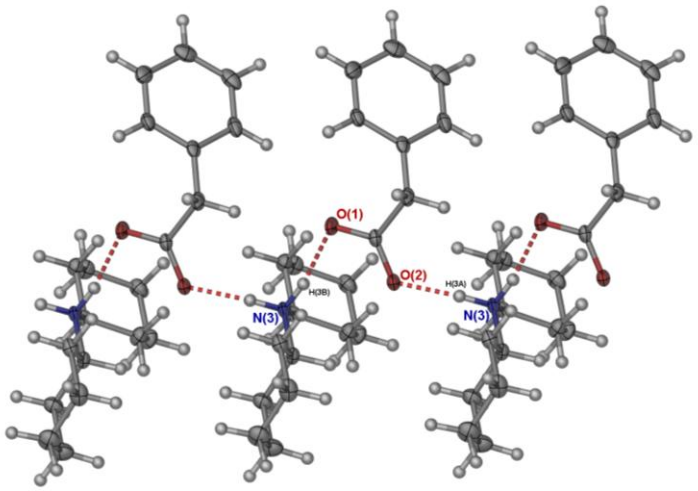

Figure 4.22 1-D hydrogen bonding in *dicyclohexylammonium phenylacetate*.

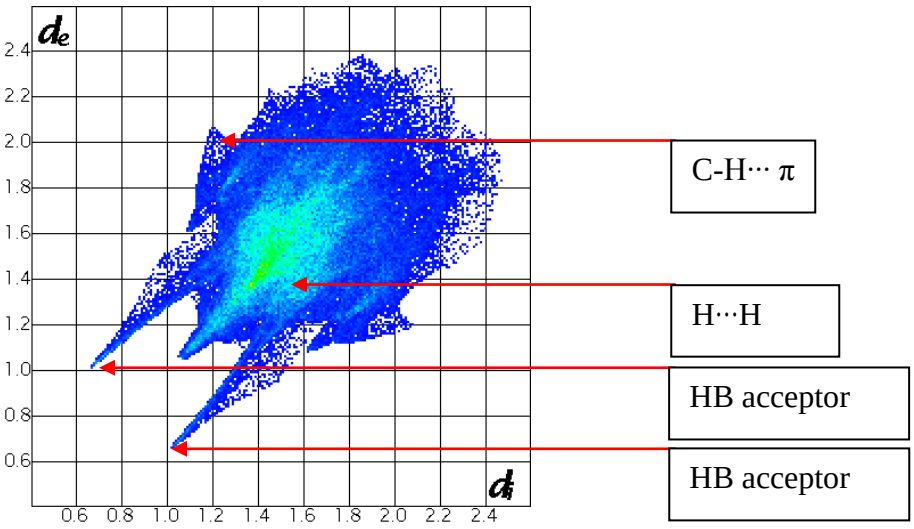

Figure 4.23 2-D fingerprint plot of *dicyclohexylammonium phenylacetate* indicating the various interactions.

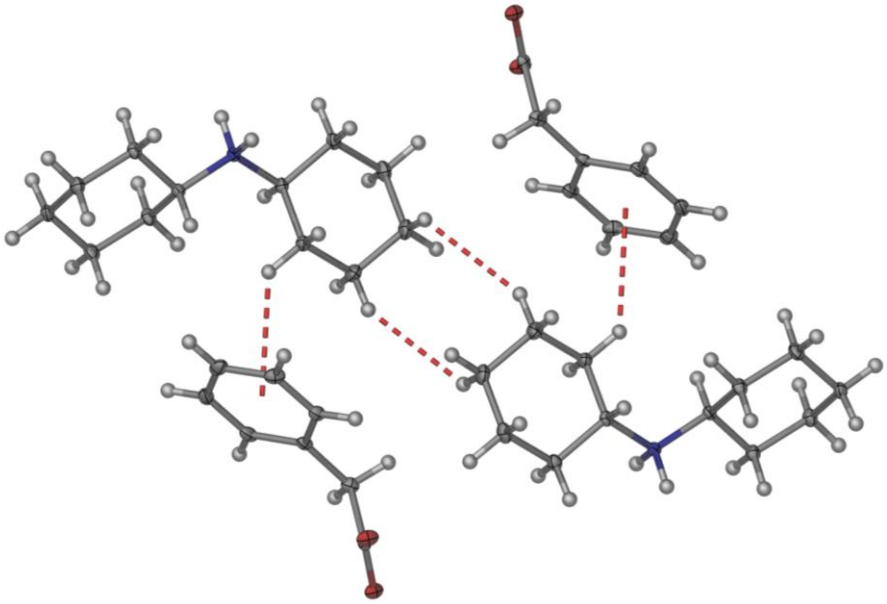

Figure 4.24 H···H interactions and C-H···π interactions in *dicyclohexylammonium phenylacetate*.

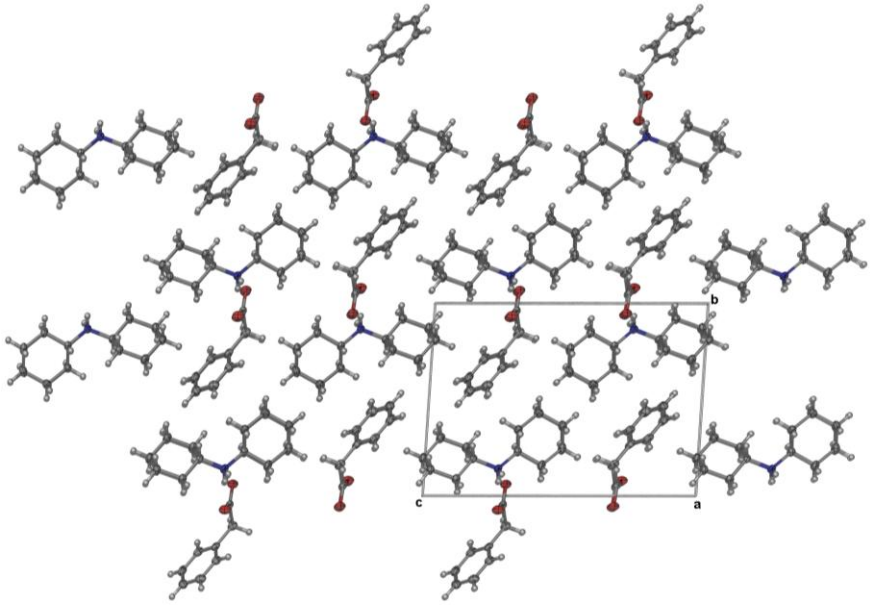

Figure 4.25 Molecular packing diagram of *dicyclohexylammonium phenylacetate*.

4.1.6 Dicyclohexylammonium diphenylacetate (6)

The salt crystallised in the triclinic space group *P1*. There are hydrogen bonds between the dicyclohexyalmmonium and the diphenylacetate [$N_{(1)}^{+}$-$H_{(1)}$···$^{-}O_{(3)}OC$ (1.852 Å), and $N_{(1)}^{+}$-$H_{(2)}$···$^{-}O_{(2)}OC$ (1.872 Å)], forming a 1-D hydrogen bonding chain along the *c*-axis, with the graph set notation $C_4^4(13)$ (Figure 4.26). The 2-D fingerprint plot generated by Crystal Explorer (Figure

4.27) has two sharp peaks due to hydrogen bonding interactions between the cation and anion. The intensity of the spots in the H···H region of the plot is an indication of multiple H···H interactions. These occur between the cyclohexylammonium C-H group and the diphenylacetate C-H groups (Figure 4.28). The fingerprint plot also indicates the presence of C-H···π interactions. These are between the C-H of the cyclohexylammonium and the π-face of the phenylacetate shown in Figure 4.28. The hydrogen bonded chains of the cations and anions are held together in sheets by C-H···π interactions. These sheets stack on top of each other with multiple H···H interactions between the sheets (Figure 4.29).

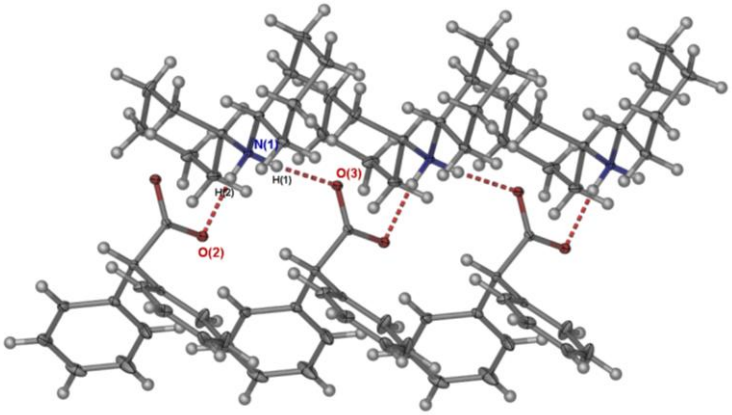

Figure 4.26 1-D Hydrogen bonding in *dicyclohexylammonium diphenylacetate*.

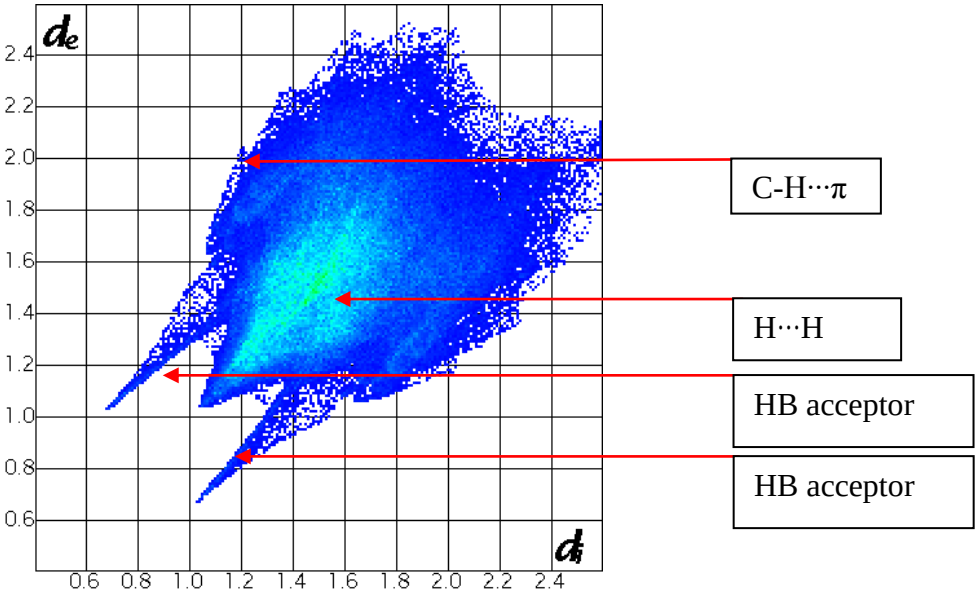

Figure 4.27 2-D fingerprint plot of *dicyclohexylammonium diphenylacetate* indicating the various interactions.

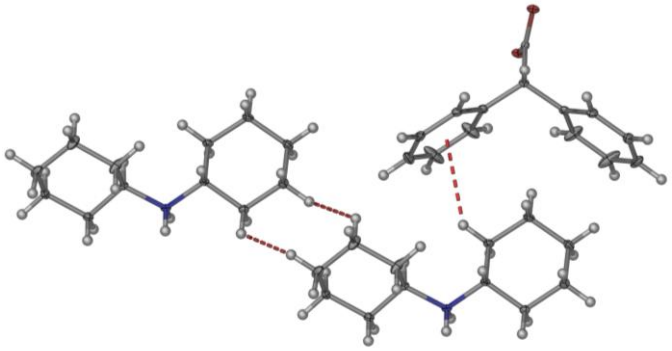

Figure 4.28 H···H interactions and C-H···π interactions in *dicyclohexylammonium diphenylacetate*.

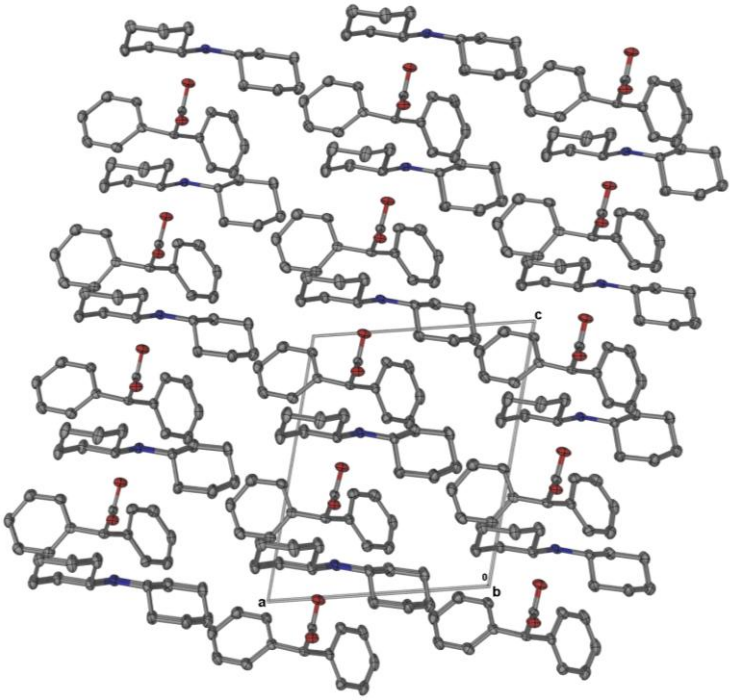

Figure 4.29 Molecular packing diagram of *dicyclohexylammonium diphenylacetate* (hydrogen atoms have been removed for clarity).

4.1.7 Dibutylammonium diphenylacetate (7)

This salt crystallised in the orthorhombic space group *Pca2₁* with two cations and anions in the asymmetric unit. There are hydrogen bonds between the dibutylammonium and the diphenylacetate [$N_{(4)}^{+}$-$H_{(4)}\cdots^{-}O_{(3)}OC$ (1.752 Å), $N_{(4)}^{+}$-$H_{(1)}\cdots^{-}O_{(1)}OC$(1.818 Å), $N_{(12)}^{+}$-$H_{(3)}\cdots^{-}O_{(2)}OC$(1.870 Å) and $N_{(12)}^{+}$-$H_{(2)}\cdots^{-}O_{(5)}OC$(1.793 Å)], forming 1-D hydrogen bonding chains

along the *b*-axis with graph set notation $C_4^4(12)$ (Figure 4.30). The two sharp peaks on the 2-D fingerprint plot (Figure 4.31) are due to the interaction between donor cation (N^+-H) and acceptor anion ($^-$OOC). The small wings on the sides of the fingerprint plot are an indication of multiple C-H···π interactions between the C-H of the phenyl group from the diphenylacetate and the π–face of the diphenylacetate (Figure 4.32), and interactions between the C-H of the dibutylammonium and the π–face of the diphenylacetate anion (Figure 4.32). Evidence of H···H interactions and alkyl-alkyl interactions are also visible between the dibutylammonium ions (Figure 4.33). The hydrogen bonded chains are held together in sheets by both the C-H···π interactions and alkyl-alkyl interactions. The sheets stack on top of each other and they are held together by the C-H···π (Figure 4.34).

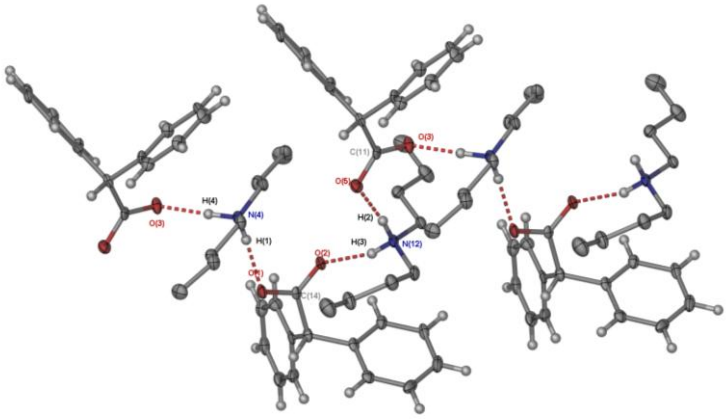

Figure 4.30 1-D hydrogen bonding (hydrogen atoms have been removed from the dibutylammonium for clarity).

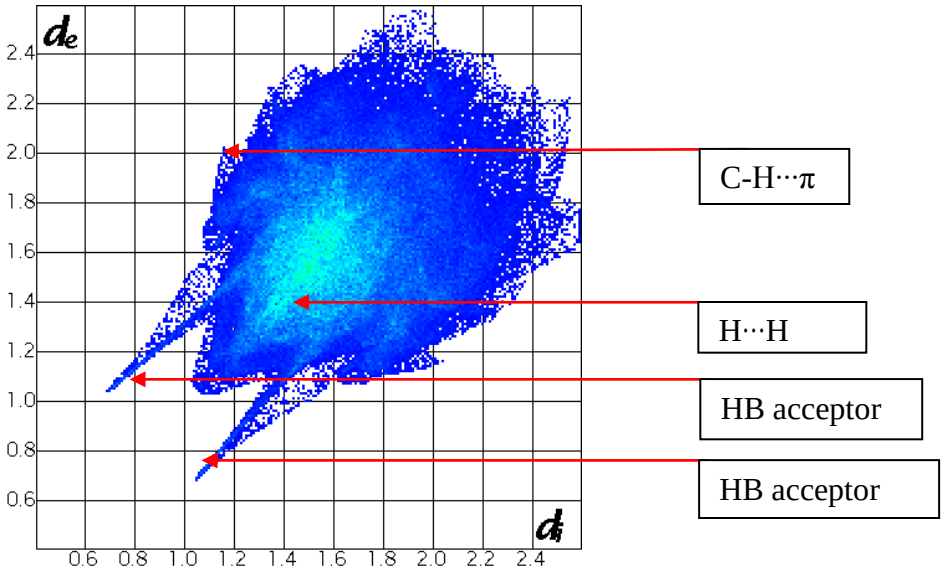

Figure 4.31 2-D fingerprint plot of *dibutylammonium diphenylacetate* indicating the various interactions.

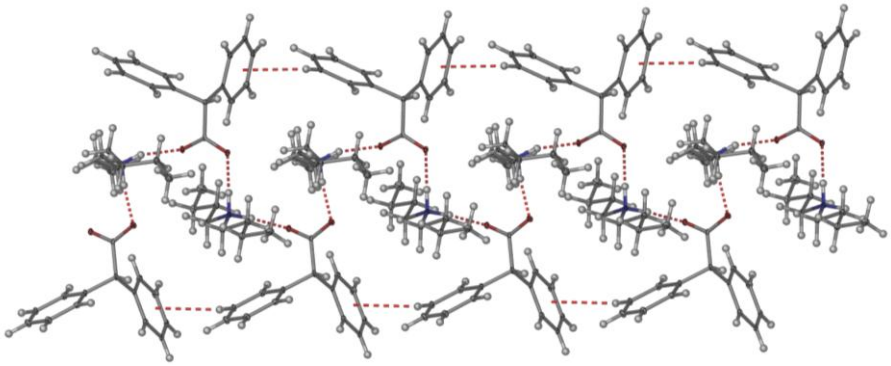

Figure 4.32 C-H···π interactions between diphenylacetate ions.

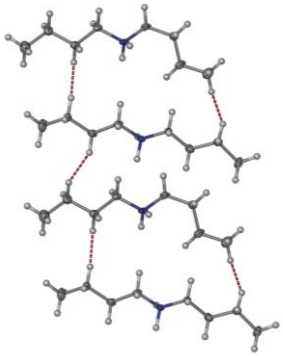

Figure 4.33 Alkyl-alkyl interaction in *dibutylammonium diphenylacetete*.

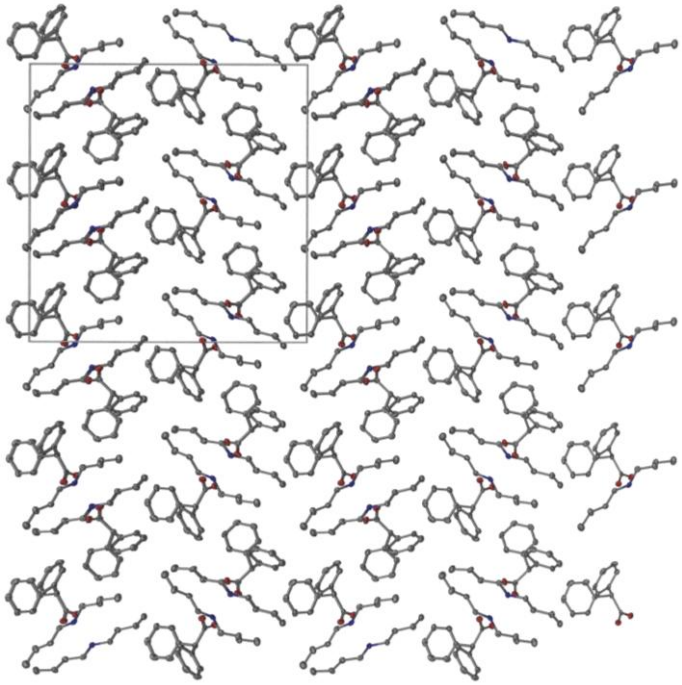

Figure 4.34 Molecular packing diagram of *dibutylammonium diphenylacetate*.

4.2 Crystal structure analysis of primary ammonium carboxylate salts

4.2.1 Propylammonium diphenylacetate (8)

This salt crystallised in the monoclinic space group *P2₁/c*. There are hydrogen bonds between the propylammonium and the diphenylacetate ions [bonds $N_{(1)}^{+}$-$H_{(1N)}\cdots^{-}O_{(2)}OC$ (1.74(2) Å), $N_{(1)}^{+}$-$H_{(3N)}\cdots^{-}O_{(1)}OC$ (1.82(2) Å) and $N_{(1)}^{+}$-$H_{(2N)}\cdots^{-}O_{(1)}OC$ (1.850(17) Å)]. The repetition of this type of hydrogen bonding forms extensive ladders along the *b*-axis (Figure 4.35). The ladder is made up of rings with the graph set notation $R_4^3(10)$. The two sharp peaks on the 2-D fingerprint plot (Figure 4.36) are due to the interaction between the donor cation (N^{+}-H) and acceptor anion ($^{-}$OOC). The plot also shows the presence of C-H···π interactions; these are between the C-H of the methylene group on the propylammnonium and the π–face of the phenyl group from the diphenylacetate (Figure 4.37). Other C-H···π interactions occur between the C-H of the phenyl group and the π–face of another phenyl group from the diphenylacetate (Figure 4.37). The plot also indicates the presence of multiple H···H interactions. This is due to the alkyl-alkyl interactions between the propylammonium groups (Figure 4.38). The hydrogen bonding ladders are held together in sheets along the *b*-axis by C-H···π interactions between the C-H of the methylene groups from the propylammonium and the π–face phenyl groups from the diphenylacetate. These hydrogen bonding sheets stack next to each other with C-H···π interactions between the C-H phenylacetate and the π–face of another phenyl group from the diphenylacetate, forming a 3-D structure (Figure 4.39).

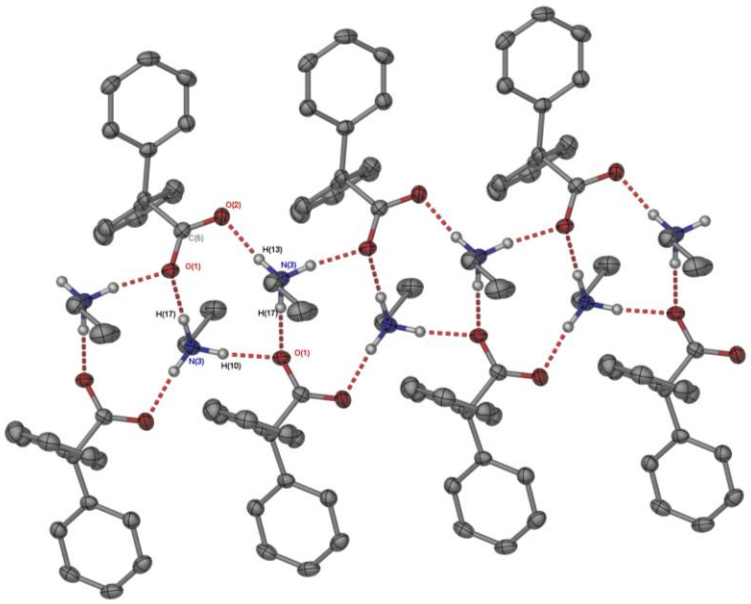

Figure 4.35 Hydrogen bonding in 8 (hydrogen atoms on anions have been removed for clarity).

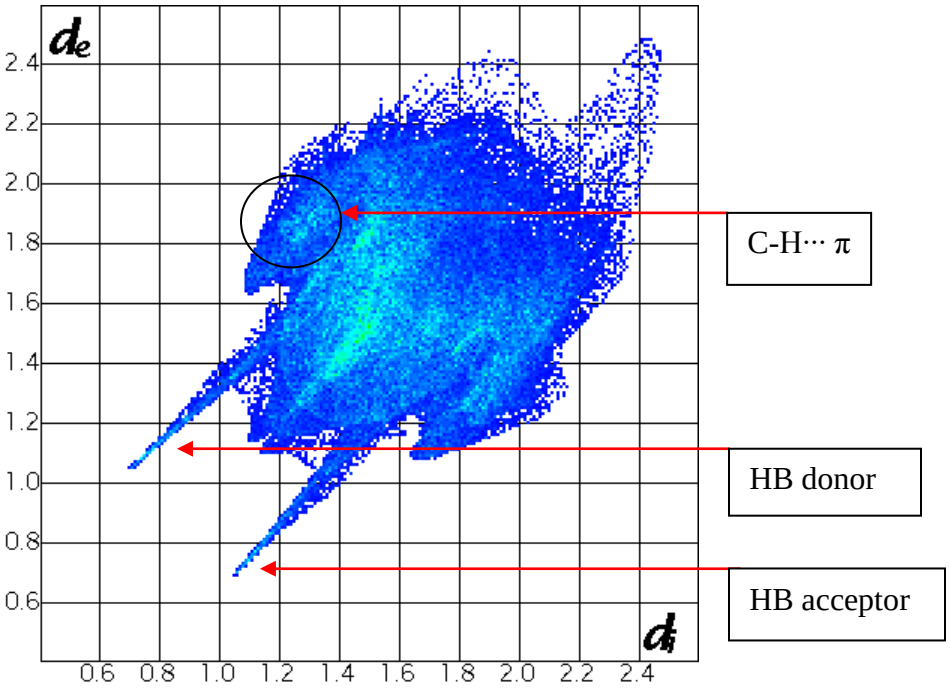

Figure 4.36 2-D fingerprint plot of *propylammonium diphenylacetate* indicating the various interactions.

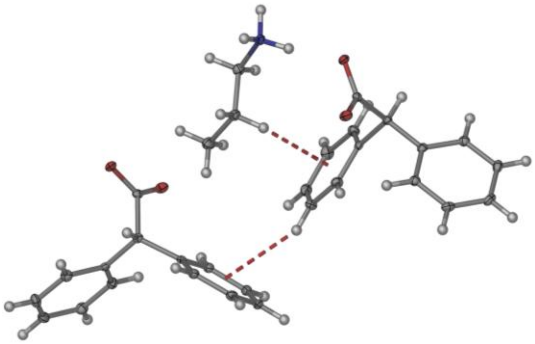

Figure 4.37 C-H···π interactions in *propylammonium diphenylacetate*.

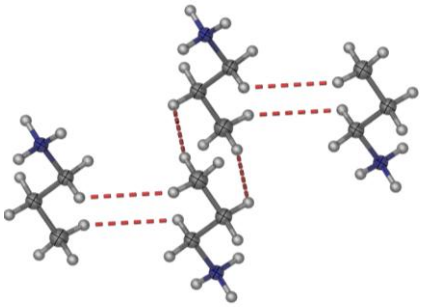

Figure 4.38 H···H interactions in *propylammonium diphenylacetate*.

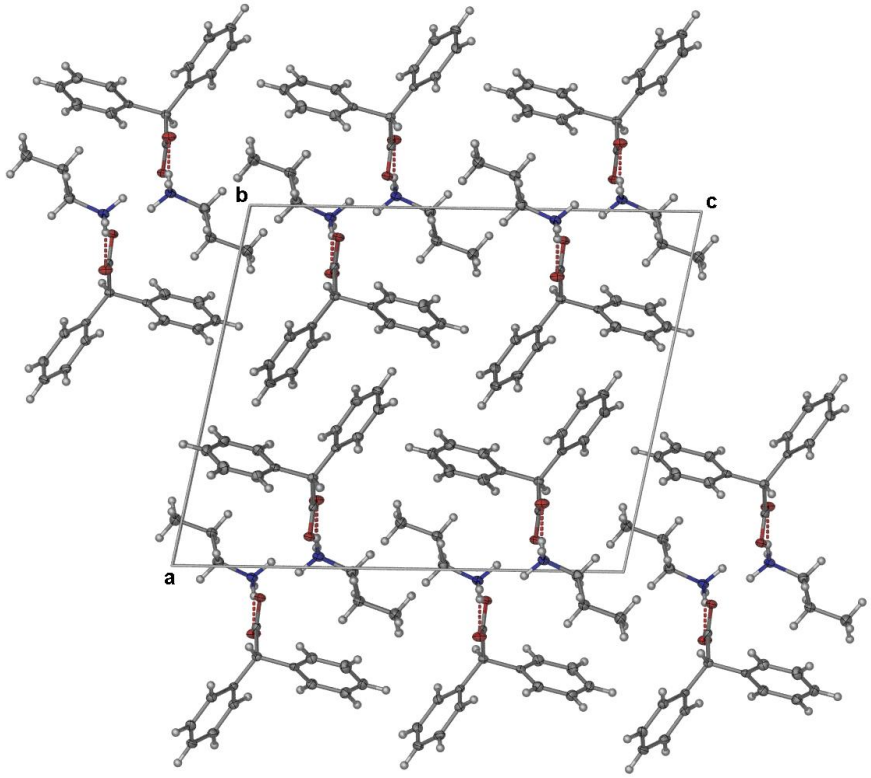

Figure 4.39 The molecular packing diagram of *propylammonium diphenylacetate*.

4.2.2 Benzylammonium formate (9)

This salt crystallised in the orthorhombic space group *Pbca*. There are hydrogen bonds between the benzylammonium and the formate ions [$N_{(1)}{}^{+}$-$H_{(3N)}\cdots{}^{-}O_{(1)}OC$ (1.820(13) Å), $N_{(1)}{}^{+}$-$H_{(1N)}\cdots{}^{-}O_{(2)}OC$ (1.846(14) Å) and $N_{(1)}{}^{+}$-$H_{(2N)}\cdots{}^{-}O_{(2)}C$ (1.938(14) Å], forming a cyclic hydrogen bonded network along the *b*-axis, with graph set notation $R_6^5(16)$ (Figure 4.40). The sharp peaks from the 2-D fingerprint plot (Figure 4.41) are due to the interactions between the donor cation (N^{+}-H) and acceptor anion ($^{-}$OOC). The plot shows evidence of C-H··· π interactions, this is due to the interaction between the C-H of the phenyl group from the benzylammonium and the π–face of the phenyl group from the benzylammonium (Figure 4.42) The cyclic hydrogen bonding nets stack next to each other due to the C-H··· π interactions between the π–face of the phenyl group from the benzylammonium and the π–face of the adjacent phenyl group of another benzylammonium in a adjacent sheet (Figure 4.42). These interactions led to the formation of a 3-D structure (Figure 4.43).

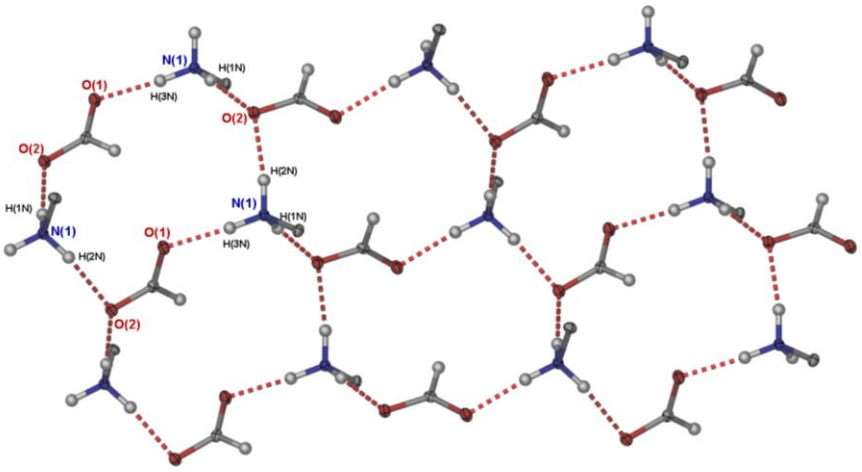

Figure 4.40 Hydrogen bonded nets in 9 (phenyl group has been removed to show hydrogen bonding networks).

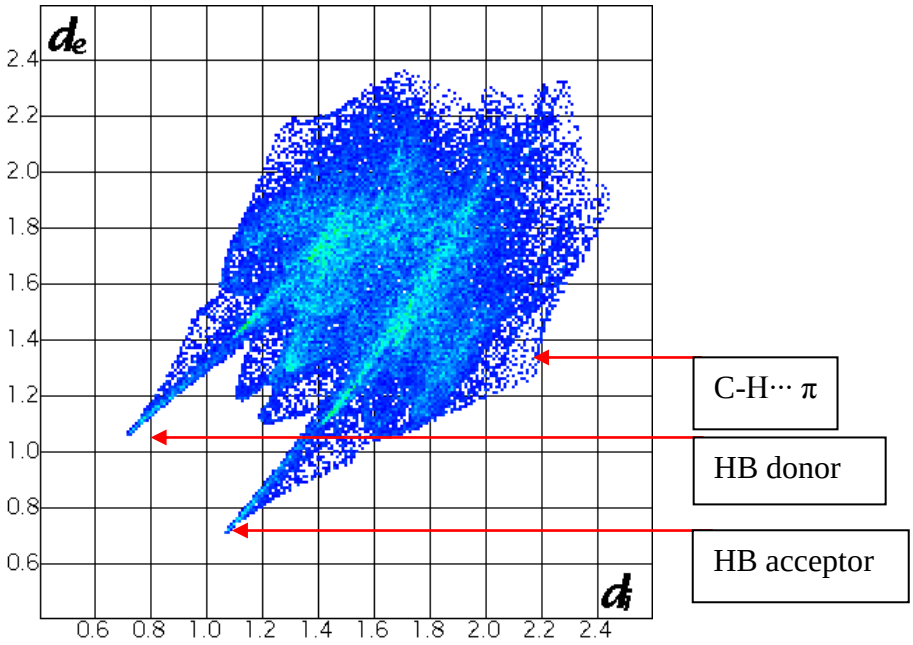

Figure 4.41 2-D fingerprint plot of *benzylammonium formate* indicating the various interactions.

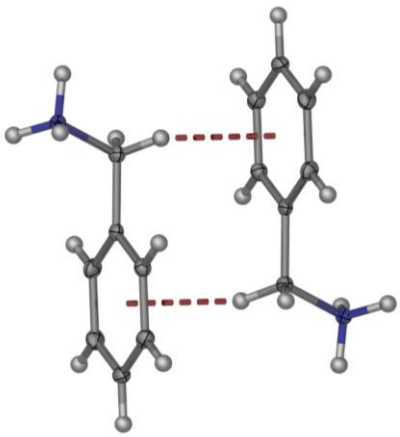

Figure 4.42 C-H···π interactions between adjacent benzylammonium ions.

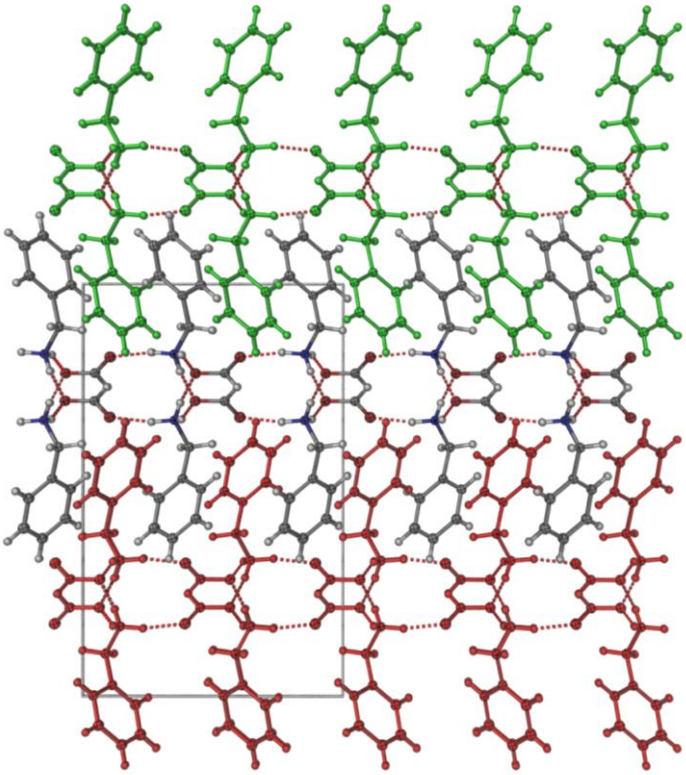

Figure 4.43 The molecular packing diagram of *benzylammonium formate*.

4.2.3 Benzylammonium acetate (10)

This salt crystallised in the monoclinic space group $P2_1/n$ with two anions and cations pairs in the asymmetric unit. There are hydrogen bonds between the benzylammonium and the acetate [$N_{(1)}^{+}$-$H_{(1N)}\cdots^{-}O_{(1)}OC$ (1.900(15) Å), N_1^{+}-$H_{(2N)}\cdots^{-}O_{(2)}OC$ (1.770(15) Å), $N_{(1)}^{+}$-$H_{(3N)}\cdots^{-}O_{(3)}C$ (1.730(16) Å), $N_{(2)}^{+}$-$H_{(4N)}\cdots^{-}O_{(1)}OC$ (1.917(16) Å), $N_{(2)}^{+}$-$H_{(5N)}\cdots^{-}O_{(4)}C$ (1.952(15) Å) and $N_{(2)}^{+}$-$H_{(6N)}\cdots^{-}O_{(4)}OC$ (1.838(15) Å)], forming hydrogen bonded nets along the *c*-axis, with graph set notation $C_4^3(11)$ (Figure 4.44). The two sharp peaks from the 2-D fingerprint plot (Figure 4.45) are due to the interaction between the donor cation (N^{+}-H) and acceptor anion ($^{-}$OOC). The 2-D fingerprint plot indicates evidence of C-H··· π interactions, which are between the C-H of the phenyl group on the benzylammonium and the π–face of the phenyl group from an adjacent benzylammonium (Figure 4.46). Evidence from the plot also indicates that π···π interactions are present, which arises due to the π···π interaction between the two benzylammonium ions (Figure 4.46). The hydrogen bonding nets stack on top of each other with C-H···π and π···π interactions between layers (Figure 4.47).

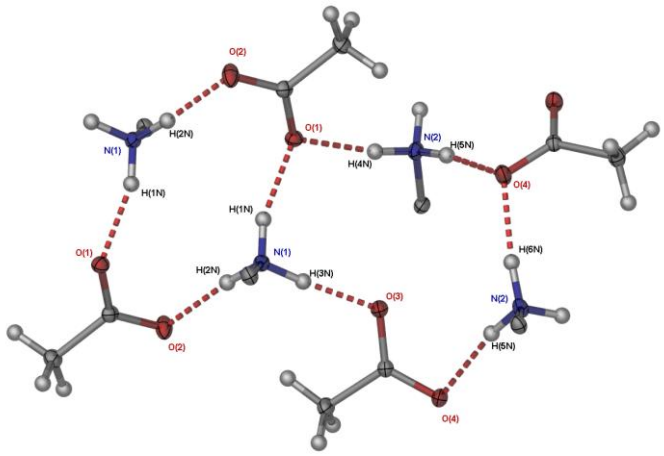

Figure 4.44 Hydrogen bonded nets in *benzylammonium acetate* (the phenyl groups from the cation have been removed for clarity).

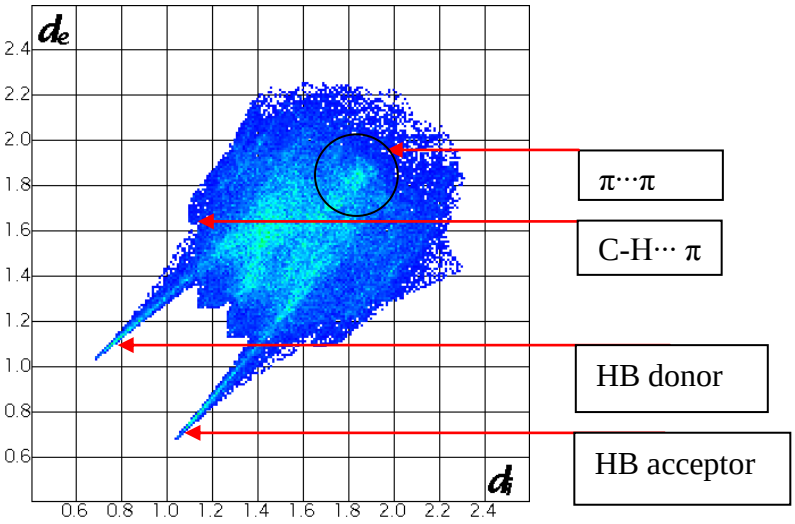

Figure 4.45 2-D fingerprint plot of benzylammonium acetate indicating the various interactions.

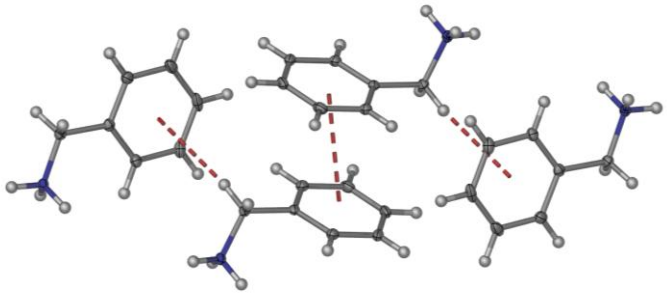

Figure 4.46 C-H···π and π···π interactions in *benzylammonium acetate*.

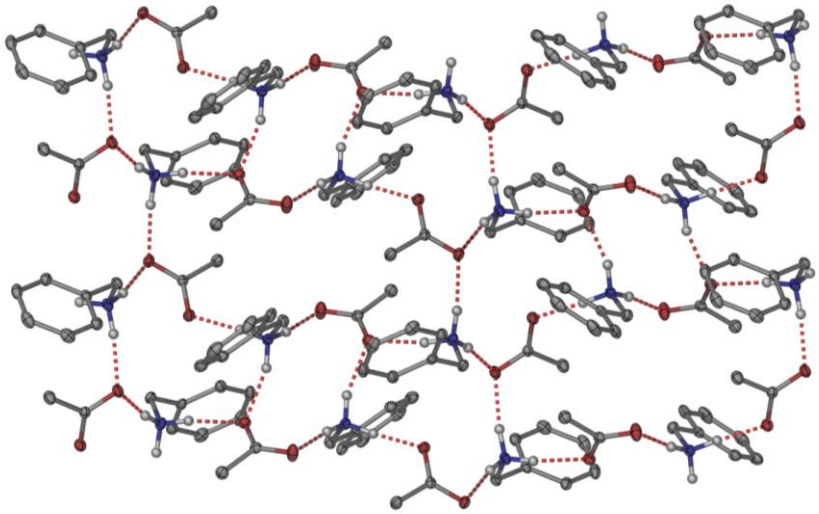

Figure 4.47 The molecular packing diagram of *benzylammonium acetate* (some hydrogen atoms have been removed for clarity).

4.2.4 Benzylammonium propionate hydrate (11)

This salt crystallised in the monoclinic space group $P2_1/c$. There are hydrogen bonds between the benzylammonium and the propionate [$N_{(1)}^{+}$-$H_{(1N)}$···$^{-}O_{(1)}OC$ (1.817(17) Å), $N_{(1)}^{+}$-$H_{(2N)}$···$^{-}O_{(2)}OC$ (1.896(15) Å), $N_{(1)}^{+}$-$H_{(3N)}$···$^{-}O_{(1)}C$ (1.907(18) Å], forming a hydrogen bonded ring, with graph set notation $R_4^3(10)$ (Figure 4.48). The two sharp peaks from the 2-D fingerprint plot (Figure 4.49) are due to the interaction between the donor cation (N^{+}-H) and acceptor anion ($^{-}$OOC). There is also a hydrogen bond between the water molecule and propionate ion [O_{1W}-H_{2W}···$^{-}O_2OC$ (2.01(2) Å)] (Figure 4.48). The 2-D fingerprint plot also indicates evidence of H···H contacts, which is due to the interaction between the benzylammonium and propionate (Figure 4.50). Evidence from the plot shows C-H··· π interactions, this is due to the interaction between the C-H of the

methyl group from the propionate and the π–face of the phenyl group from the benzylammonium. Another C-H··· π interaction interaction is visible between the C-H of the benzylammonium and the π–face of an adjacent benzylammonium (Figure 4.51). The hydrogen bonding rings formed by the cation and anion interaction between benzylammonium and propionate are held together by a hydrogen bonding interaction between the water molecules. The C-H···π interactions between the C-H of the methyl group from the propionate and the π–face of the phenyl group from the benzylammonium form extended sheets. These sheets stack next to each other with C-H··· π interactions of the C-H of the benzylammonium and the π–face of an adjacent benzylammonium between sheets, forming the 3-D structure (Figure 4.52).

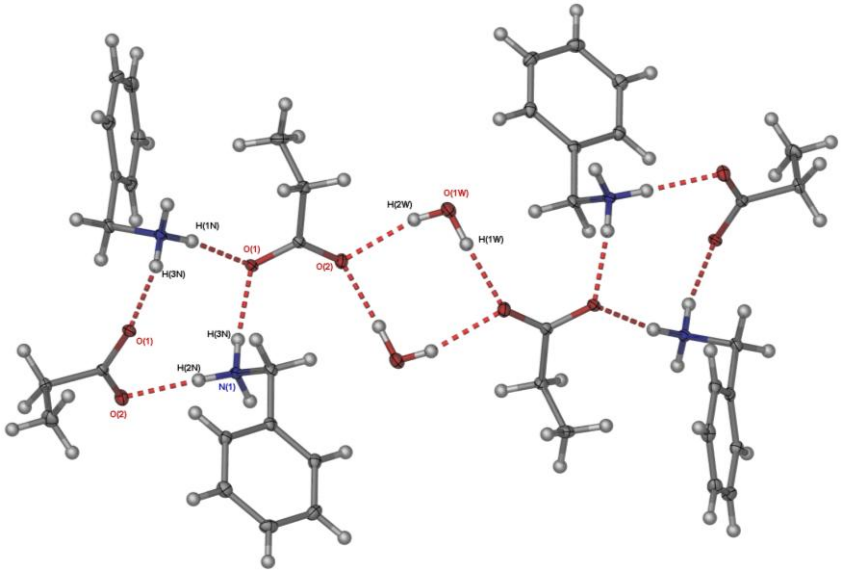

Figure 4.48 Hydrogen bonding in *benzylammonium propionate hydrate*.

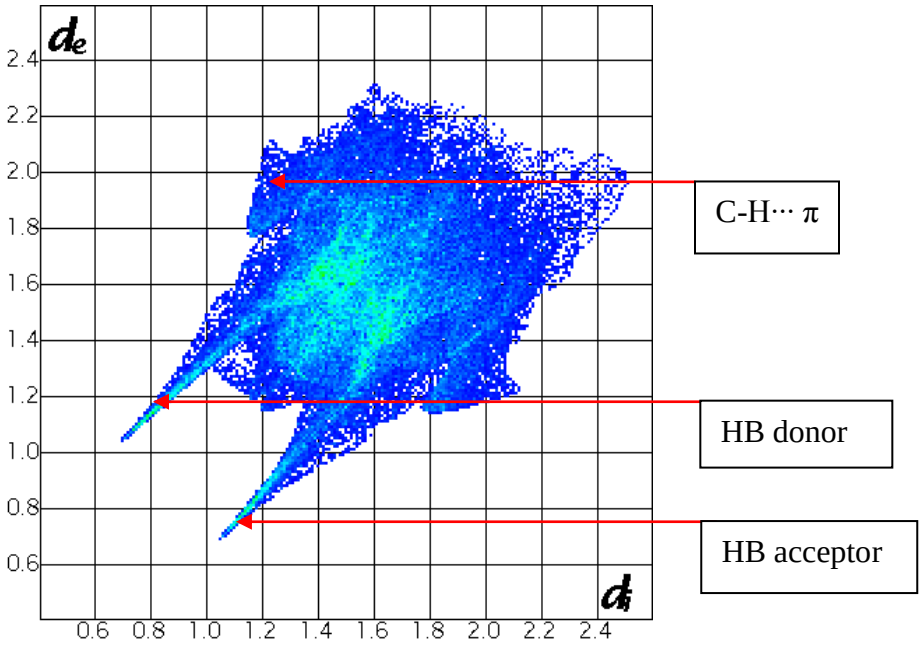

Figure 4.49 2-D fingerprint plot of *benzylammonium propionate hydrate* indicating the various interactions.

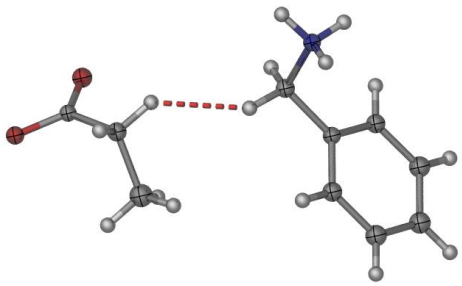

Figure 4.50 H···H contacts in *benzylammonium propionate hydrate*.

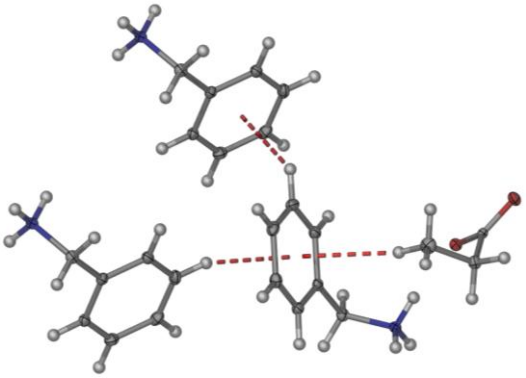

Figure 4.51 C-H···π interactions in *benzylammonium propionate hydrate*.

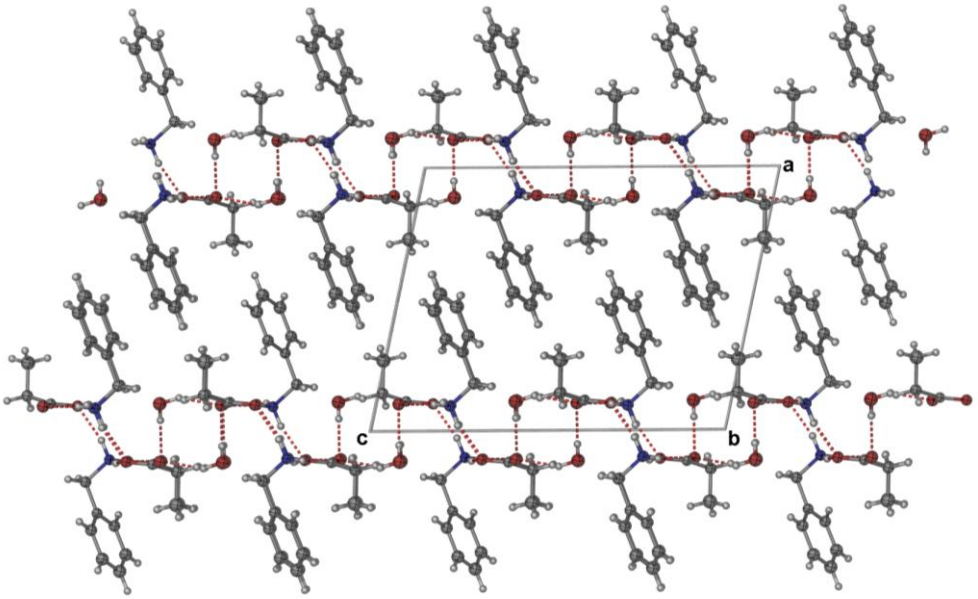

Figure 4.52 Molecular packing diagram of *benzylammonium propionate hydrate*.

The thermogram of 11 (Figure 4.53) does not show complete loss of water from the structure. An initial loss shown on the thermogram could be from loss of surface water. With an increase in temperature the thermogram shows the complete decomposition of the crystal structure. Upon examining the crystal structure (Figure 4.56), it is clear that the water molecules act as a bridge between cation-anion chains, holding the structure together. If these water molecules are removed between the cation-anion chains the crystal structure would collapse. Therefore the loss of water due to the increase in temperature results in the complete decomposition of the crystal structure.

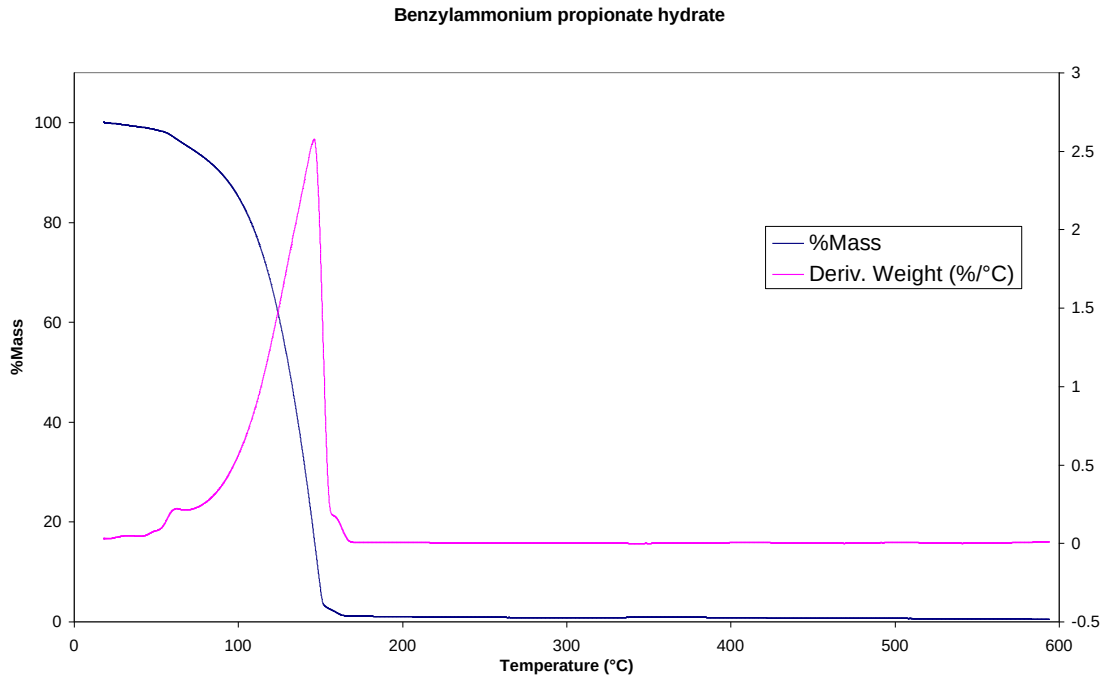

Figure 4.53 TGA of *benzylammonium propionate hydrate*.

4.2.5 Cyclohexylammonium acetate (12)

This salt crystallised in the monoclinic space group *C2/c*. There are hydrogen bonds between the cyclohexylammonium and the acetate [$N_{(1)}^{+}$-$H_{(1N)}\cdots^{-}O_{(2)}OC$ (1.860(14) Å), $N_{(1)}^{+}$-$H_{(2N)}\cdots^{-}O_{(2)}OC$ (1.872(16) Å) and $N_{(1)}^{+}$-$H_{(3N)}\cdots^{-}O_{(1)}C$ (1.824(14) Å], forming hydrogen bonding ladders along the *b*-axis, with graph set notation $R_4^3(10)$ (Figure 4.54). This structure shows a similar hydrogen bonding pattern to that of *propylammonium diphenylacetate* **(9)**. The two sharp peaks from the 2-D fingerprint plot (Figure 4.55) are due to the interaction between the donor cation (N^{+}-H) and acceptor anion ($^{-}$OOC). Additional hydrogen bonding interactions between the C-H of the cyclohexylammonium and the O of the acetate further strengthen the hydrogen bonding interactions in the structure (Figure 4.56). The intensity of the spots in the H···H intermolecular region of the 2-D fingerprint plot indicates that multiple H···H interactions are present within the structure. This is due to the interaction between the two cyclohexylammonium ions (Figure 4.57). The hydrogen bonding ladders are close packed into sheets, with H···H interactions between the C-H groups from the cyclohexylammonium ions. These sheets stack next to each

other with additional H···H interaction between the C-H groups of the cyclohexylammonium ions (Figure 4.58).

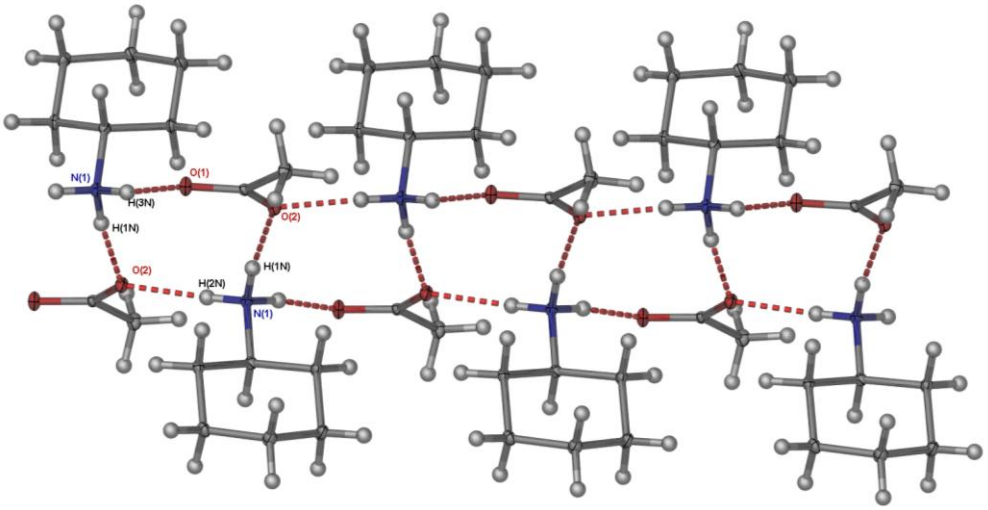

Figure 4.54 Hydrogen bonding ladders in *cyclohexylammonium acetate*.

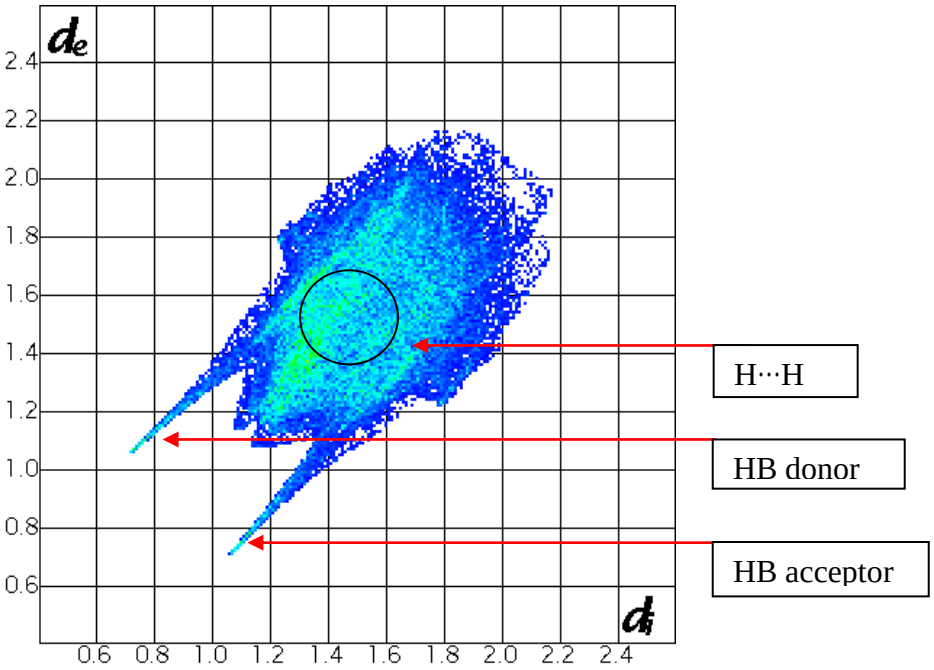

Figure 4.55 2-D fingerprint plot of *cyclohexylammonium acetate* indicating the various interactions.

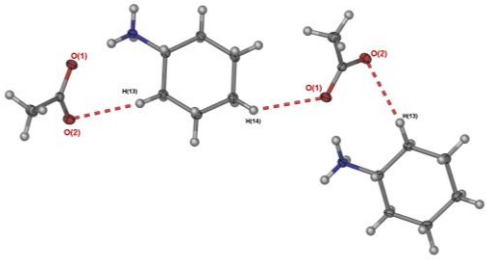

Figure 4.56 C-H···O interactions in *cyclohexylammonium acetate*.

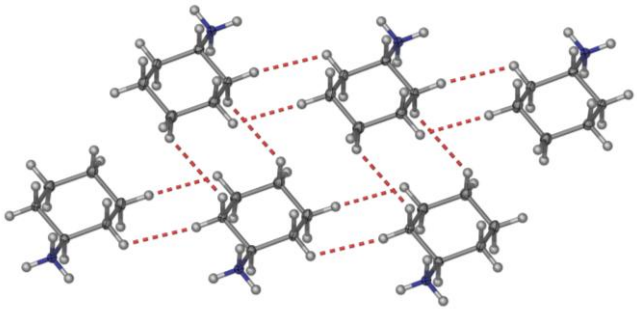

Figure 4.57 H···H contacts in *cyclohexylammonium acetate.*

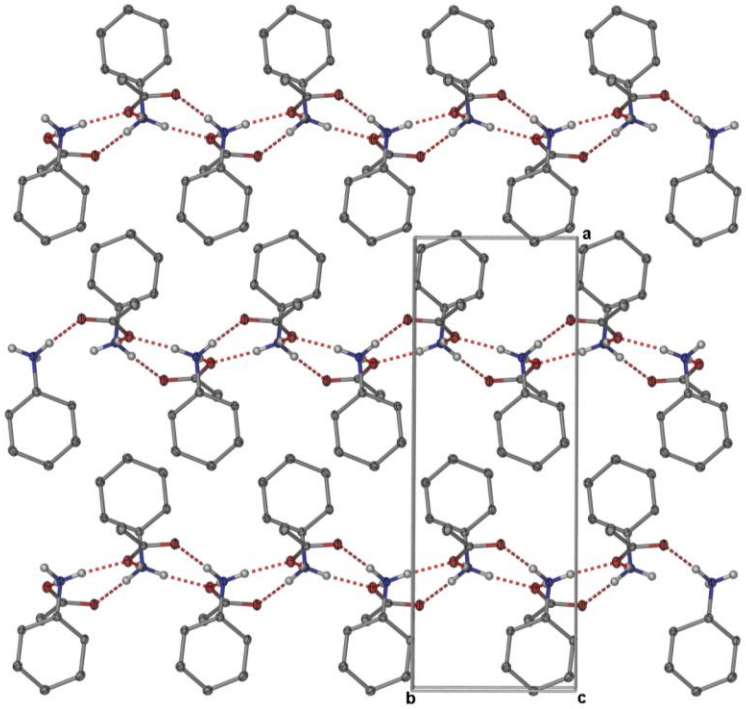

Figure 4.58 The molecular packing diagram of *cyclohexylammonium acetate* (some hydrogen atoms have been removed for clarity).

4.2.6 Anilinium benzoate benzoic acid (13)

This combination of acid and base resulted in the formation of a co-crystal of a salt, which contains both the un-protonated acid and the cation and anion salt. The co-crystal of a salt crystallised in the monoclinic space group $P2_1/n$. There are hydrogen bonds between anilinium and benzoate [$N_{(1)}^{+}$-$H_{(1N)}\cdots^{-}O_1OC$ (1.867(19) Å), $N_{(1)}^{+}$-$H_{(2N)}\cdots^{-}O_{(2)}OC$ (1.84(3) Å) and $N_{(1)}^{+}$-$H_{(3N)}\cdots^{-}O_{(2)}OC$ (1.92(3) Å, N_1^{+}-$H_{(3N)}\cdots^{-}O_{(3)}C$ (2.71(2) Å], forming a hydrogen bonding ring, with graph set notation $R_4^4(12)$ (Figure 4.59). There is another hydrogen bond between the benzoic acid and benzoate [O_4-$H_{3N}\cdots O_1$ (1.70(4) Å)] (Figure 4.59). The two sharp peaks from the 2-D fingerprint plot (Figure 4.60) are due to the interaction between the donor cation (N^{+}-H) and acceptor anion ($^{-}$OOC). The 2-D fingerprint plot shows evidence for C-H···π interactions, which form between the C-H of the phenyl group from the benzoic acid and the π–face of the phenyl group from the anilinium. An additional C-H···π interaction between a C-H on the benzoic acid and the π–face of the benzoate is also present (Figure 4.61). Evidence from the 2-D fingerprint plot also indicates that π···π interactions are present; this is due to the π–face of the anilinium to π–face of the benzoic acid (Figure 4.62). The hydrogen bonding rings formed by the cation-anion interactions are held together by the additional hydrogen bonding between the benzoic acid and the benzoate ion. These hydrogen bonding ladders are held together by C-H···π interactions between the phenyl groups and the anilinium forming extended sheets. These sheets stack on top of one another via π···π interactions between the π–face of anilinium and the π–face of benzoic acid resulting in the 3-D structure shown in Figure 4.62.

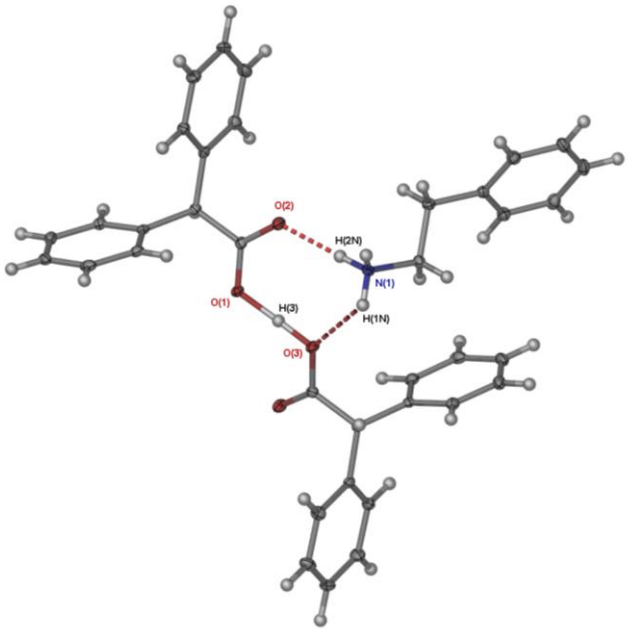

Figure 4.59 Hydrogen bonding in *anilinium benzoate benzoic acid*.

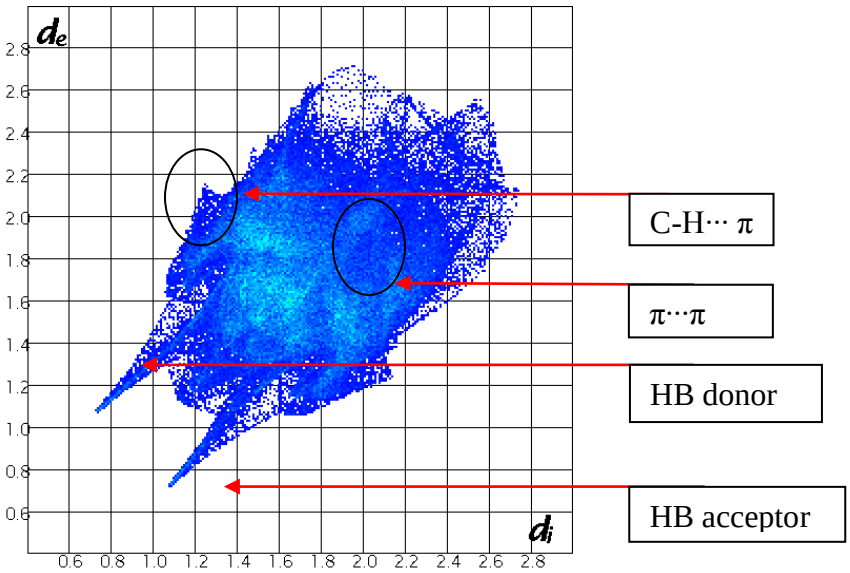

Figure 4.60 2-D fingerprint plot of *anilinium benzoate benzoic acid* indicating the various interactions.

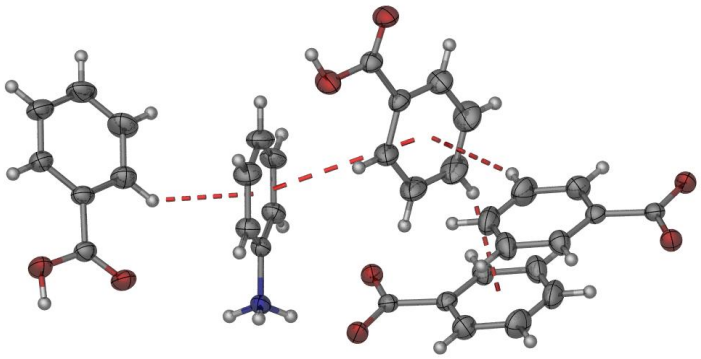

Figure 4.61 C-H···π and π···π interactions in *anilinium benzoate benzoic acid*.

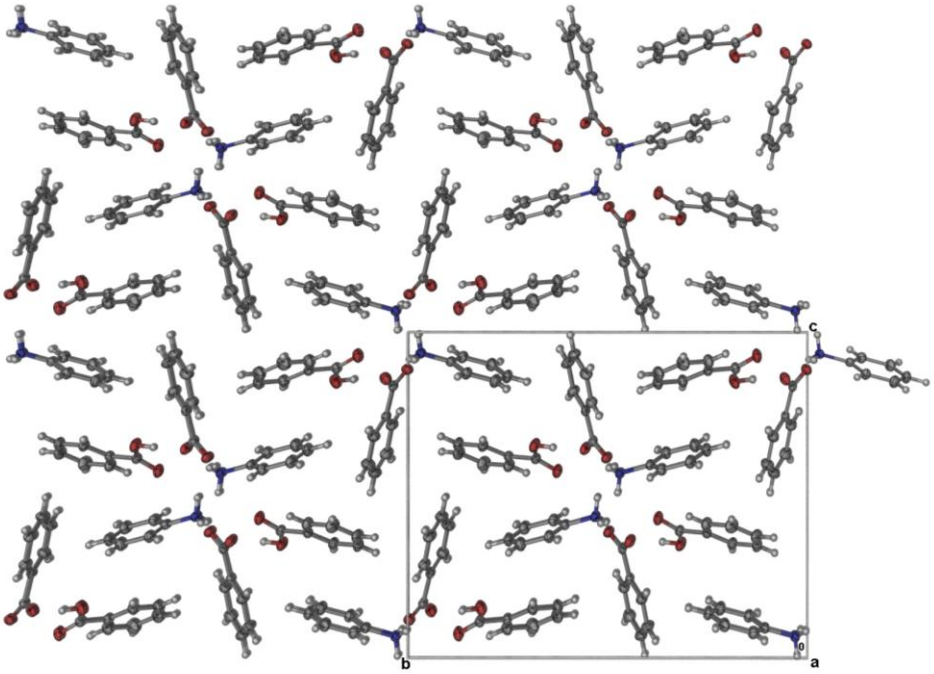

Figure 4.62 The molecular packing diagram of *anilinium benzoate benzoic acid*.

4.2.7 1-Phenylethylammonium diphenylacetate diphenylacetic acid (14)

This combination of acid and base resulted in the formation of a co-crystal of a salt, which crystallised in a monoclinic space group *P2₁ /c*. There are hydrogen bonds between the 1-phenylethylammonium and diphenylacetate [$N_{(1)}^{+}$-$H_{(1N)}$···$^{-}O_{(3)}OC$ (2.258(14) Å), $N_{(1)}^{+}$-$H_{(1N)}$···$^{-}O_{(4)}OC$ (2.095(3) Å), $N_{(1)}^{+}$-$H_{(2N)}$···$^{-}O_{(2)}OC$ (1.863(17) Å) and $N_{(1)}^{+}$-$H_{(3N)}$···$^{-}O_{(3)}OC$ (1.910(16) Å], as well as between the diphenylacetic acid and the diphenylacetate [$O_{(3)}$-$H_{(3)}$ ···$O_{(3)}$ (1.33(2) Å)]. This results in a hydrogen bonding ring with graph set notation $R_3^2(8)$ (Figure 4.63). The hydrogen atom involved in hydrogen bonding between the diphenylacetate anion and the diphenylacetic acid is positioned almost equidistant from both oxygen atoms, indicating that this is a strong hydrogen bond.

The two sharp peaks on the 2-D fingerprint plot (Figure 4.64) are due to the interaction between the donor cation (N^{+}-H) and acceptor anion ($^{-}$OOC). Evidence from the 2-D fingerprint plot indicate that there are multiple C-H···π interactions. This arises due to the interaction between the C-H of the phenyl group from the diphenylacetatic acid and the π–face of the 1-phenylethylammonium (Figure 4.65). There is another C-H···π interaction between the C-H of the diphenylacetate and the π–face of another diphenylacetate (Figure 4.66). The hydrogen bonding chain is held together in sheets by C-H···π interactions between 1-phenylethylammonium and diphenylacetic acid. These sheets stack on top of one another and are further extended by C-H···π interactions between the C-H of the diphenylacetate with the π–face of another phenylacetate, resulting in the 3-D structure (Figure 4.67)

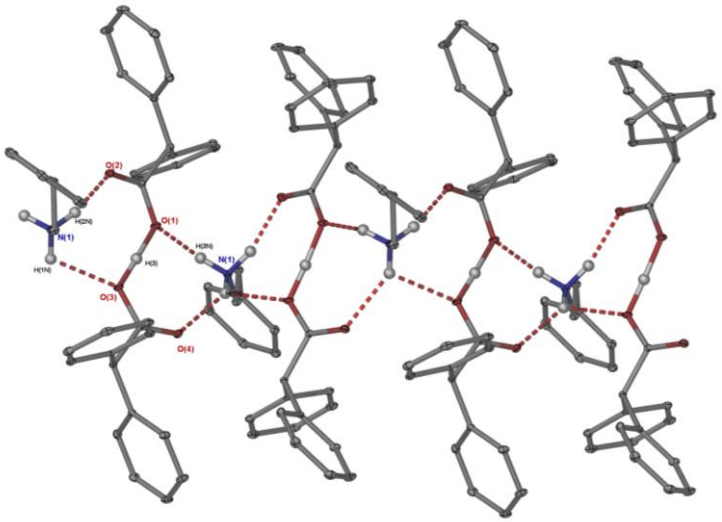

Figure 4.63 Hydrogen bonding in 14 (some hydrogen atoms have been removed for clarity).

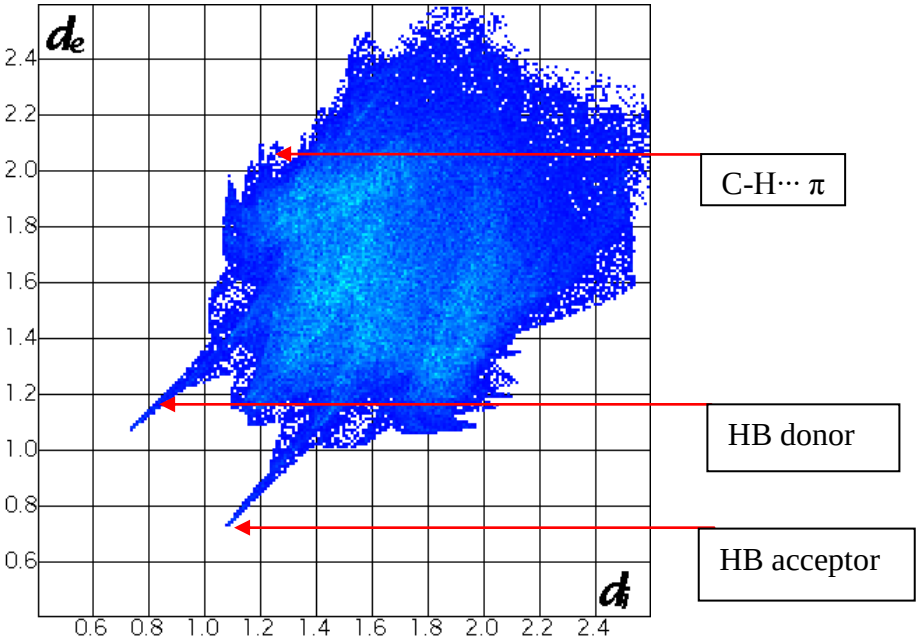

Figure 4.64 2-D fingerprint plot of *1-phenylethanammonium diphenylacetate* indicating the various interactions.

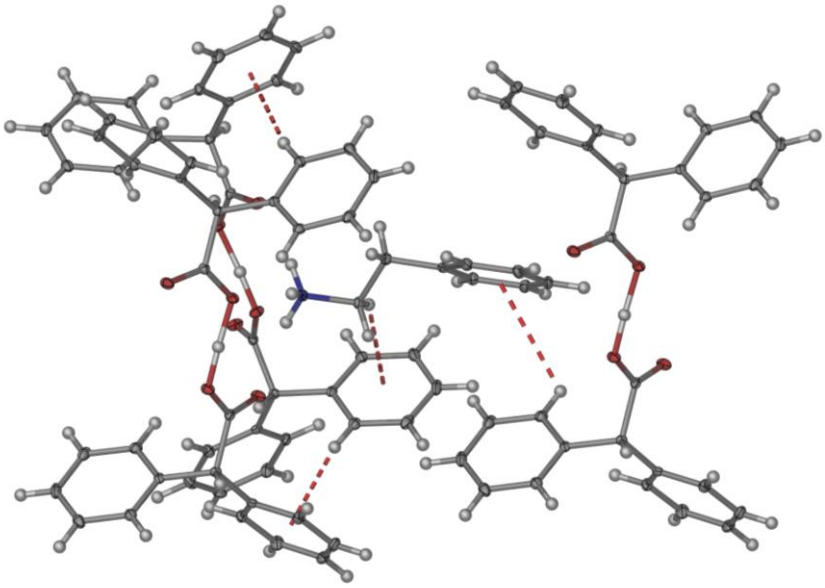

Figure 4.65 C-H··· π between 1-phenylethanammonium and diphenylacetic acid.

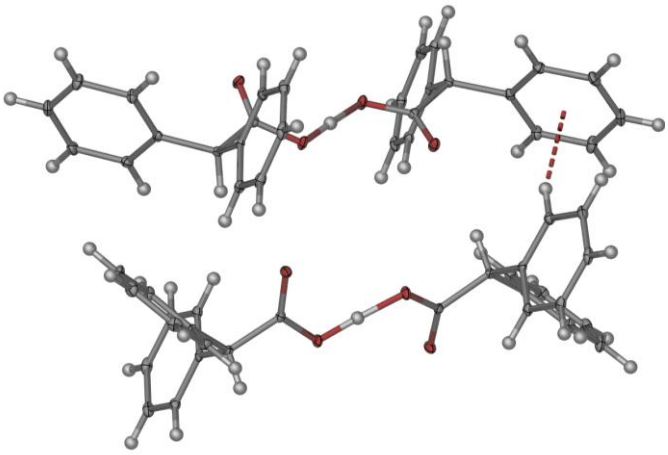

Figure 4.66 C-H··· π between diphenylacetate ions.

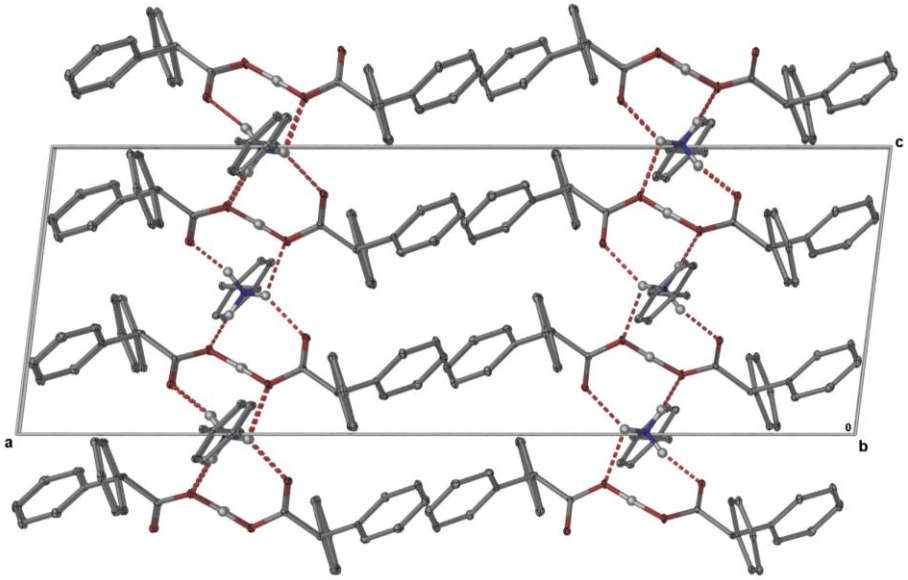

Figure 4.67 The molecular packing diagram of *1-phenylethanammonium diphenylacetate diphenylacetic acid*.

4.2.8 Cyclohexylammonium benzoate (15)

The salt crystallised in the orthorhombic space group $P2_12_12_1$ with five cation-anion pairs units in the asymmetric unit. There are twelve hydrogen bonds between the cyclohexylammonium and the benzoate [$N_{(21)}^{+}$-$H_{(21N)}$···$^{-}O_{(11)}OC$ (1.77(3) Å), $N_{(21)}^{+}$-$H_{(23N)}$···$^{-}O_{(32)}OC$ (1.87(3) Å), $N_{(21)}^{+}$-$H_{(22N)}$···$^{-}O_{(12)}OC$ (1.95(3) Å), $N_{(41)}^{+}$-$H_{(42N)}$···$^{-}O_{(12)}OC$ (1.90(3) Å), N_{41}^{+}-$H_{(41N)}$···$^{-}O_{(32)}OC$ (1.82(3) Å), $N_{(41)}^{+}$-$H_{(43N)}$···$^{-}O_{(31)}OC$ (1.76(3) Å), $N_{(61)}^{+}$-$H_{(61N)}$···$^{-}O_{(51)}OC$ (1.75(3) Å), $N_{(61)}^{+}$-$H_{(62N)}$···$^{-}O_{(71)}OC$ (1.95(2) Å), $N_{(61)}^{+}$-$H_{(63N)}$···$^{-}O_{(52)}OC$ (1.82(3) Å), $N_{(81)}^{+}$-$H_{(82N)}$···$^{-}O_{(71)}OC$ (2.00(3) Å), $N_{(81)}^{+}$-$H_{(81N)}$···$^{-}O_{(52)}OC$ (1.80(2) Å) and $N_{(81)}^{+}$-$H_{(8N)}$···$^{-}O_{(7)}OC$ (1.78(3) Å)]. This results in 3 different hydrogen bonded ladders along the *a*-axis, with graph set notation $R_4^3(10)$ (Figure 4.68). The two sharp peaks on the 2-D fingerprint plot (Figure 4.69) are due to the interaction between the donor cation (N^{+}-H) and acceptor anion ($^{-}$OOC). Evidence from the 2-D fingerprint plot indicates that H···H interactions are present, this interaction is due to close packing between the C-H groups of the of two cyclohexylammonium ions (Figure 4.70). Evidence from the fingerprint plot indicates the presence of multiple C-H···π interactions, these interactions are between the C-H of the phenyl group of the benzoate and the π–face of another phenyl group of the benzoate (Figure 4.71). Another C-H···π interaction is between the C-H of the phenyl group of the benzoate and the π–face of another phenyl group of the benzoate (Figure 4.72). The three distinct hydrogen bonding ladders are close-packed into sheets (Figure 4.73). These sheets stack on top of one another via multiple C-H···π interactions, forming the 3-D structure (Figure 4.74).

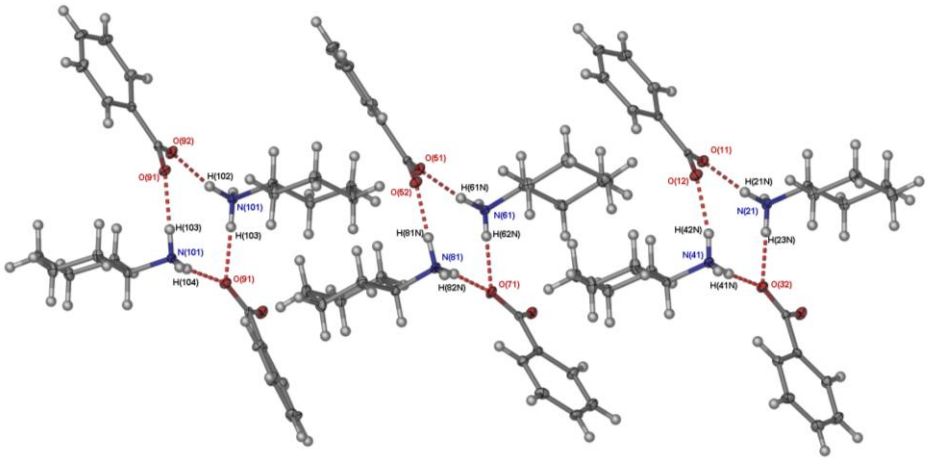

Figure 4.68 Hydrogen bonding in *cyclohexylammonium benzoate*.

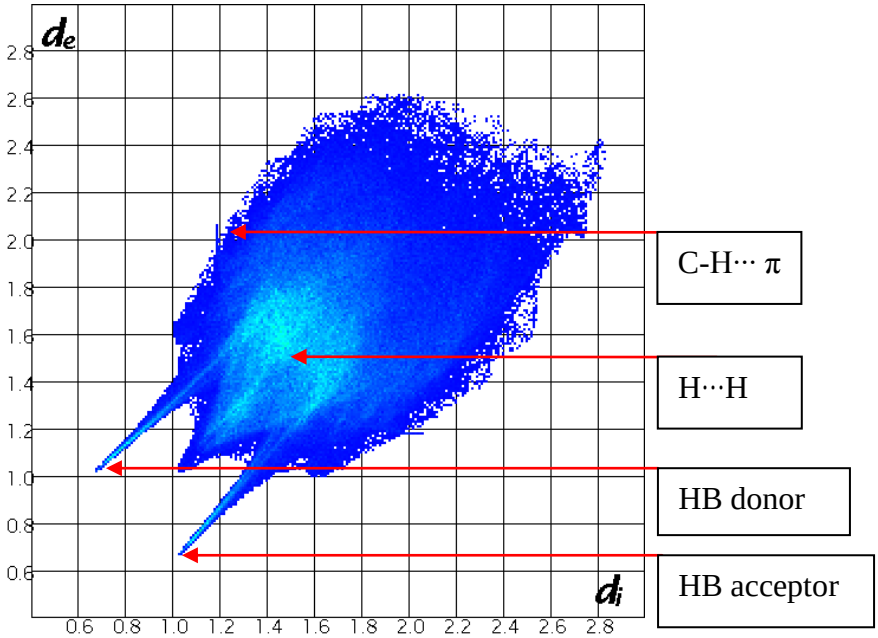

Figure 4.69 2-D fingerprint plot *cyclohexylammonium benzoate* indicating the various interactions.

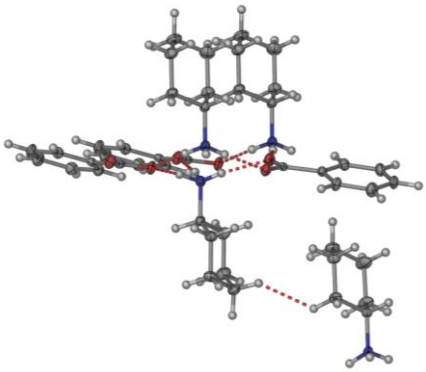

Figure 4.70 H···H interactions between the cyclohexylammonium ions.

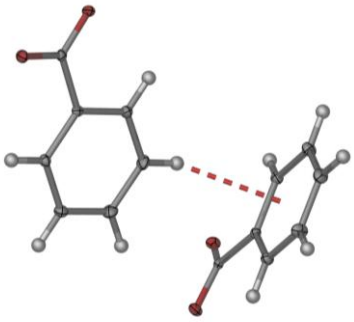

Figure 4.71 C-H··· π between benzoate ions.

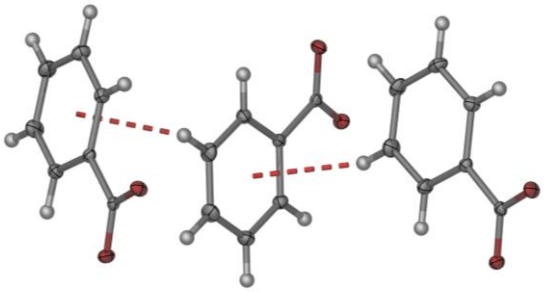

Figure 4.72 Second C-H··· π between benzoate ions.

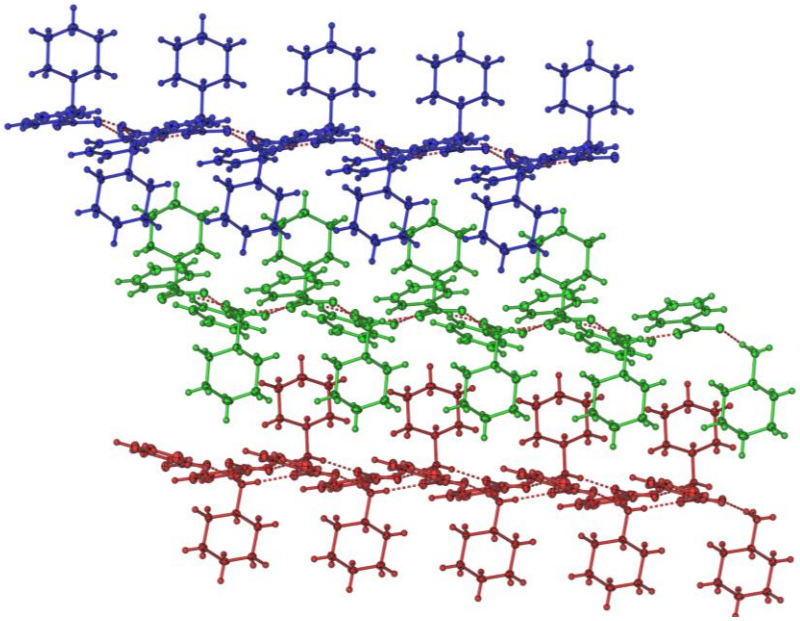

Figure 4.73 Three different hydrogen bonding sheets in *cyclohexylammonium benzoate*.

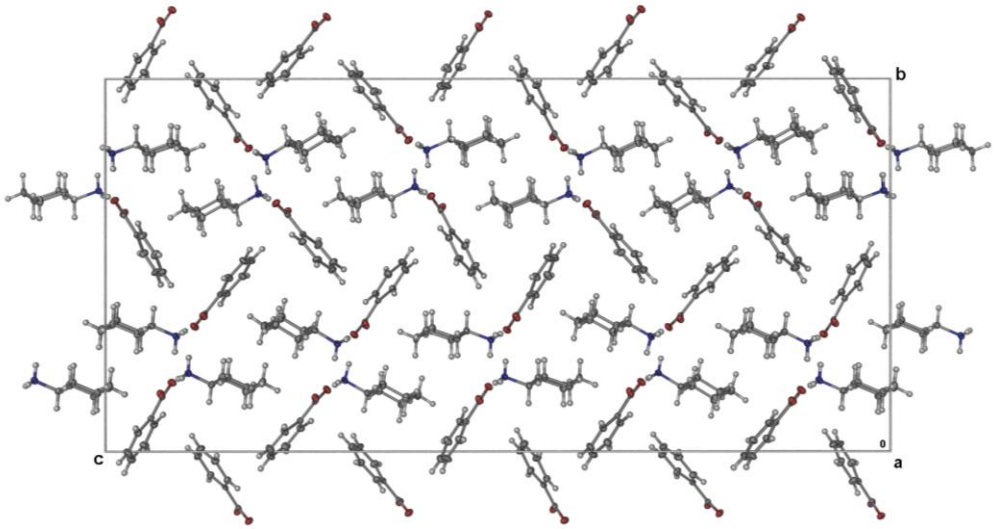

Figure 4.74 The molecular packing diagram *cyclohexylammonium benzoate*.

4.3 Crystal structure analysis of ammonium carboxylate salts

4.3.1 Ammonium benzoate (16)

This salt crystallised in the orthorhombic space group *Pbca*. There are hydrogen bonds between the ammonium and the benzoate forming a 3-D cube [$N_{(7)}^{+}$-H $_{(1)}\cdots^{-}O_{(2)}OC$ (1.948 Å), $N_{(7)}^{+}$-$H_{(2)}\cdots^{-}$ $O_{(2)}OC$ (2.009 Å), $N_{(7)}^{+}$-$H_{(6)}\cdots^{-}O_{(1)}OC$ (1.882 Å), $N_{(7)}^{+}$-$H_{(7)}\cdots^{-}O_{(1)}OC$ (2.200 Å)] (Figure 4.75). The graph set notations for the different hydrogen bonding rings making up the cube are $R_4^4(12)$, $R_4^3(10)$ and $R_4^2(8)$ (Figure 4.76). The two sharp peaks on the 2-D fingerprint plot (Figure 4.77) are due to the interaction between the donor cation (N^{+}-H) and acceptor anion ($^{-}$ OOC). Evidence from the 2-D plot indicates that C-H$\cdots$ π interactions are present; this is due to the C-H of the phenyl group of the benzoate and the π–face of the benzoate (Figure 4.78). The plot shows that H$\cdots$H interactions are present, this arises due to the close packing between C-H groups of the two benzoate ions interacting with each other (Figure 4.79). The hydrogen bonding stacks of ladders (or ladders of cubes) are held together by multiple C-H$\cdots$π interactions between the benzoate ions into stacks of sheets (Figure 4.80).

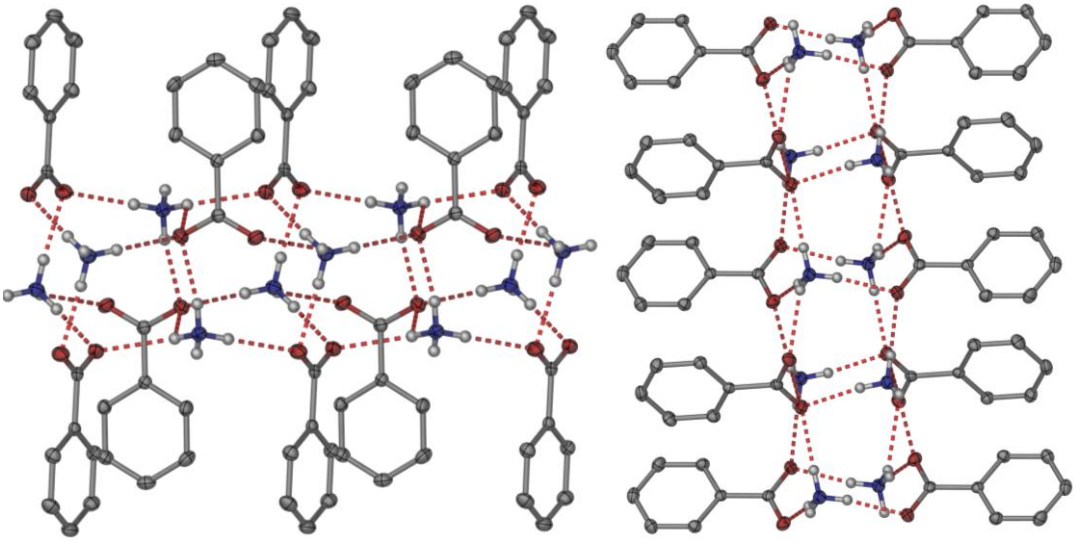

Figure 4.75 Cube hydrogen bonding in *ammonium benzoate*.

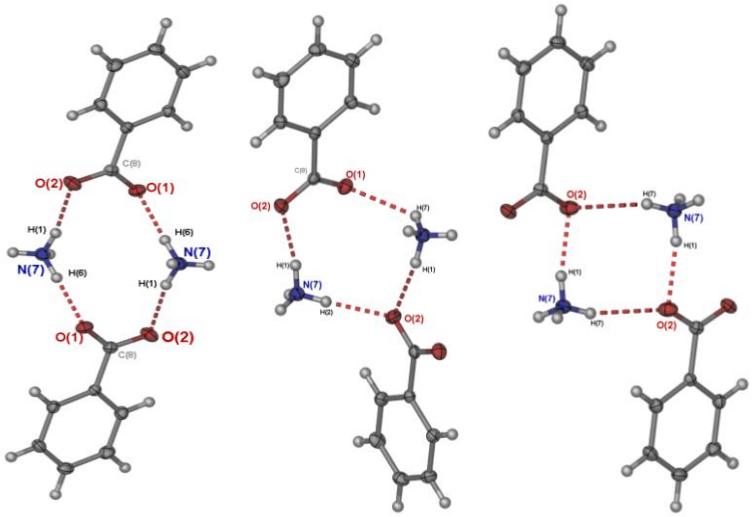

Figure 4.76 Various H-bonding rings observed in *ammonium benzoate*.

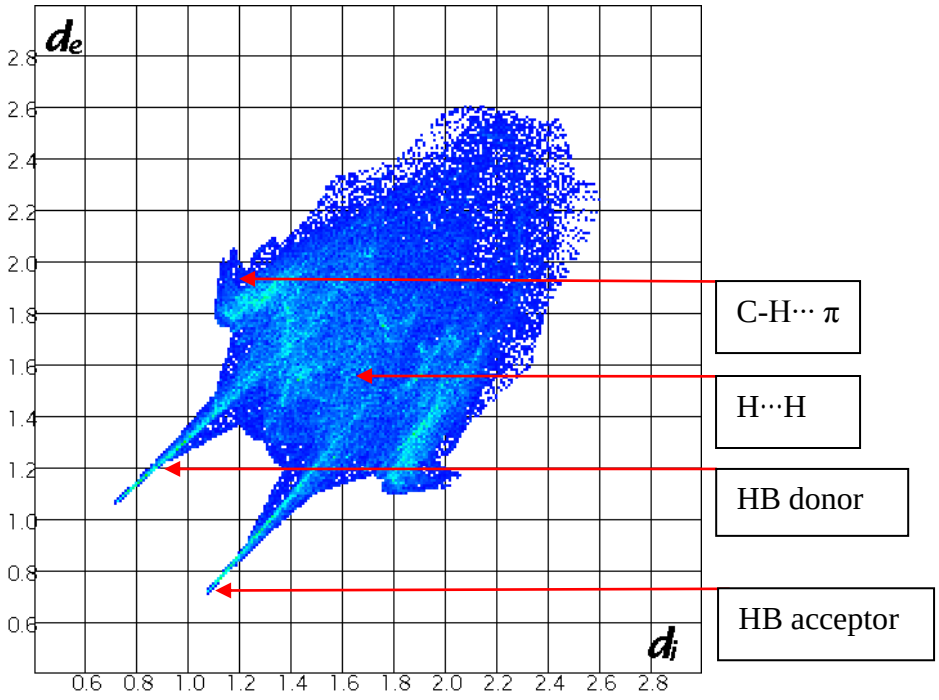

Figure 4.77 2-D fingerprint plot of *ammonium benzoate* indicating the various interactions.

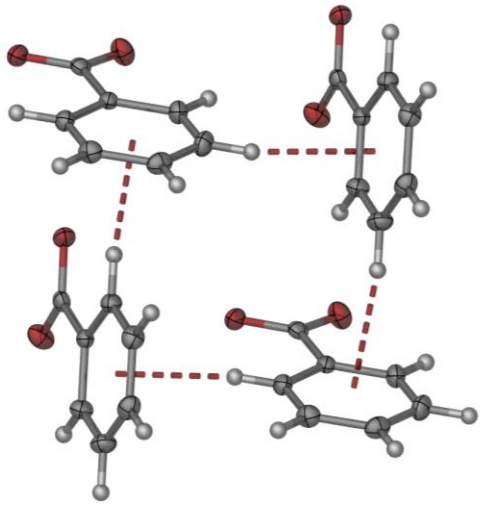

Figure 4.78 C-H···π interaction between benzoate ions.

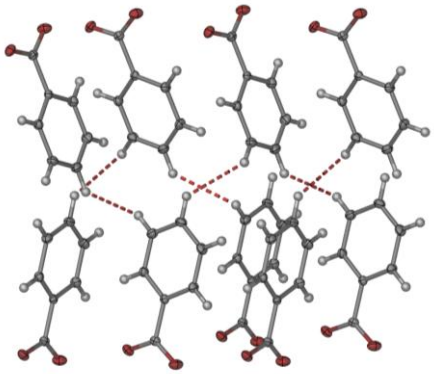

Figure 4.79 H···H contacts between benzoate ions.

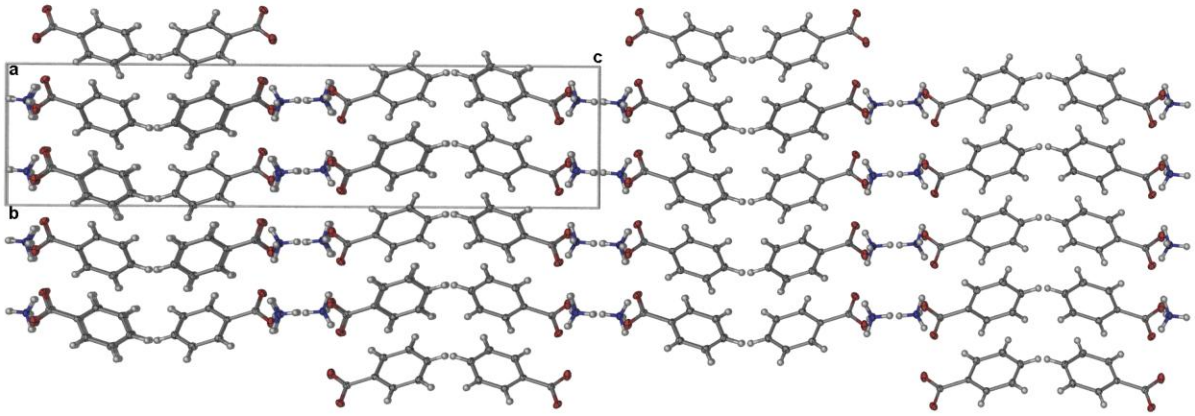

Figure 4.80 The molecular packing diagram of *ammonium benzoate*.

4.4 DISCUSSION

In total, 16 new crystal structures have been determined in the course of this study. Of these, 2 are hydrates and 2 are co-crystals of salts. All of these new materials show cation-anion interactions in the solid state, and all have extensive hydrogen bonding. The motifs seen in these structures will be compared to the results obtained from the CSD survey conducted in Chapter 3. This section will look at structural similarities between the CSD survey and the experimental work done, and it will give a detailed analysis of why these specific motifs formed over others. The rules formulated in chapter 3, which predict the formation of ring-stacking and ring-laddering in primary ammonium carboxylate salts, will be tested on the experimental results.

4.4.1 AMMONIUM CARBOXYLATE SALTS

The results from the CSD survey for ammonium carboxylate salts show that the crystal structures can form nets, ring-stacking and ring-laddering. Upon investigating the nine crystal structures obtained from the CSD survey, four formed nets (Figure 4.81); this is because both the cation and anion were small. The remaining five structures display both ring-laddering and ring-stacking similar to our *ammonium benzoate salt* (Figure 4.82) which formed stacks of ladders due to the additional cation-anion interactions i.e. C-H···π interaction from the benzoate anion.

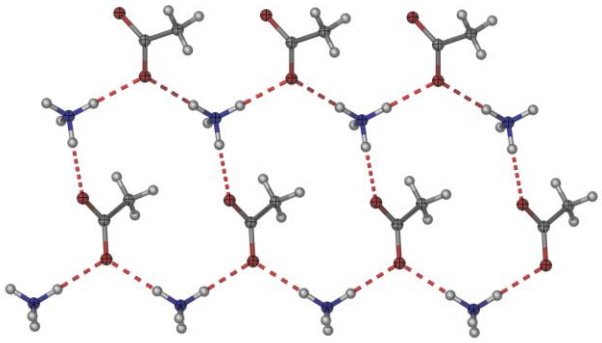

Figure 4.81 Nets in *ammonium acetate* (AMACET).

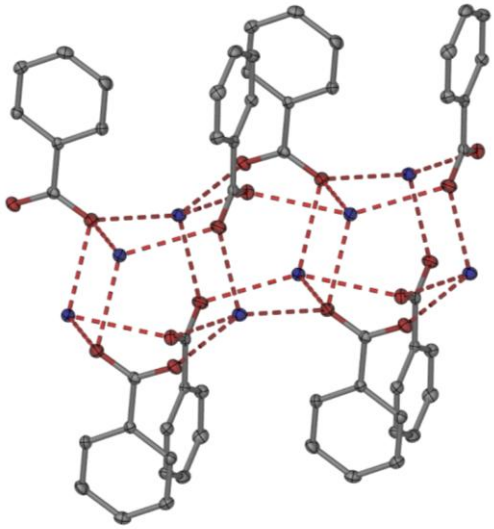

Figure 4.82 Ring-stacking and ring-laddering in *ammonium benzoate* (hydrogen atoms have been removed for clarity).

4.4.2 **PRIMARY AMMONIUM CARBOXYLATE SALTS**

The results from the CSD survey for primary ammonium carboxylate salts show that the crystal structures can form nets, ring-stacking and ring-laddering. The survey showed that the formation of ring-stacking in primary ammonium carboxylate salts is statistically low; and our experimental work did not yield any crystal structures displaying the ring-stacking phenomenon. Within the eight crystal structures obtained from the primary ammonium carboxylate salts experiments, one formed a hydrate and two formed co-crystal of a salt. The remaining five structures could further be subdivided into three structures which form ring-laddering (Figure 4.83) and the remaining two structures formed nets (Figure 4.84). The results from the CSD survey indicated that ring-laddering will dominate over the formation of nets and ring-stacking in primary ammonium carboxylate salts. Upon investigating the crystal structures obtained from the CSD survey which formed ring-laddering rules could be formulated which can aid in predicting the formation of ring-laddering.

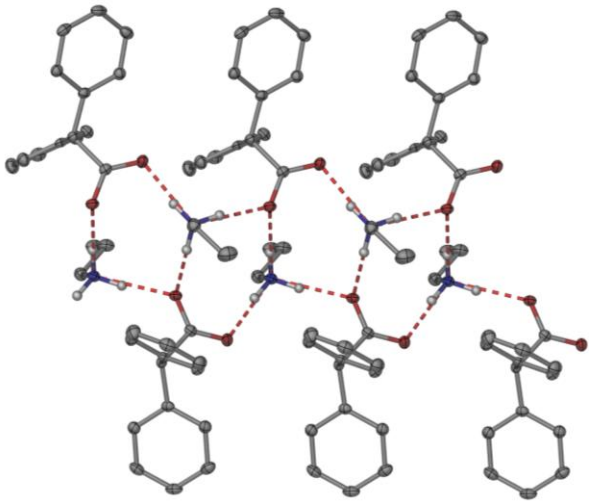

Figure 4.83 ***Propylammonium diphenylacetate*** **forming ring-laddering.**

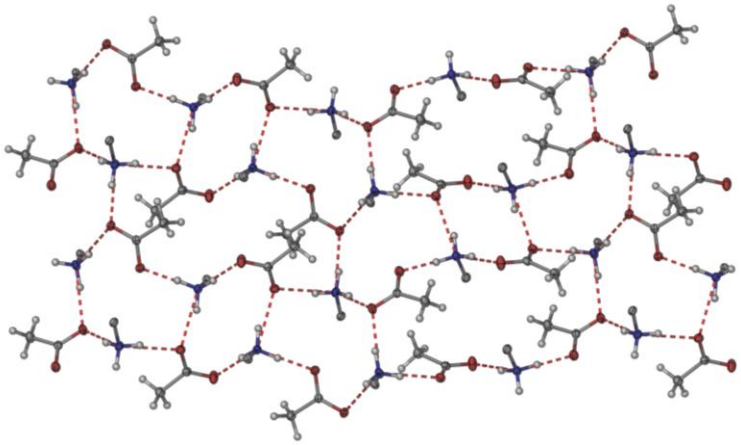

Figure 4.84 Diagram of *benzylammonium formate* showing the formation of nets (phenyl group has been removed for clarity).

If the cation is viewed down the C-N^+H_3 bond and the molecule has a large cross-sectional area (perpendicular to the plane) (Figure 4.85), the structure will form ring-laddering (Figure 4.86). This appears to be a steric effect. Ideally any crystal structure would maximise electrostatic forces to maximise the Coulombic energy within its 3-D crystal lattice (Figure 4.87). However, in ammonium carboxylate salts the packing is directly affected by steric effects of both the cation and the anion. Therefore the size of the cation and anion will influence the mode of packing in crystal lattice, thus affecting the electrostatic forces. The steric interactions between ions will interrupt the formation of nets, resulting in ladders or stacks.

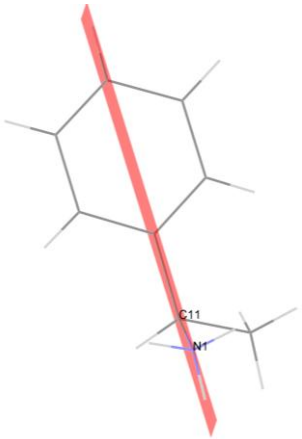

Figure 4.85 C-N^+H_3 plane (large cross-sectional area) in AFINEJ.

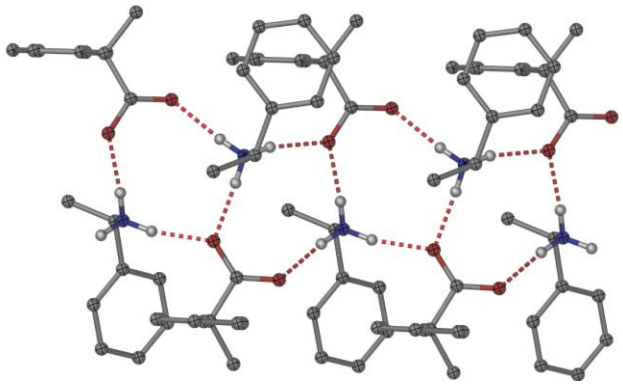

Figure 4.86 Ring-laddering in AFINEJ (some hydrogen atoms have been removed for clarity).

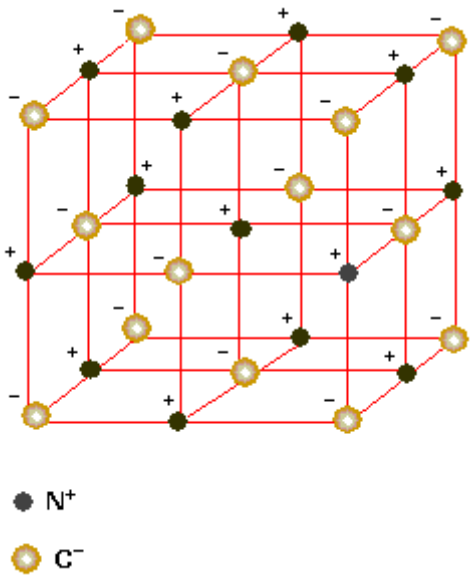

Figure 4.87 Ideal packing to maximize electrostacic forces.

The rule for predicting the formation of ring-laddering was applied to *benzylammonium formate* (Figure 4.88) and it was expected that the crystal structure would display ring-laddering due to the large cross-section it displayed after viewing the cation down the C-$N^{+}H_3$ bond, but it forms nets (Figure 4.89). The size of the formate ion plays an important role in the formation of nets in *benzylammonium formate*. The small formate ion allows the formation of the more electrostatically favourable nets (Figure 4.89), and it resembles the packing in Figure 4.87.

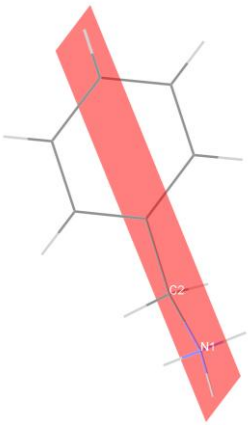

Figure 4.88 Benzylammonium cation showing the plane through the N and C atoms.

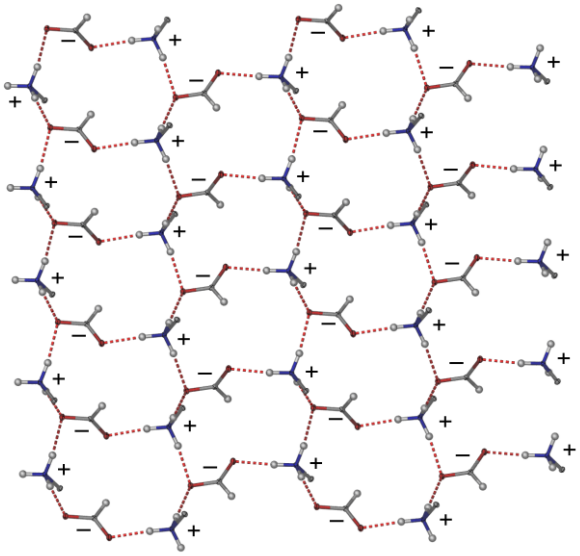

Figure 4.89 *Benzylammonium formate* maximizing electrostatic forces (phenyl groups have been removed from cation for clarity).

Another rule could be formulated upon investigating the primary ammonium carboxylate salts is that if the cation is viewed down the C-$N^{+}H_3$ bond and the molecule has a small cross-sectional area (parallel to the plane) (Figure 4.90), the molecule will form nets (Figure 4.91). The *benzylammonium formate* and *benzylammonium acetate* crystals both form nets. Also in *benzylammonium acetate* we see the cation in both conformations.

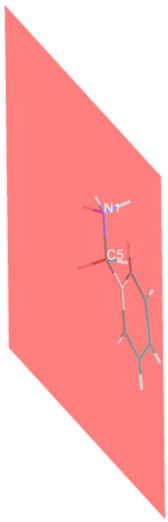

Figure 4.90 Plane through N and C atoms in benzylammonium ion.

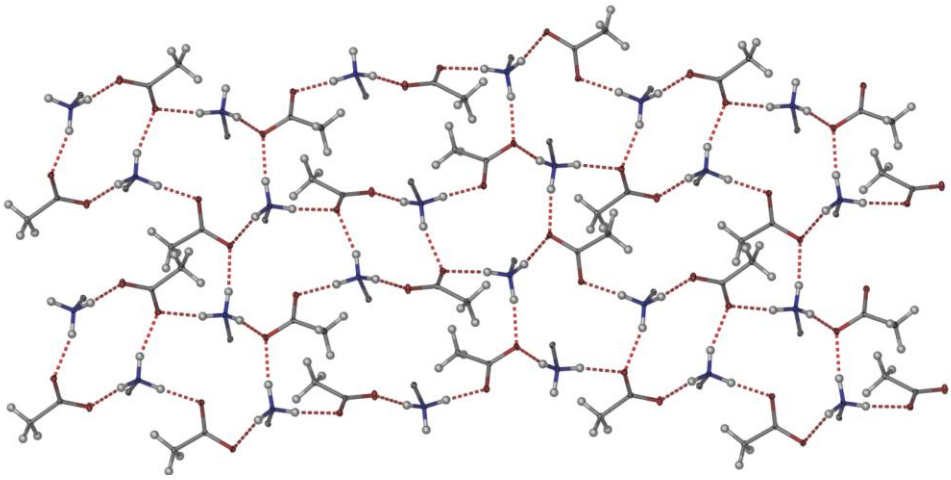

Figure 4.91 *Benzylammonium acetate* forming nets (phenyl groups have been removed from cation for clarity).

The cation in cyclohexylammonium was inspected by viewing it down the C-$N^{+}H_3$ bond (Figure 4.92); this cation has a large cross-section. This structure obeys the rule and forms extended ladders (Figure 4.93).

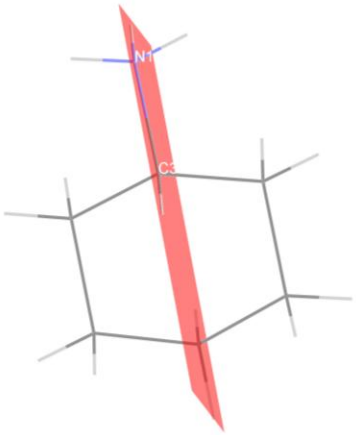

Figure 4.92 Plane between the N and C of cyclohexylammonium ion form the *benzylammonium acetate*.

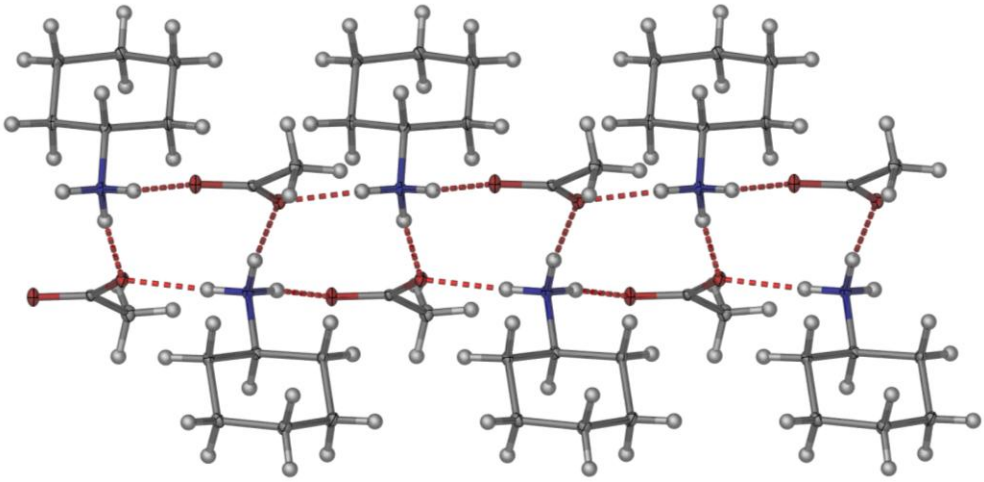

Figure 4.93 Ring-laddering in *cyclohexylammonium acetate*.

The cation in cyclohexylammonium benzoate was inspected by viewing it down the C-$N^{+}H_3$ bond (Figure 4.94); it has a large cross-section. This structure obeys the rule and forms extended ladders (Figure 4.95).

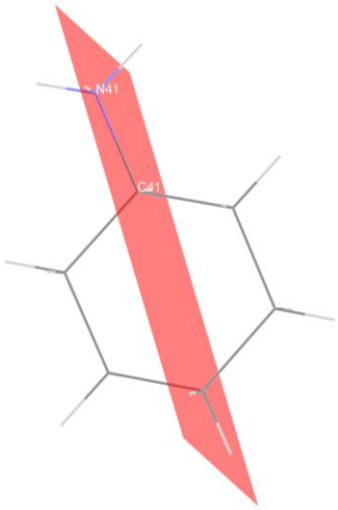

Figure 4.94 Plane through the N and C of the cyclohexylammonium ion.

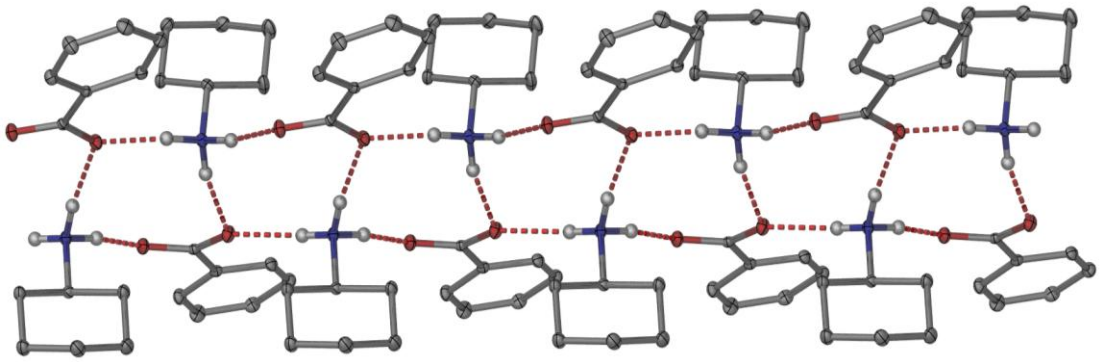

Figure 4.95 Ring-laddering in *cyclohexylammonium benzoate* (some hydrogen atoms have been removed for clarity).

The cation in *propylammonium diphenylacetate* was inspected by viewing it down the C-$N^{+}H_3$ bond (Figure 4.96), it has a large cross-section. This structure obeys the rule and forms extended ladders (Figure 4.97).

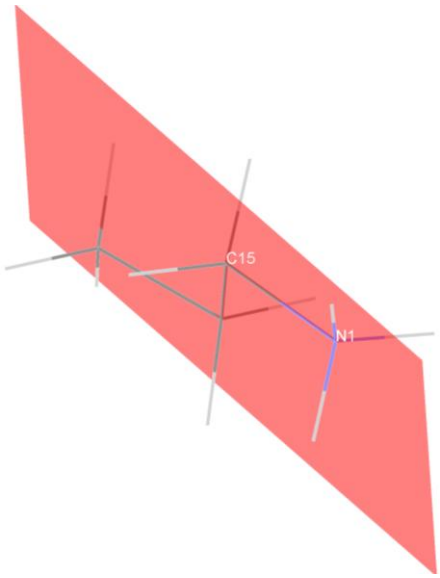

Figure 4.96 Plane through the N and C of the propylammonium ion.

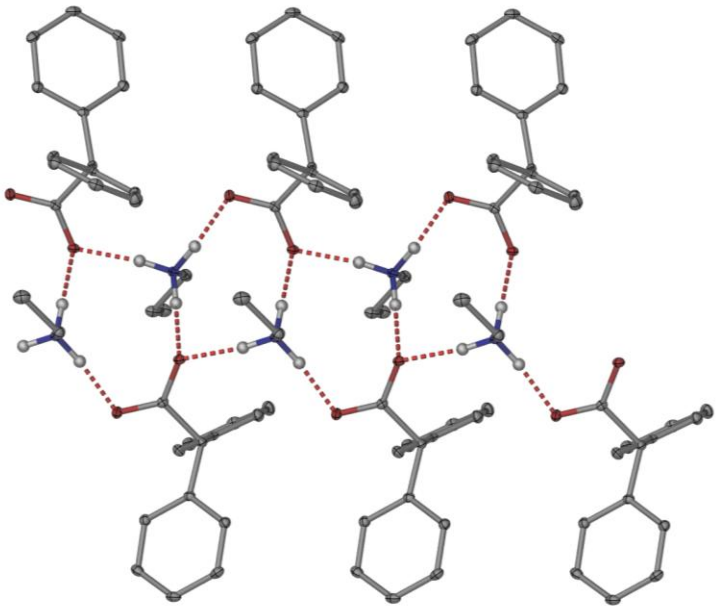

Figure 4.97 Ring-laddering in *propylammonium diphenylacetate*.

The formation of cubes in primary ammonium carboxylate salts is due to the size of both the cation and anion. If the cation and anion are large it will hinder the formation of extended ladders, it will form a discrete cubes. Our experimental work did not yield any crystal structures that display the formation of a cube but an example from the CSD survey does (Figure 4.98).

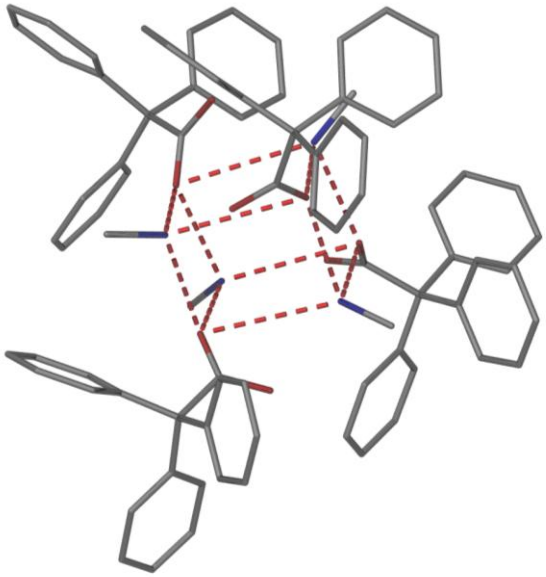

Figure 4.98 Cube in *n-Butylammonium triphenylacetate* (MIBTOH).

4.4.3 SECONDARY AMMONIUM CARBOXYLATE SALTS

The results from the CSD survey on secondary ammonium carboxylate salts show that these salts exclusively form 0-D, 1-D and ladders motifs. Seven crystal structures were obtained from the secondary ammonium carboxylate salts experiments, of which one formed a hydrate. In the remaining six structures four formed 1-D chains (Figure 4.99), the remaining two structures forms the discrete 0-D network (Figure 4.100). The results from the CSD survey for secondary ammonium carboxylate salts show that the formation of 0-D networks will be dominant over that of 1-D networks but the experimental results reflect the opposite, this is because of the steric effects from the anion. In all four of the structures forming the 1-D networks the anion is fairly large which favours the formation of 1-D chains, i.e. dibutylammonium *diphenylacetate*, dibutylammonium *diphenylacetate*, dicyclohexyalammonium *phenylacetate* and dicyclohexylammonium *diphenylacetate*. The size of both the cation and anion influences the formation of both the 0-D and 1-D networks. Therefore the experimental results reflect the formation of the 1-D network over 0-D networks. The anions from the secondary ammonium carboxylate salts in the CSD were smaller than the diphenylacetic acid used in our experiments which explains the formation of 1-D networks in our experimental work.

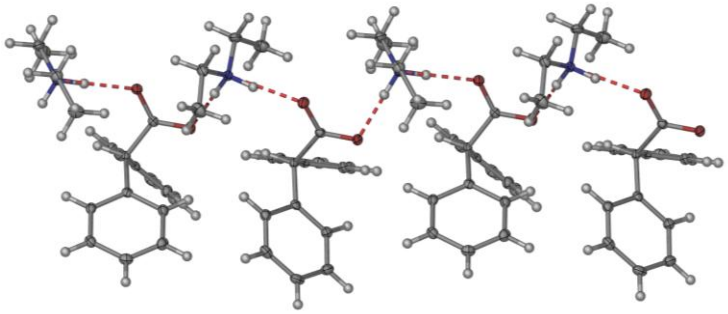

Figure 4.99 *Diethylammonium diphenylacetate* forming a 1-D hydrogen bonding network.

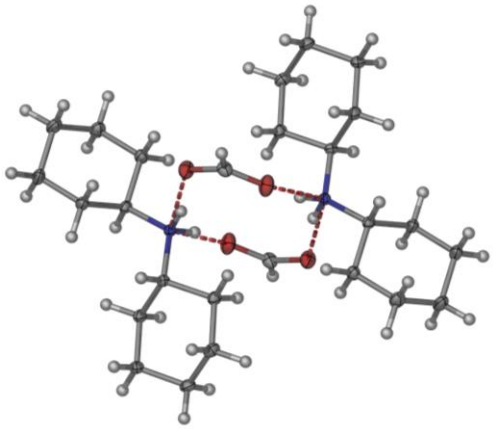

Figure 4.100 ***Dicyclohexylammonium formate*** **forming a 0-D hydrogen bonding networks.**

CONCLUSIONS

Sixteen new structures were obtained from the experimental results, which confirm the CSD results that cation anion size is significant in the formation of structural motifs in ammonium carboxylate salts.

REFERENCES:

1 L. J. Barbour, *J. Supramol. Chem.*, 2001, **1**, 189; J. L. Atwood and L. J. Barbour, *Cryst. Growth Des.*, 2003, **3**, 3.

2**.** *POV-Ray for Windows, Version 3.6.1a.icl8.win32*, Persistence of Vision Team, Persistence of Vision Pty. Ltd., 2003-2004.

3. S. K. Wolff, D. J. Grimwood, J. J. McKinnon, D. Jayatilaka and M. A. Spackman, *Crystal Explorer 2.1 (381)*, University of Western Australia, Perth, 2007.

4. M. A. Spackman and J. J. McKinnon, *CrystEngComm*, 2002, 378.

5. "It is important to recognise that the use of spherical electron densities does not assume anything about the electron distribution in either the molecule or the crystal, which is well known to be anisotropic about each nucleus. The spherical electron distribution at each atomic site are the basic of Hirshfeld's stockholders partitioning scheme, but they also result in relatively trivial computations to determine the isosurface." (From reference 4).

6. M. C. Etter and J.C. McDonald. *Acta. Cryst*. 1990, 256.

7. M. C. Etter, *Acc. Chem. Res*., 1990, **23,** 120.

8. A. Ballabh, D. R. Trivedi and P. Dastidar, *Cryst. Growth Des.*, 2005, **5**, 1545; D.R. Trivedi and P. Dastidar, *Cryst. Growth Des*., 2006, **6**, 1022.

Summary and Future Work

The concept of ring-stacking and ring-laddering is mainly useful in contexts where maximization of Coulombic energy plays a role in determining the solid-state structures.[1] Due to the electrostatic interactions between the ammonium and the carboxylates, this is a perfect system to apply the ring-stacking and ring-laddering concept to, as Coulombic energy plays an important role in the crystal structures of ammonium carboxylates.

The analysis and classification of secondary ammonium carboxylate salt motifs was fairly straightforward, due to the imbalance of electrostatic and steric factors. The secondary ammonium carboxylate salts have large cations so steric factors dominate over electrostatic factors in these crystal structures. This prevents the formation of nets, ring-stacking and ring-laddering.

The classification of ammonium carboxylate salt motifs was also fairly straightforward, due to the size of the cation. The cation in ammonium carboxylate salts is small which allows electrostatic factors to dominate and thus the formation of nets is frequent. Therefore the formation of stacks and ladders is directly dependent on the anion size and functionality (i.e. π···π, C-H···π and alkyl-alkyl interactions).

In the primary ammonium carboxylate salts there is a balance between electrostatics and steric factors, and the vast number of primary ammonium carboxylate crystal structures available in the CSD made it an obvious candidate to formulate rules to predict the formation of nets, ring-laddering and ring-stacking. The formation of ring-stacking in primary ammonium carboxylate salts is mainly due to the size of the cation and anion; if both the cation and anion are large ring-stacking will occur.

This study of the structural chemistry of ammonium carboxylate salts demonstrates that comparable motifs exist with in the secondary, primary and ammonium carboxylate salts. The extensive CSD surveys together with a steric-specific experimental study, resulted in the successful formulation of rules for "predicting" the formation of specific ammonium carboxylate

salt motifs. Finally it is now possible to "predict", to some extent, the formation of nets, ring-stacking and ring-laddering in primary ammonium carboxylate salts. If the cation and anion are small, this favours the formation of nets. If the cation and anion are large, this favours the formation of cubes. The formation of nets and ring-laddering can now be predicted based on viewing the cation down the $C\text{-}N^{+}H_3$ bond: if the cross-section is small the formation of nets is favoured. If the cross-section of the cation viewed down the $C\text{-}N^{+}H_3$ bond is large it favours the formation of ring-laddering.

FUTURE WORK

The results of this study suggest a number of specific future experimental objectives. The CSD does not contain any structures with small cations and anions in secondary ammonium carboxylate salts; it would be interesting to see if these structures would display 0-D, 1-D and ring-laddering motifs. The primary ammonium carboxylate salts were mainly obtained from grinding experiments, upon investigating the powder patterns of these salts they were different from the predicted powder pattern of the crystal structures obtained. This would suggest that the solid salts obtained from the grinding experiments exist in different forms. It would be interesting to investigate these different forms and see if they obey the rules for predicting the formation of ring-stacking and ring-laddering. The primary and secondary ammonium carboxylate salts formed hydrates, *dicyclohexylammonium formate hydrate* and *benzylammonium propionate hydrate*. The *dicyclohexylammonium formate hydrate* formed water channels within the crystal lattice; only TGA studies were done on this crystal and it would be interesting to do some hot-stage microscopy and variable temperature PXRD. The variable temperature PXRD would be used to check for phase changes within the hydrate crystal structure.

A number of more general questions have also arisen. Is it possible to quantify the effect of sterics on these packing motifs? This would involve measuring cross-sectional areas of cations and anions and predicting what conformation is most likely. It would also be interesting to investigate the effect of interactions such as $\pi - \pi$ stacking on the formation of stacks and ladders in these salts. Finally, it would be interesting to investigate whether these ideas could be applied to other organic systems.

REFERENCES:

1. A. D. Bond, *Coord. Chem. Rev.*, 2005, **249**, 2035-2055.